Reduction of the Antenna Coupling in a Bi-static, FM-CW Radar System

By

Frederich T. Malan

Thesis presented in partial fulfilment of the requirements for the degree of
Master of Science in Electronic Engineering
at the University of Stellenbosch

Department of Electrical and Electronic Engineering,
University of Stellenbosch,
Private Bag X1, Matieland 7602, South Africa.

Supervisor: Prof. K.D. Palmer
December 2011

Declaration

By submitting this thesis electronically, I declare that the entirety of the work contained therein is my own, original work, that I am the sole author thereof (save to the extent explicitly otherwise stated), that reproduction and publication thereof by Stellenbosch University will not infringe any third party rights and that I have not previously in its entirety or in part submitted it for obtaining any qualification.

December 2011

Abstract

A well-known problem with FM-CW radar systems is the leakage of transmitter power into the receiver which leads to the making of close-in targets, and can severely limit the system dynamic range performance. This thesis considers two solutions to this radar system problem for a low frequency radar operating in the VHF band.

The first method to suppress coupling is using separate transmit and receive antennas designed in such a way as to reduce coupling between them. The second is to design a negative feedback loop as part of the radar receiver where the feedback loop adaptively reduces the amount of transmitter leakage through to the receiver.

This project details the realisation of these two solutions. A number of antenna designs are modelled in software and simulated to determine their characteristics of which the transmit-to-receive coupling is the key parameter. As no low coupling configuration could be found a simple configuration is chosen and practical measurements are taken. These antennas are then used in the radar system that is to be built.

An FM-CW radar system is designed and simulated using software with a negative feedback loop being designed and implemented into the radar simulation.

A practical radar system is then made inclusive of the feedback loop. Measurements are then taken to determine the efficacy of the feedback loop.

Uittreksel

'n Bekende probleem met FM-CW radar stelsels is die lekkasie van versender krag tot in die ontvanger wat lei tot die maak van nabye teikens en kan die stelsel se dinamiese sendbereik steng beperk. Hierdie tesis oorweeg twee oplossings tot hierdie probleem vir 'n lae frekwensie radar wat in die VHF band werk.

Die eerste metode wat na gekyk word om die koppeling te onderdruk is om die twee antennas van die radar stelsel so te ontwerp sodat die hoeveelheid koppeling tussen hulle verminder is. Die tweede is om 'n negatiewe terugvoerlus as deel van die ontvanger te ontwerp. Hierdie terugvoerlus sal die versender lekkasie sein aanpassend in die ontvanger verminder.

In hierdie projek word die realisering van bogenoemde oplossings uiteengeset. 'n Paar verskillende antenna ontwerpe word gemodelleer in sagteware en word gesimuleer om hul karakteristieke te bepaal. Die belangrikste van hierdie faktore is die versender na ontvanger koppeling. Sienend dat geen ontwerp met 'n lae genoeg koppeling gevind kon word nie, is 'n eenvoudige ontwerp gekies en praktiese metings daarvan geneem. Hierdie antennas word dan gebruik in die radar stelsel wat gebou sal word.

'n FM-CW radar stelsel word ontwerp en gesimuleer in sagteware. Die negatiewe terugvoerlus word ook ontwerp en geïmplementeer in die radar simulasie.

'n Praktiese radar stelsel word dan gemaak insluitend die terugvoerlus. Metings word dan geneem om die effektiwiteit daarvan te bepaal.

Acknowledgements

I wish to dedicate this in memory of my father.

I further wish to thank the following people:

- Prof. K.D. Palmer, for all his help, his knowledge and insight and most of all his patience.
- Jonathan for all his help and the time he took to explain the basics to me.
- My mother for all her support and patience.
- My friends for the distractions that kept me sane.

Table of Contents

List of Figures

List of Tables

Nomenclature

AM	Amplitude Modulation
ADC	Analog to Digital Converter
BHR	Borehole Radar
CS	Chip Select
CLK	Clock
CW	Continuous Wave
DFRRW	Delta- Frequency Ramp Rate Word
DFTW	Delta- Frequency Tuning Word
DAC	Digital to Analog Converter
DDS	Direct Digital Synthesizer
FPGA	Field-Programmable Gate Array
FM-CW	Frequency Modulated Continuous Wave
FM	Frequency Modulation
FTW	Frequency Tuning Word
FUD	Frequency Update
GPR	Ground Penetrating Radar
I-channel	In-phase channel
IORESET	Input/Output Reset
IF	Intermediate Frequency
LFM	Linear Frequency Modulation
LO	Local Oscillator
LNA	Low-Noise Amplifier
LPF	Low-pass Filter
NLFM	Non-Linear Frequency Modulation
NCO	Numerically Controlled Oscillator
POW	Phase Offset Word
PQF	Polyphase Quadrature Filter
PRF	Pulse Repetition Frequency
Q-channel	Quadrature phase channel

RF	Radio Frequency
Rx	Receive
RPC	Reflected Power Canceller
SCLK	Serial Data Clock
SDIO	Serial Data Input/Output
SYSCLK	System Clock
Tx	Transmit
VHF	Very High Frequency

Chapter 1

Introduction

1.1 Background Information

1.1.1 A Brief History of Radar

The history of radar stretches back more than a century. Its invention first started with the discovery of radio waves. In 1886 a German physicist named Heinrich Hertz started experimenting with radio waves. He found that an electric current traveling rapidly back and forth in a conducting wire would radiate electromagnetic waves into the surrounding space. Today we call these waves *radio waves*. Hertz was the first to demonstrate experimentally the generation and detection of these waves. These discoveries inevitably lead to the invention of the radio by Nikola Tesla and even further to that of radar. (1)

The first detection of a target by radar was achieved by Christian Hulsmeyer, a German engineer, who demonstrated a ship detection device to the German Navy in 1903. However, the range of the device was so limited that little interest was generated. (2)

Following the First World War, there was a great surge in radio technology. By the early 1930's, the basic technologies that would lead to radar were known to radio researchers throughout much of the world. In 1935 radio-based detection and ranging was first

demonstrated by Robert Watson Watt et al. in Great Britain. It was not until the outbreak of World War II that radar first became widely used. The name radar came from the acronym RADAR, coined by the U.S. Navy in 1940 for the then-secret "radio detection and ranging" technique. [3]

Today, radar has evolved to become considerably cheaper and more accurate. For example, radar can now be found in Intelligent Parking Assist System in cars, traffic speed cameras and even in radar speed signs, as pictured in Figure 1.1.

Figure 1.1 – Picture of a radar speed sign by RadarSign [4]

1.1.2 Ground Penetrating Radar and Borehole Radar

Ground Penetrating Radar (GPR) is a sub-section of radar widely used in industry. The possibility of detecting buried objects remotely has fascinated mankind over centuries. GPR has been found to be an especially attractive option. [5]

GPR refers to the use of high and medium power radio and microwave frequency signals to generate an image of any underground object or anomaly without physical removal of the ground surrounding the object. This form of radar generally has applications for discovering of structures under the earth's surface, geological or otherwise, but also for

non-destructive studying of the internal structure of non-geological objects, for example building condition assessment. [6]

GPR is commonly used in the mining industry and for archaeological investigations, but it has a very diverse field of use, fields such as medicine, building construction and assessment to name but a few. In the mining industry GPR can be used to find mineral and ore deposits. GPR is also used in maritime archaeology to find sunken ships buried under sand. [7]

Figure 1.2 shows some examples of how GPR can be used.

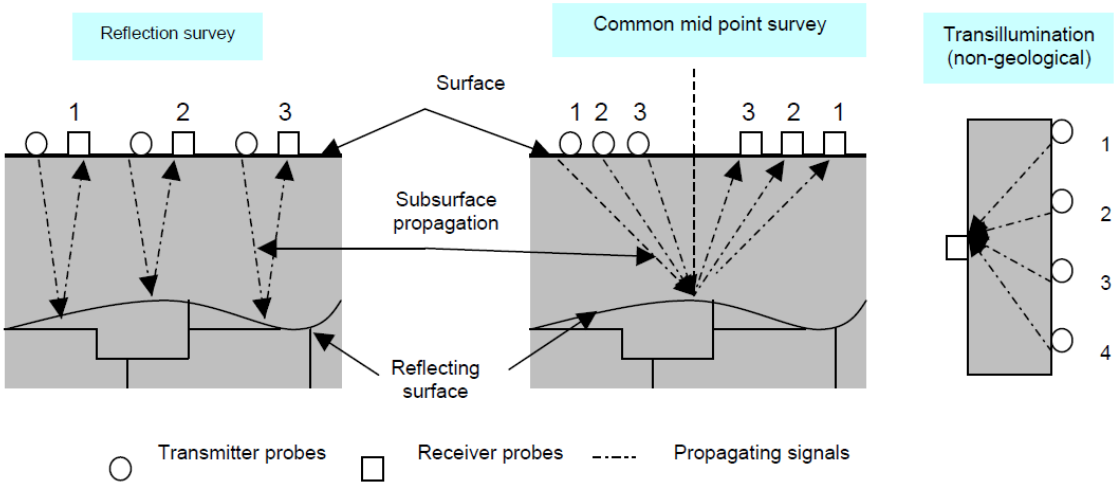

Figure 1.2 – The progression of three generic GPR deployment topologies [6]

Borehole Radar (BHR) uses the same principles as GPR, but where the GPR transmits and receives the radar signal from aboveground, the BHR does this from underground. An example of a BHR system is shown in Figure 1.3.

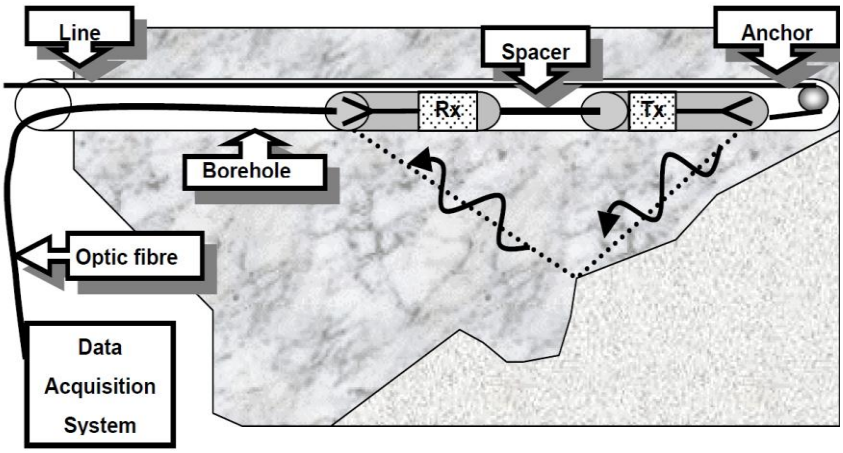

Figure 1.3 – Diagram of a borehole radar system [8]

1.2 Project Description

1.2.1 Objective

The aim of this project was to determine if linear frequency modulated continuous wave (FM-CW) radar technology could yield a low cost, high performance borehole radar system. The radar system should be designed to work underground in the mining industry. For this application typical system specifications are: a range resolution of 1 m, with a maximum unambiguous range of 100 m. The radar must consist of separate transmit and receive antennas with the electronics and battery pack in between. To fit into a borehole, the physical layout of the radar system had to be designed to fit into a cylinder that has a diameter of 28mm and a length of 600mm, excluding antennas. Figure 1.4 shows a diagram of how the BHR must look.

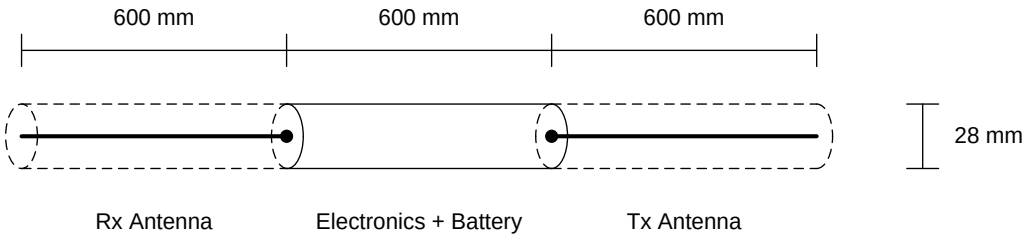

Figure 1.4 – Diagram of the borehole radar design with dimensions

The project would detail the design of the radar system, the manufacturing of its components and the tests and measurements performed on the system.

1.2.2 Problem statement

A well-known problem with continuous wave (CW) radars is the isolation between transmitter and receiver and consequently the leakage of the transmit signal into the receiver. With pulsed radar isolation can be achieved by using time gating, however, CW radar transmits and receives signals continuously and simultaneously. Normally it is necessary for radar to detect reflected signals of the order of -90 dBm, which is nearly impossible when simultaneously receiving a transmitter leakage signal in the order of +30 dBm or possibly more.

The following two problems with the leakage signal are apparent:

- Firstly noise from the transmitter can overshadow signals from valid targets;
- Secondly the power leaking into the receiver can saturate or even damage some components.

1.2.3 Proposed solutions

The following two possible solutions to the above stated problem were investigated:

- The first concerns the design of the transmit and receive antennas. The design of these antennas must ensure that the coupling between the transmit and receive antennas is minimized so as to reduce the transmitter leakage.
- The second possible solution is the use of a negative feedback loop in the receiver. The use of a negative feedback loop in the receiver will adaptively reduce the amount of transmitter leakage within itself.

A combination of the above two solutions can be used to improve the overall effectiveness of the transmitter leakage suppression.

1.2.4 Thesis outline

The outline of the thesis is as follows:

- Chapter 2 provides a brief explanation of the theoretical and mathematical working of FM-CW radar.
- Chapter 3 looks at the design of a number of antennas. Different antenna designs are simulated in computational electromagnetic software to determine their characteristics. The focus of the simulation is on the amount of coupling between the different antennas
- The details for the design of the FM-CW radar system are given in Chapter 4. In this chapter the radar concept from Chapter 2 is used to create a block diagram of a basic FM-CW radar system. Additional features such as quadrature modulation and the negative feedback loop are also developed in this chapter. Lastly a block diagram of the complete system is presented.
- In Chapter 5 the block diagram developed in Chapter 4 is broken down into its individual components. Each of these individual components is discussed separately with suitable components being chosen to implement each. Each component is also tested and their measurements presented.
- In Chapter 6 the two possible solutions to the transmitter leakage problem are tested. In the case of the antennas, the selected antennas are measured to determine the amount of isolation between them. For the feedback loop, the constructed radar system is tested and the amount of leakage cancellation measured. The chapter concludes with a summary of the work done and the results obtained. Recommendations for further development and revisions to the design are also provided.

Chapter 2

Introduction to FM-CW Theory

This chapter summarizes the theory behind FM-CW radar.

2.1 The Doppler Effect

Because the Doppler Effect is the basis of CW radar, a brief description of the Doppler Effect is provided in this section.

The Doppler Effect is well known in the fields of optics and acoustics. It states that if a source of oscillation, for example a vehicle sounding a siren, is moving relative to an observer, it will result in an apparent change, or shift, in frequency.

Figure 2.1 shows waves emitted by a source moving from right to left. The wavelengths are shorter on the left side of the source and longer on the right. [9]

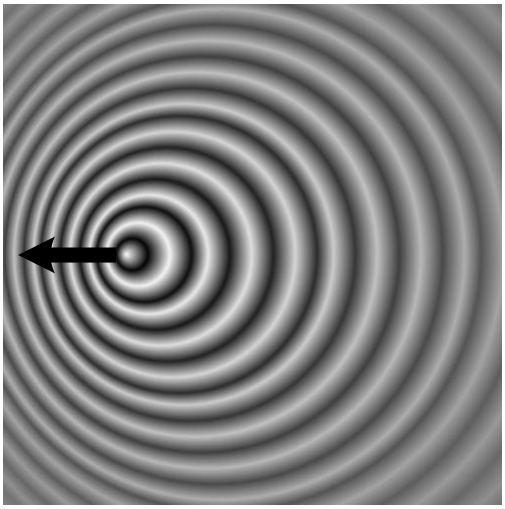

Figure 2.1 – Visual representation of the Doppler Effect [9]

The formula for Doppler shift can be determined from the relationship between the observed frequency, f, and emitted frequency, f_0, of waves in a medium. [10]

$$f = \left(\frac{v \pm v_o}{v \pm v_s} \right) f_0 \qquad (2.1)$$

Where, v is the velocity of waves in the medium

v_o is the velocity of the observer relative to the medium; positive if the source is moving away from the observer.

v_s is the velocity of the source relative to the medium; positive if the observer is moving toward the source.

For the case of electromagnetic waves, i.e. for radar, where the radar is usually stationary, Equation (2.1) becomes [11]:

$$f_r = \left(\frac{c + v_r}{c - v_r} \right) f_t \qquad (2.2)$$

Where, f_r is the frequency observed by the radar,

f_t is the frequency transmitted or scattered by the source or target,

c is the speed of light,

v_r is the relative velocity of the target with respect to the radar.

The Doppler shift frequency, also known as the "beat frequency", is the difference between the frequencies emitted by the radar and target [11].

$$f_d = f_r - f_t = f_t\left(\frac{2v_r}{c - v_r}\right) \tag{2.3}$$

The velocity of the electromagnetic waves, in this case light, is much greater than the relative speed of the observer or source, $c \gg v_o, v_s$, therefore Equation (2.3) becomes [11]:

$$f_d = \frac{2v_r}{c} f_t \tag{2.4}$$

2.2 CW Radar

CW radar is a radar system that transmits a continuous flow of radio energy at a constant frequency. It is also known as continuous-wave Doppler radar. [12]

The Doppler Effect is the basis of CW radar. CW radar can measure the Doppler shift of an oscillation source and determine the relative velocity between the radar and source. [13]

Figure 2.2(a) illustrates a block diagram of a simplified CW radar.

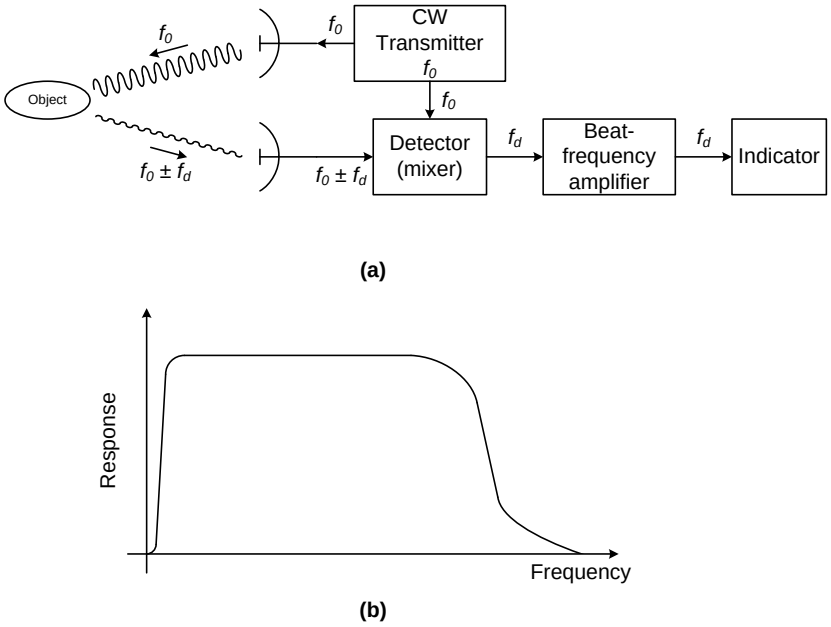

Figure 2.2 – (a) Block diagram of a simple CW radar; (b) Response characteristic of the beat-frequency amplifier [11]

The transmitter generates a continuous signal of constant frequency f_0 (an unmodulated signal), which the antenna then radiates. An object intercepts this transmitted signal and scatters a portion of it back to the radar, where it is received by the receiving antenna. The system has two separate antennas to avoid interruption of the continuous signal transmission.

From Equation (2.4), in Section 2.1, it can be seen that if a target has a velocity, v_r, relative to the radar, the received signal will have a shifted frequency of amount $\pm f_d$. This shifted frequency is known as the Doppler shift or beat frequency. A positive Doppler shift corresponds to a target moving towards (decreasing in distance with respect to) the radar and negative if it is moving away. The received signal, at frequency $f_0 \pm f_d$, is heterodyned (mixed) with the transmitter signal, f_0, and filtered to produce the beat frequency f_d. The sign of f_d is however lost in the process.

A beat-frequency amplifier eliminates echoes from stationary targets and amplifies the Doppler frequency signal to a level where it can operate an indicating device (e.g.

earphones or a frequency meter). Figure 2.2(b) shows the frequency response of such an amplifier. It shows that stationary targets with a dc-component will be suppressed. [11]

In some CW radar applications it is of interest to know whether a target is approaching or receding. If the echo signal, f_d, lies below the carrier, f_0, the target is receding and above the carrier if it is approaching, as illustrated in Figure 2.3.

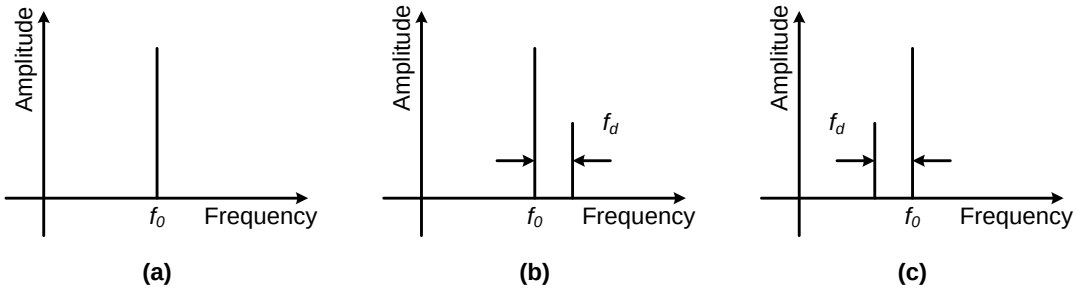

Figure 2.3 – Spectra of received signals. (a) No Doppler shift, no relative target motion; (b) Approaching target; (c) Receding target [11]

The sign of the Doppler shift, and therefore the direction of the target motion, may be found by splitting the received signal into two channels, as illustrated in Figure 2.4. The signal in channel B is phase shifted by 90° in respect to the signal in channel A. These two signals are then separately mixed with the received signal. This process is called quadrature modulation and is used in newer radar systems to retain phase information normally lost in the analog to digital conversion process.

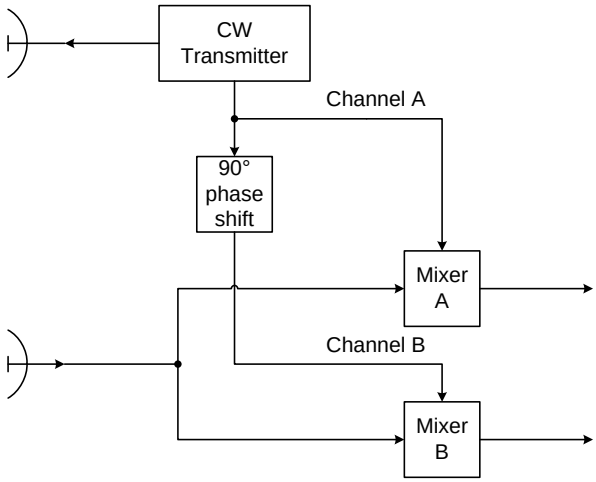

Figure 2.4 – Measurement of Doppler direction using quadrature modulation [11]

The two resulting difference signals are as follows.

$$\begin{aligned} S_A &= \sin(\pm\omega_d t + \varphi) \\ S_B &= \sin(\pm\omega_d t + \varphi + \frac{\pi}{2}) \\ &= \cos(\pm\omega_d t + \varphi) \end{aligned} \qquad (2.5)$$

Where, S_A and S_B are the signals after mixers *A* and *B* respectively,
$\omega_d = 2\pi f_d$ and is the radial frequency form of the Doppler shift,
φ_A and φ_B are the phases of each signal,
$\frac{\pi}{2}$ is the 90° phase shift.

The sign of the phase for each signal will be positive if the target is approaching, and negative if it is receding. The sign of ω_d, and therefore the target's motion, may be determined according to whether the output of channel *B* leads or lags that of channel *A*. [11]

Advantages of CW radar are that it is technologically simple to design and compact in size when manufactured. [14] It has the ability to measure velocity with extreme accuracy by means of the Doppler shift in the frequency of the echo signal. [15] Another advantage is that it has no pulsing, as in a pulsed radar system, and therefore no minimum or maximum ranges, although the transmitter power does impose a practical limit on this. [16] The main

disadvantage of CW radar is that it can only detect moving targets, as motionless targets do not cause a Doppler shift.

Applications of the simple, unmodulated CW radar is for the measurement of relative velocities of moving targets, for example as police speed monitors, rate-of-climb meters in vertical-take-off aircraft or in sports to track ball and equipment parameters, for example the Trackman system used in golf. [17]

2.3 FM-CW Radar

CW radar only determines relative velocity by means of the Doppler shift and is unable to measure range to targets. To include range information, the transmitted signal is modulated. Pulse radar is an example of one form of modulation, namely amplitude modulation (AM). Frequency modulation (FM) is the other technique used to determine range and is one of the main focuses for this project.

Thus by combining the measurement of Doppler shift and Frequency modulation, FM-CW radars determine relative velocity and measure the range to the target.

2.3.1 Signal Description

Frequency modulated continuous wave (FM-CW) radar also transmits a continuous flow of radar energy as with CW radar, but the frequency of the signal is rapidly increased or decreased at regular intervals.

Figure 2.5 shows such a signal where the amplitude is at a constant level but the frequency increases with time.

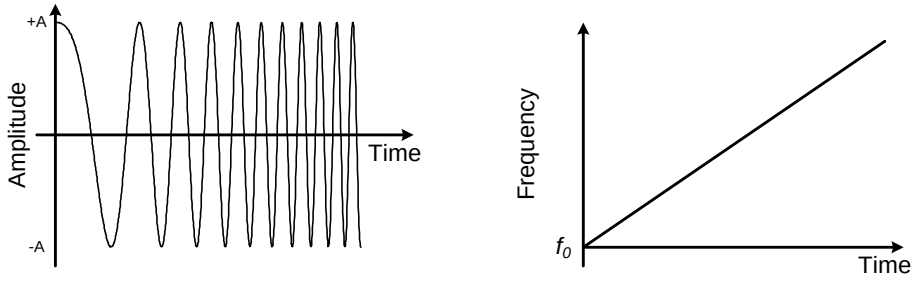

Figure 2.5 – Chirp waveform

This signal is called a "chirp" signal. Mathematically this is represented by the following:

$$S_{chirp} = A\cos(\psi(t)\cdot t)$$
$$\psi(t) = f_0 t \qquad (2.6)$$

Where, S_{chirp} is the chirp signal,
A is the amplitude of the signal,
f_0 is the carrier frequency (frequency the signal starts at).

In practical CW radar the frequency cannot be continuously changed in one direction only. It has to be reset or changed in the other direction and this process is then repeated at a constant rate.

There are numerous methods to employ frequency modulation and Figure 2.6 shows the three modulation waveforms most often used, namely sawtooth, triangular and sinusoidal modulation.

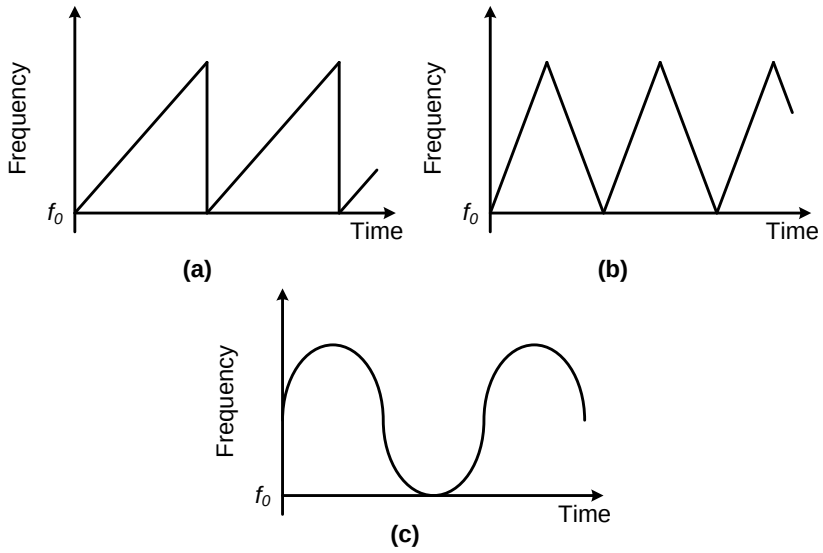

Figure 2.6 – Modulation Waveforms. (a) Sawtooth; (b) Triangular; (c) Sinusoidal

The sawtooth and triangular waveforms are linear waveforms (linear frequency modulation, LFM) and the sinusoidal is non-linear (NLFM). The sawtooth modulation waveform is used in this project, but for the purpose of explanation the triangular waveform will be used.

Figure 2.7 illustrates Frequency-time relationships in an FM-CW radar.

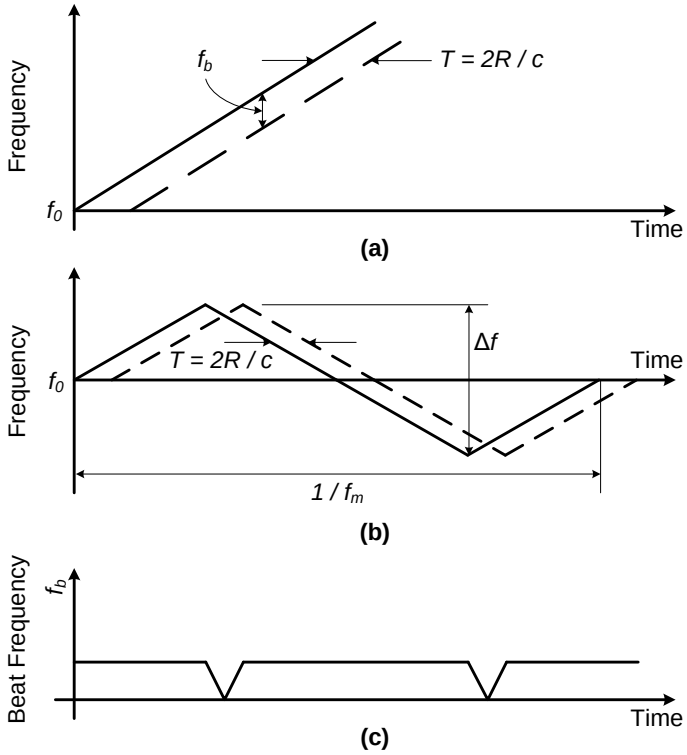

Figure 2.7 – Frequency-time relationships in FM-CW radar. Solid curve represents transmitted signal; dashed curve represents echo. (a) Linear frequency modulation; (b) Triangular frequency modulation; (c) Beat note of (b) [11]

A signal is generated at start frequency f_0, and then its frequency is linearly increased as a function of time, the solid curve in Figure 2.7(a). Figure 2.7(b) shows the process where the frequency is modulated at a rate of f_m over a range of Δf, where Δf *is* the bandwidth of the signal. f_m is also known as the pulse repetition frequency or PRF. The rate of frequency change $\dot{f}_0$ is given by [18]:

$$\dot{f}_0 = 2 f_m \Delta f \qquad (2.7)$$

2.3.2 Range Equation

If there is no Doppler frequency shift, the received signal, the dashed curve in Figure 2.7(a) and (b), is shifted only in time. This is due to the time delay caused by the distance the

radar signal has to travel between the radar and the target. If R is this distance, the signal has to traverse this distance twice, at the speed of light. The time delay T is then given by:

$$T = \frac{2R}{c} \tag{2.8}$$

Where, T is the time delay,
R is the distance between the target and radar,
c is the speed of light.

The difference signal produced by mixing the transmitted signal with the received signal is known as the beat frequency or beat note, Figure 2.7(c). From this beat frequency the distance R can be determined.

When there is no Doppler frequency shift, the beat note $f_b = f_r$ where f_r is the beat frequency due only to the target's range. Therefore the beat frequency is [11]:

$$f_r = \dot{f}_0 T = \frac{2R}{c}\,\dot{f}_0 \tag{2.9}$$

For triangular frequency modulation, using Equations (2.7) and (2.9), the beat frequency will be [11]:

$$f_r = \frac{2R}{c} \cdot 2 f_m \Delta f = \frac{4R f_m \Delta f}{c} \tag{2.10}$$

From this the range can be determined [11].

$$R_S = \frac{f_b c}{2 f_m \Delta f}$$
$$R_T = \frac{f_b c}{4 f_m \Delta f} \tag{2.11}$$

Where, R_S = range for sawtooth modulation,
R_T = range for triangular modulation.

2.3.3 Range Equation with Doppler Effects

The above is only for stationary targets, where there is no Doppler frequency shift. The Doppler frequency shift causes the received signal; the dashed curve in Figure 2.7(a) and (b), to be shifted up or down, Figure 2.8(a). On the up portion of the slope, the Doppler shift term subtracts from the beat frequency and ads on the down portion, as illustrated in Figure 2.8(b) [11].

$$f_b(up) = f_r - f_d$$
$$f_b(down) = f_r + f_d \qquad (2.12)$$

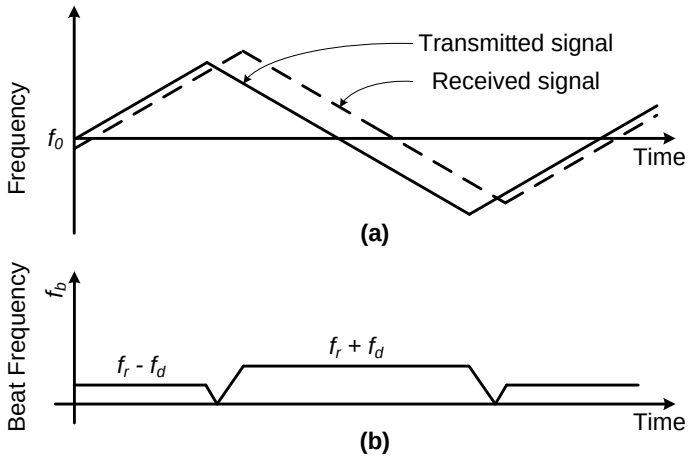

Figure 2.8 – Frequency-time relationships in FM-CW radar when the received signal is shifted in frequency by the Doppler Effect. (a) Transmitted (solid curve) and echo (dashed curve) frequencies; (b) Beat frequency [11]

2.3.4 Unambiguous Range and Range Resolution

The maximum unambiguous range is limited by the pulse repetition frequency f_m. This is the same for both pulsed and FM-CW radar and is given by [11]:

$$R_{unamb} = \frac{c}{2 f_m} \tag{2.13}$$

The bandwidth of the radar (Δf) determines the range resolution and is inversely proportional to it. A practical approximation for this is [11]:

$$\Delta R_{\min} > \frac{c}{2\Delta f} \tag{2.14}$$

2.3.5 Functional Block Diagram

As in the case of the CW radar system, Figure 2.2(a), the FM-CW system consists of a transmitter, two separate antennas for transmission and reception and a heterodyne receiver. The difference now is that the transmitter has a frequency modulator that modulates the signal frequency to the desired waveform before it is transmitted. The received signal is similarly heterodyned in the receiver to generate the beat frequency. The beat frequency is then amplified and limited to remove any amplitude fluctuations. The beat frequency is then measured with, for example, a frequency counter to determine the range. Figure 2.9 shows a block diagram of a typical FM-CW radar system.

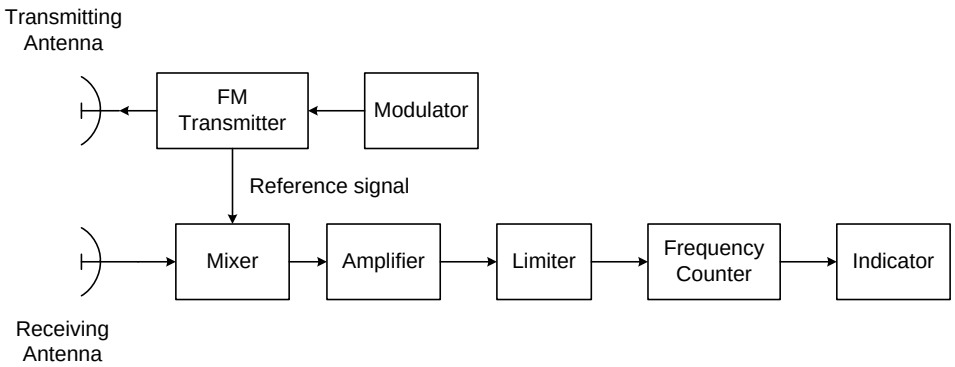

Figure 2.9 – Block diagram of a typical FM-CW radar [11]

2.3.6 Example of FM-CW radar in Aircraft Altimeter

The above block diagram is a basic form of a FM-CW radar system and various methods and additional components are used to improve on this system or used to modify the function thereof. An improved adaptation of this radar system is shown in Figure 2.10 which is used in aircraft altimeters.

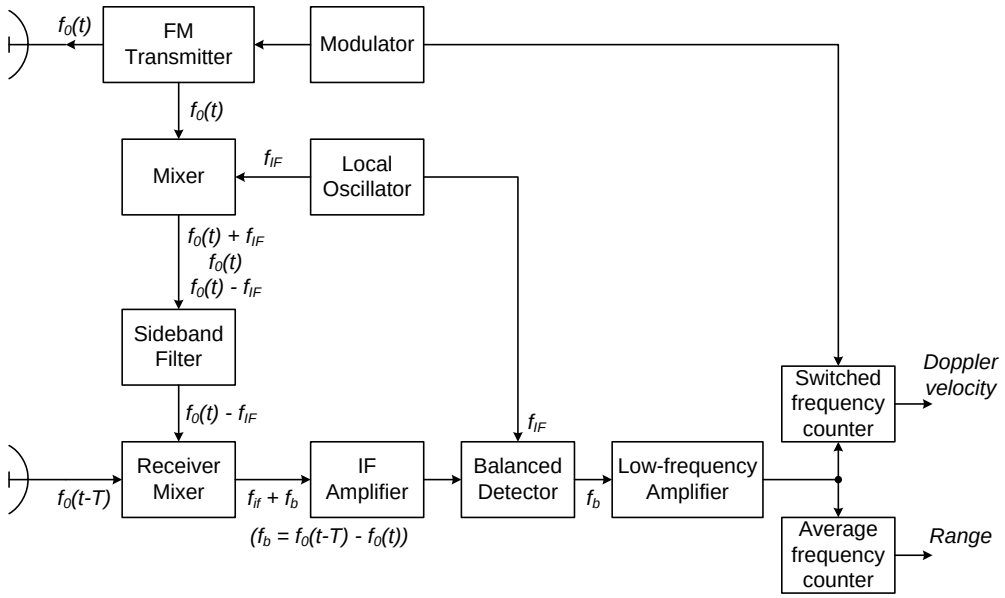

Figure 2.10 – Block diagram of FM-CW radar using sideband superheterodyne receiver [11]

An altimeter is used in aircraft to measure the height of the vehicle above the surface of the earth. The relative short distances and large radar cross section of the earth allows for low transmitter power and low antenna gain. The relative motion between the aircraft and the earth is small and therefore the Doppler frequency shift may usually be neglected.

Chapter 3

Antenna Design and Simulation

The first step taken in designing the radar system was to design the antennas. This chapter shows a number of antenna designs that were simulated and then their simulation results were compared.

For the purpose of modelling the antennas, a number of different designs were created. Each design was then simulated and certain specifications determined. There are four key parameters that needed to be determined from the model results and used for determining each antenna's effectiveness. These results are the antennas': Input Impedance, Reflection Coefficient (S_{11}), Coupling (S_{21}) and Gain.

For this project the frequency specifications for the design of the antennas were that the antennas must work within the 50 MHz to 350 MHz frequency band. They should also show quantifiable levels of coupling.

The software used for the antenna modelling was Computer Simulation Technology's (CST) Microwave Studio and FEKO. Both are fast and accurate 3D computational electromagnetic analysis software suites.

3.1 Modelling of the Antennas

The radar would consist of two separate transmit and receive antennas with the electronics and battery pack in between, as mentioned in Section 1.2.1. To fit into a borehole, the radar system had to be designed to fit into a cylinder of diameter 28mm and length 1800mm, as illustrated in Figure 3.1.

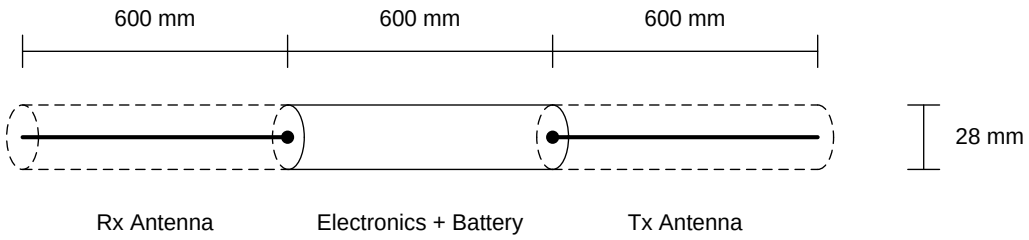

Figure 3.1 – Borehole radar design with dimensions

The design constraints of the radar system limited the antenna design so that each would fit into a cylinder of diameter 28mm and length 600mm. With this constraint on the design of the antennas, it was decided to design a dipole antenna as well as several variants thereof.

3.1.1 Dipole Antenna

Figure 3.2 shows the model for the dipole antenna.

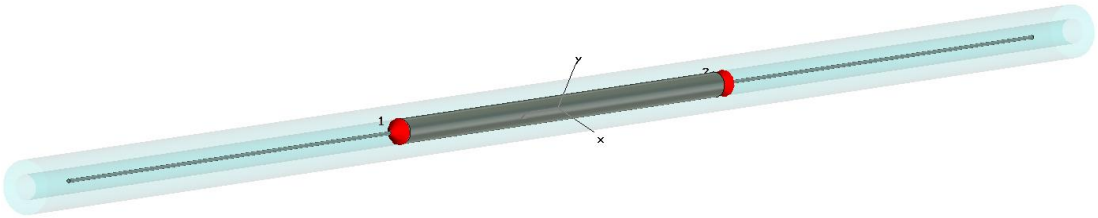

Figure 3.2 – CST model of Dipole Antenna

The dipole antenna model consists of two monopole antennas opposing each other in a single plane. The first monopole is fed with the signal and is used for the transmission of

signals, whereas the other acts as the receiver. This antenna configuration is called a Bullhorn Antenna.

3.1.2 Wu-King Antenna

The Wu-King antenna is a resistively-loaded dipole antenna. This means that instead of a solid wire monopole, it is instead interspersed with resistive elements. The values for these resistive elements increase exponentially the further they are placed from the feed. These values are an important variable in the design of the Wu-King Antenna. One of the purposes of modelling the antenna is to determine for what values of the resistive elements the best results can be obtained. Figure 3.3 shows the model for the Wu-King Antenna impedance.

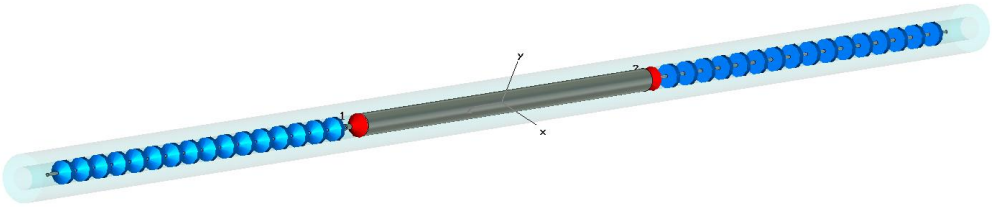

Figure 3.3 – CST model of Wu-King Antenna showing the interspersed resistive elements

In the antenna model used for this project, the resistive elements are given starting values that range from 58 Ohm to 1680 Ohm based on an available prototype model.

3.1.3 Folded Dipole Antenna

Figure 3.4 illustrates a Folded Dipole Antenna.

Figure 3.4 – FEKO model of the Folded Dipole

The folded dipole antenna design consists of two monopole antennas whose tips are folded back and terminated at the feed point, as illustrated in Figure 3.4. This antenna in its general form is compact in size, provides good signal gain and has a greater bandwidth compared to the dipole antenna. [19]

3.2 Simulation Results

This section details the results obtained from the simulation of the antennas.

3.2.1 Input Impedance

Figure 3.5 illustrates the input impedance results of the Dipole Antenna.

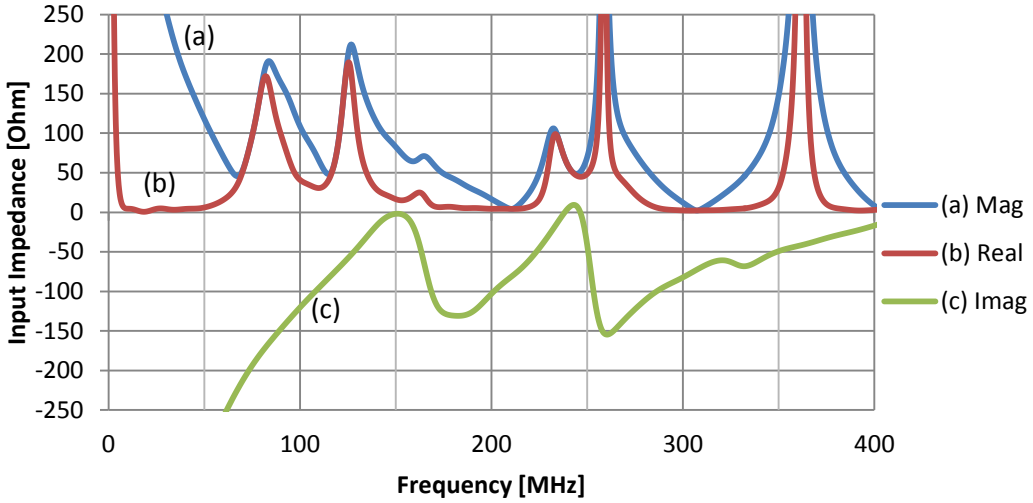

Figure 3.5 – Simulated input impedance of Dipole Antenna

Figure 3.6 illustrates the input impedance results of the Wu-King Antenna.

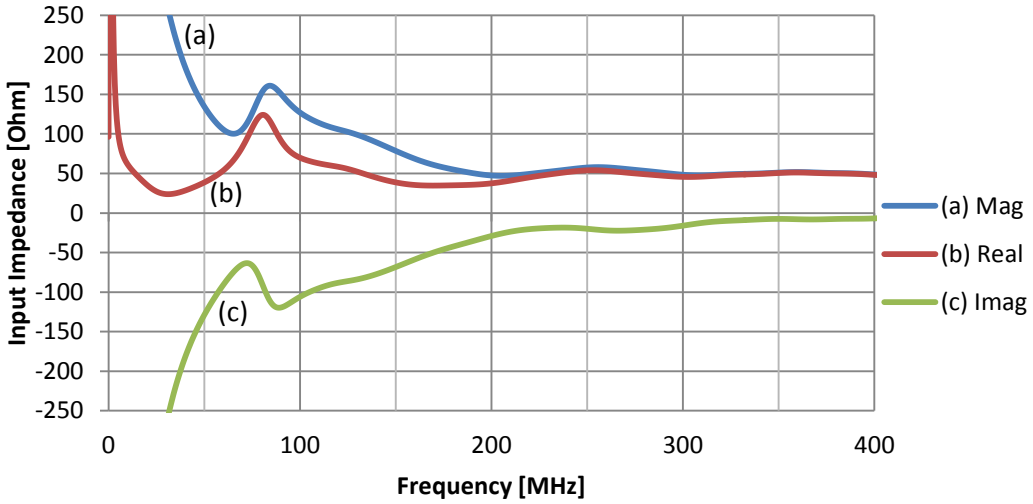

Figure 3.6 – Simulated input impedance of Wu-King Antenna

Figure 3.7 illustrates the input impedance results of the Folded Dipole Antenna.

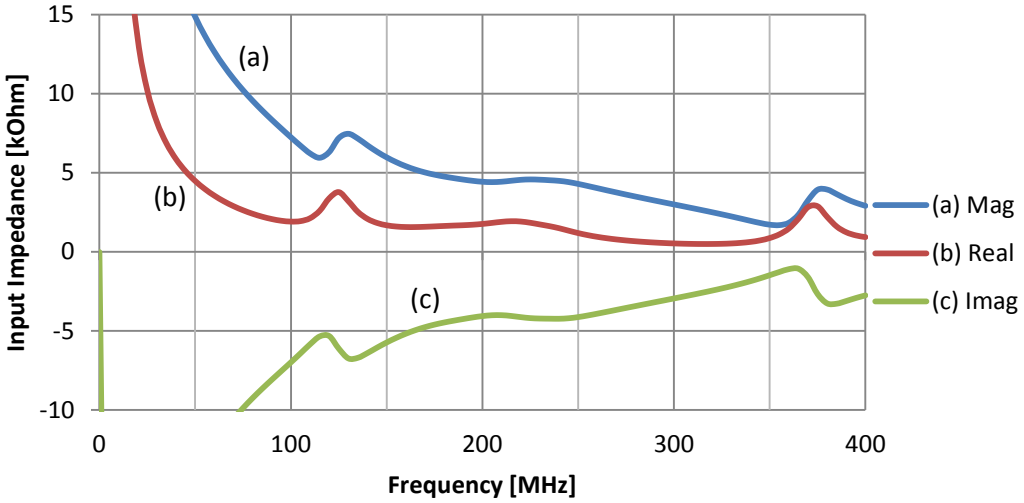

Figure 3.7 – Simulated input impedance of Folded Dipole Antenna

The nominal target value for the input impedance of the antennas is chosen as 50 Ohm so that the antenna is matched to standard amplifiers. From the results given in Figure 3.6 it can be seen that the input impedance stays relatively constant at 50 Ohm for the Wu-King antenna. None of the other antenna models besides the dipole comes close to the desired 50 Ohm. An impedance matching network can be used to reduce the impedance of the other antennas to 50 Ohm.

3.2.2 Reflection Coefficient (S_{11})

Figure 3.8 illustrates the reflection coefficient results for the Dipole Antenna.

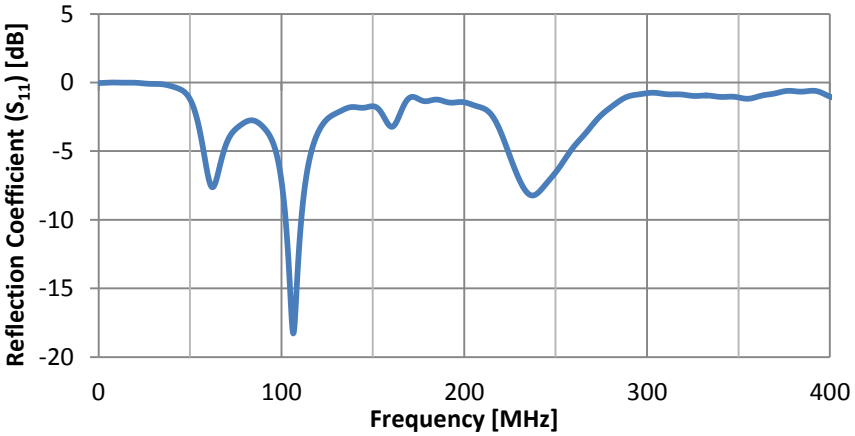

Figure 3.8 – Simulated reflection coefficient of Dipole Antenna

Figure 3.9 illustrates the reflection coefficient results for the Wu-King Antenna.

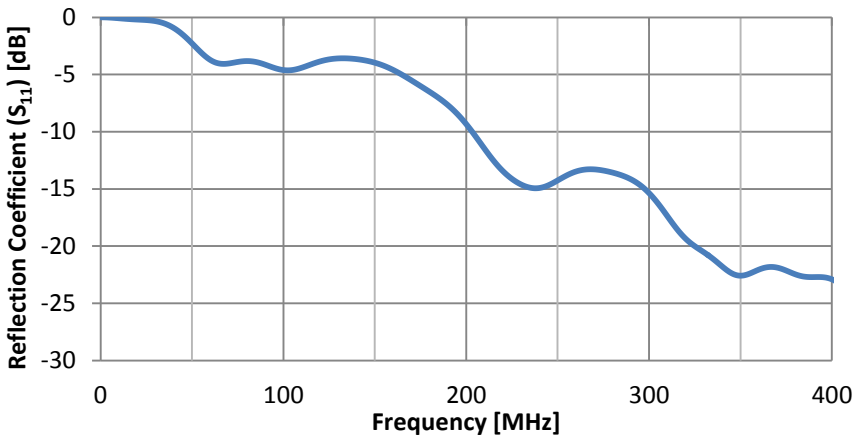

Figure 3.9 – Simulated reflection coefficient of Wu-King Antenna

Figure 3.10 illustrates the reflection coefficient results for the Folded Dipole Antenna.

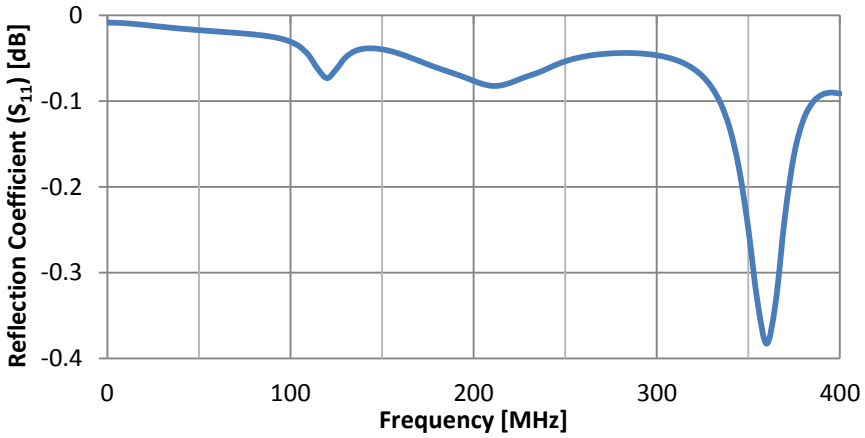

Figure 3.10 – Simulated reflection coefficient of Folded Dipole Antenna

The reflection coefficient of each antenna shows that they have different resonant frequencies. This is however not a crucial factor in the design of the antennas for this project. The only requirement is that the resonant frequency falls within the frequency band used in the radar system. Also, if necessary, a feed network can be designed to place the resonant frequency within the required frequency band. The results also show that the

simulated antennas' reflection coefficient are very poor, typically an S_{11} of below –10 dB is desired over the entire band.

3.2.3 Coupling (S_{21})

Figure 3.11 illustrates the coupling results of the Dipole Antenna.

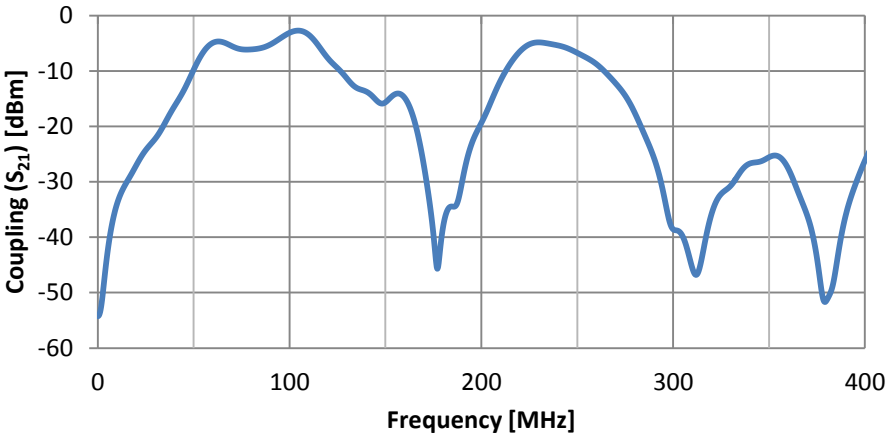

Figure 3.11 – Simulated coupling of Dipole Antenna

Figure 3.12 illustrates the coupling results of the Wu-King Antenna.

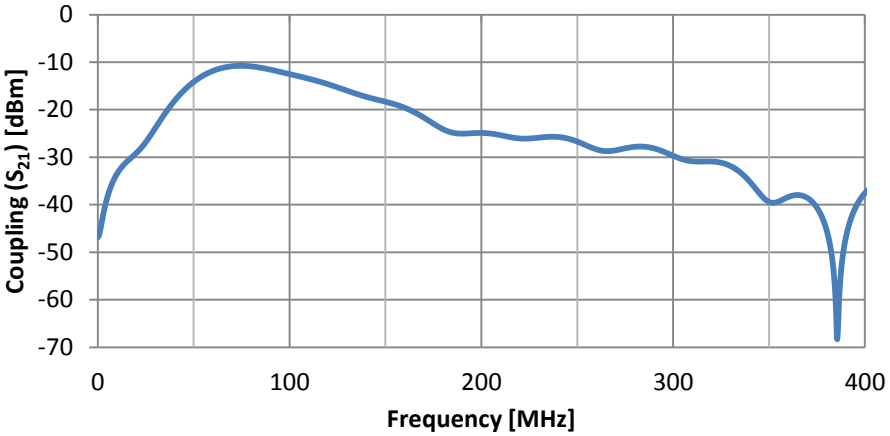

Figure 3.12 – Simulated coupling of Wu-King Antenna

Figure 3.13 illustrates the coupling results of the Folded Dipole Antenna.

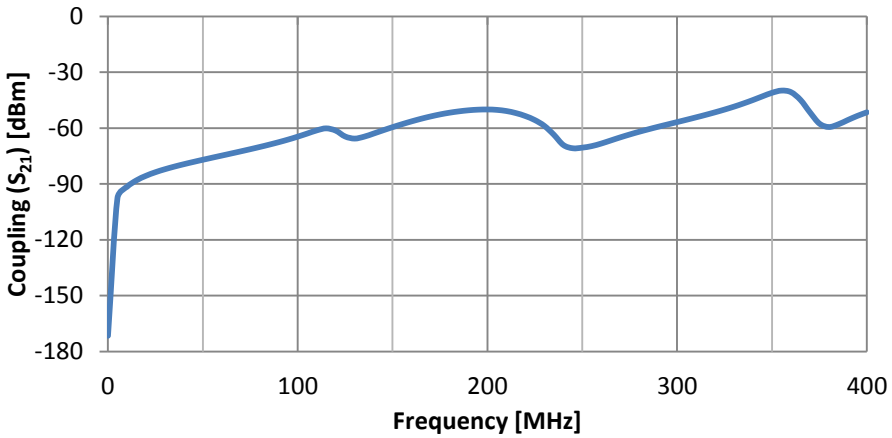

Figure 3.13 – Simulated coupling of Folded Dipole Antenna

The coupling of both the Dipole and Wu-King antennas, Figure 3.11 and Figure 3.12, is high and therefore undesirable. The folded dipole model has a much lower coupling value. A low coupling value is desired so that the transmitted signal does not interfere with the received signal.

3.2.4 Gain

Figure 3.14 shows the orientation of the antenna.

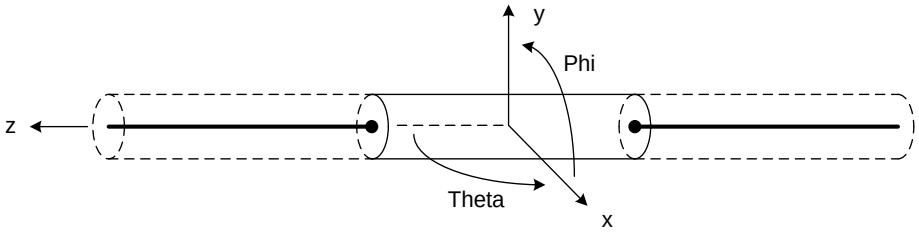

Figure 3.14 - Orientation of antenna

Figure 3.15 illustrates the maximum realized gain results that were calculated in the zx-plane, $Theta = 90^{\circ}$ and $Phi = 0^{\circ}$ for the Dipole Antenna.

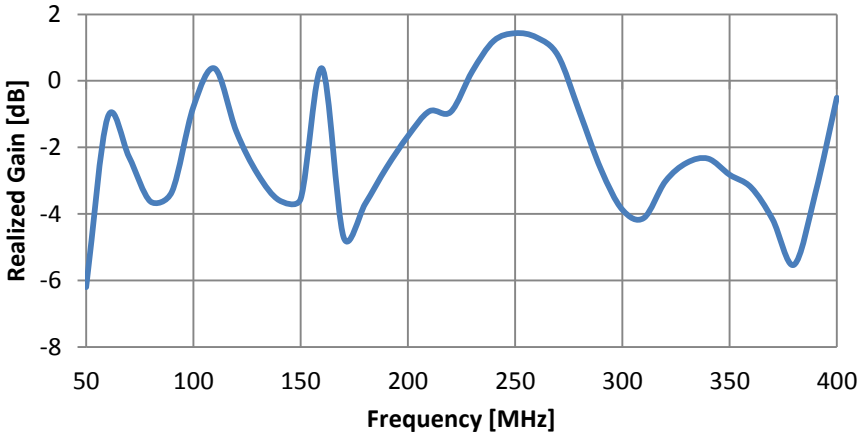

Figure 3.15 – Simulated realized gain of Dipole Antenna

Figure 3.16 illustrates the maximum realized gain results that were calculated in the zx-plane, $Theta = 90^{\circ}$ and $Phi = 0^{\circ}$ for the Wu-King Antenna.

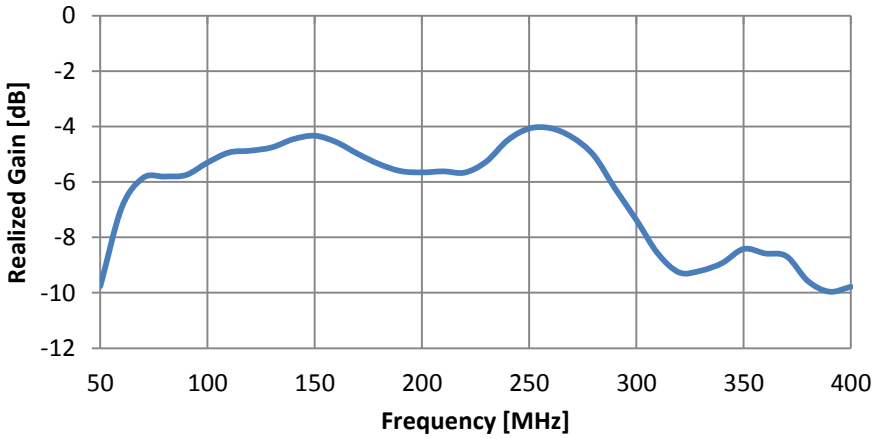

Figure 3.16 – Simulated realized gain of Wu-King Antenna

Figure 3.17 illustrates the maximum realized gain results that were calculated in the zx-plane, $Theta = 90^{\circ}$ and $Phi = 0^{\circ}$ for the Folded Dipole Antenna.

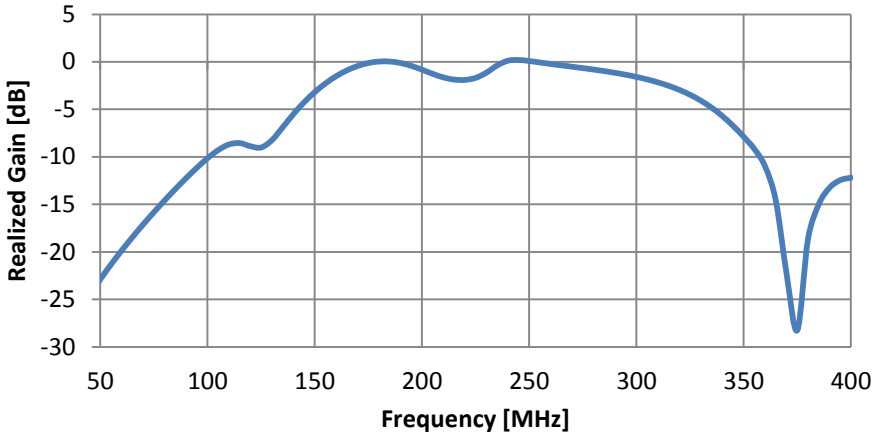

Figure 3.17 – Simulated realized gain of Folded Dipole Antenna

The max realized gain of all the simulated antennas are more or less the same but the Wu-King and Folded Dipole are flatter.

3.2.5 Conclusion

The antenna simulation results summarized in Table 3.1 show that each antenna design has its pros and cons.

Table 3.1 – Summary of Antenna Parameters

	Avg. S_{11} [dB]	Avg. S_{21} [dBm]	Avg. Gain [dB]
Dipole	-2.36	-21.3	-2.13
Wu-King	-13.9	-28.6	-6.45
Folded Dipole	-0.0692	-62.9	-12.5

Some antennas have a better gain than others, whereas another might have a wider or narrower bandwidth (which is better depends on the application) than the other. Relative easy methods could be employed to improve the impedance matching or the gain of a design, for example using impedance matching.

However the most important aspect of the antenna design for this project is the coupling between the transmit and receive antennas. The results in Section 3.2.3 show that the

Dipole and Wu-King antenna both have coupling levels of between -5 and -10 dB, which is very high and unacceptable for a normal radar system. The Folded Dipole antenna shows an improved coupling level of about -60 dB. The problem is that there is indeed still coupling present.

Other antenna designs were also examined and simulated to determine their levels of coupling. These also showed very high levels of coupling and would therefore also be rejected for use in a normal radar system. These antennas are derivations of the folded dipole in Section 3.1.3 but with different layouts. The simulation results are given in Appendix A.2.

Methods can be employed to improve, for example, the bandwidth or the impedance of an antenna, but the coupling between antennas cannot be resolved as easily. Not without redesigning the antenna entirely. Because of the design constraints of the radar system, the two antennas cannot be physically shielded from each other. The coupling would therefore never be zero when using a bi-static FM-CW radar system. A method to further reduce the coupling within the radar system needed to be examined.

Chapter 4

System Block Diagram Design

The original purpose of this project was to design a simplistic and inexpensive borehole-radar system. The radar would consist of separate transmit and receive antennas with the electronics and battery pack in between.

The radar system is of bi-static design and it can be expected that the performance of a short range system is adversely affected if the two antennas are not well "shielded" from each other. This adverse effect is caused by the transmitter leakage signal that enters the receiver due to the coupling between the antennas. Another method was needed to reduce the coupling between the antennas because of the physical constraints on the shape of the design, the two antennas could not be physically "shielded" from each other.

The first method that was looked at was to design the antennas so that their radiation patterns do not overlap at all or as little as possible, thus reducing the coupling between them. A number of antenna designs were simulated and their results compared. However it was found that the antennas were ineffective at limiting the effect of transmitter leak through and it was decided to pursue a second method proposed which is direct cancellation. From general control systems engineering it is known that a feedback loop can be used to reduce certain signals or parameters within a system and so an

implementation of such a feedback loop in the radar system was investigated to reduce the coupling between the antennas.

This chapter first briefly discusses the basic FM-CW radar system mentioned in Chapter 2 and then introduces the feedback loop to suppress the transmitter leakage signal. Additional features and components are added to this design concept in order to create a practical system that can be tested and measured to obtain results.

4.1 FM-CW Radar Sub-Systems

The block diagram of an FM-CW radar system consists of a signal generator, transmitter circuitry, the transmit and receive antennas, receiver circuitry and some kind of indicator. Figure 4.1 shows a diagram of such a basic FM-CW radar system.

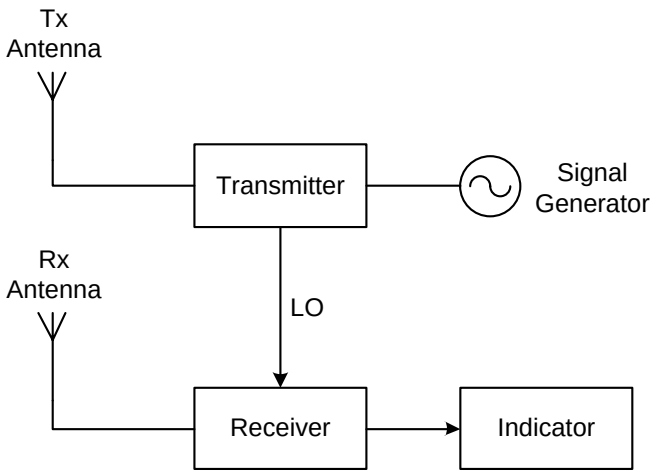

Figure 4.1 – Concept of a basic FM-CW radar system

4.1.1 Signal Generator

The signal generator is used to generate the FM-CW signal. This device should be capable of frequency modulation, i.e. it should be able to sweep the frequency of its output signal.

4.1.2 Transmitter

The purpose of the transmitter is to amplify the generated signal to the desired power level. In the case of FM-CW radar, the transmitted signal is also used as the local oscillator (LO) signal that is used for mixing the received (RF) signal. Therefore the transmitter circuitry also splits the transmit signal.

4.1.3 Receiver

The function of the receiver is divided into the following three steps:

- It amplifies the low-power RF signal without adding any excess noise to it.
- Then it mixes the RF signal with the LO signal to form the intermediate frequency (IF) signal.
- Lastly, it filters out any unwanted frequency components and noise within the signal.

This type of receiver is known as a superheterodyne receiver.

4.1.4 Indicator

The indicator is the term adopted here for the device that is used to extract information from the radar signal. In this case, it should extract range information and the Doppler frequency shift from the signal.

4.2 Basic Radar System

Section 4.1 only outlines a concept of the radar system and components need to be chosen to make this a practical system. Figure 4.2 shows the basic radar design implemented with practical components.

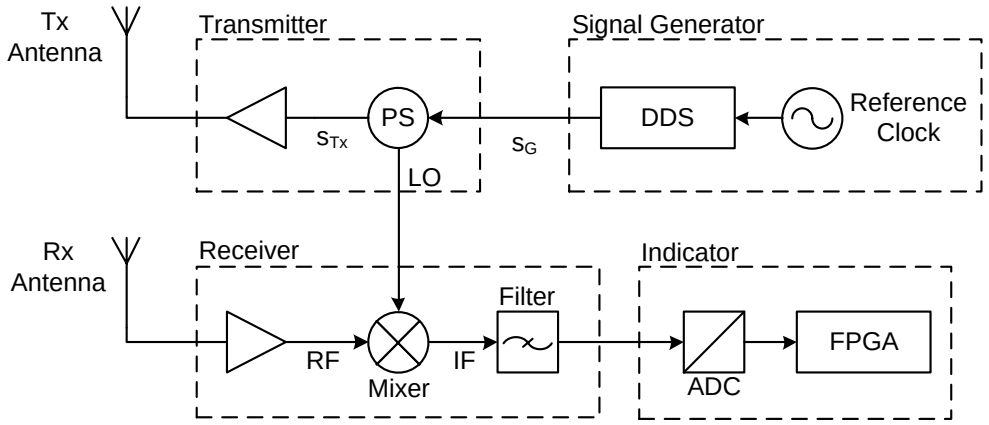

Figure 4.2 – Basic radar design with components

4.2.1 Signal Generator

A direct digital synthesizer (DDS) with frequency sweeping capability is used to generate the FM-CW signal. A 1GHz reference clock drives the internal clock of the DDS that enables it to generate frequencies of 400+ MHz. [20]

The FM-CW signal was chosen to have a bandwidth of 300 MHz and a sweep time of 20 us. This would give the radar a maximum unambiguous range of 3000 m and a range resolution of 0.5 m in air.

4.2.2 Transmitter

A power splitter, abbreviated as PS in Figure 4.2, splits the generated signal (S_G) into the transmit signal (S_{Tx}) and the LO signal that enters the mixer in the receiver. The amplifier in the transmitter is used to amplify the transmit signal to the desired power level before it is transmitted by the transmit (Tx) antenna.

4.2.3 Receiver

The receiver circuitry first amplifies the low-power RF signal to a desired power level; this is done with a low-noise amplifier (LNA) to reduce the noise that can be added to the

signal. The RF signal is then down-mixed, or down-converted, using a mixer and the LO signal to form the IF signal. The IF signal is then filtered to remove unwanted frequency components from the signal before it is sent to an indicator. This IF filter should compensate so that far and near targets have the same signal amplitude.

4.2.4 Indicator

In this project the indicator used is a field-programmable gate array (FPGA) device and therefore the analog radar signal has to be converted to a digital signal with an analog to digital converter (ADC).

4.3 Quadrature Modulation

The next step in implementing the design of the system was to add quadrature modulation to the receiver. Quadrature modulation is used to retain the received signal's phase information that is used to determine the sign of the Doppler frequency. The sign of the Doppler frequency indicates the direction of the target's motion.

To determine the sign of the Doppler frequency, the LO signal from the transmitter is split into two channels. The first channel is processed the same way as in the simple radar system of Figure 4.2. The second channel is processed similarly, except for a 90° phase shift introduced into the LO signal. The signal in the first channel is called the in-phase ("I") signal and the second the quadrature ("Q") signal. Figure 4.3 shows the concept of quadrature modulation and how the mixing of these I and Q signals with the RF signal forms the IF_I and IF_Q signals. (The same result can be obtained when phase shifting the RF signal by 90° instead of the LO.)

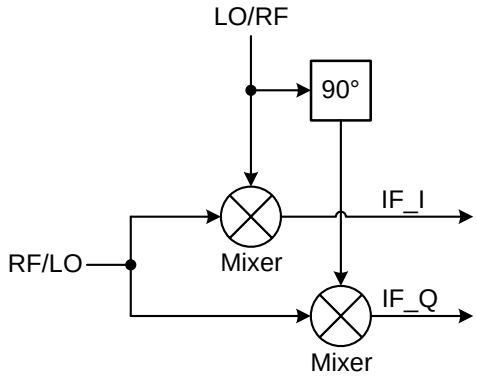

Figure 4.3 – Quadrature Modulation concept

To implement quadrature modulation, a component was needed to split the LO or RF signal into the I and Q signals. This is done by using a polyphase quadrature filter (PQF), which is the PQF component at the input of the receiver in Figure 4.4. Components have been added to the receiver to split the LO signal and to process both the I and Q channel signals. The indicator also now possesses an ADC with two channels to convert the IF_I and IF_Q channels separately. Section 5.3 describes the PQF component in further detail as well as its design.

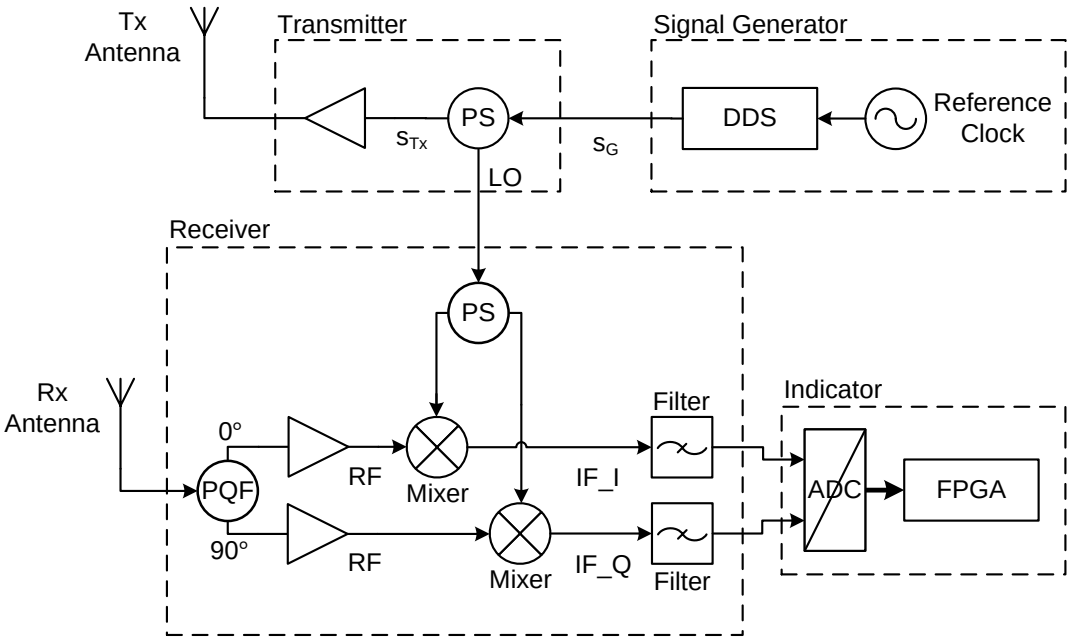

Figure 4.4 – Radar system with Quadrature Modulation

To determine the sign of the Doppler frequency, one must first look at the signals. If the transmit signal, and therefore the LO signal, is given by

$$LO(t) = E_0 \cos(\omega_0 t) \tag{4.1}$$

The RF signal from a moving target will be

$$RF(t) = k_1 E_0 \cos[(\omega_0 \pm \omega_d)t + \phi] \tag{4.2}$$

Where, E_0 = amplitude of transmitter signal,

k_1 = a constant determined from the radar equation,

ω_0 = angular frequency of transmitter,

ω_d = Doppler angular frequency shift,

ϕ = a constant phase shift, which depends on range of initial detection.

The difference signal, in other words the IF signal after filtering the mixed LO and RF signals, in the I channel (IF_I) is given by [14]

$$I(t) = k_2 E_0 \cos[\pm\omega_d t + \phi] \tag{4.3}$$

The difference signal in the Q channel (IF_Q) is given by [14]

$$Q(t) = k_2 E_0 \cos[\pm\omega_d t + \phi + \pi/2] \tag{4.4}$$

If the target is approaching (positive Doppler), the signals from the two channels are [14]

$$I(t)^+ = k_2 E_0 \cos[\omega_d t + \phi] \quad Q(t)^+ = k_2 E_0 \cos[\omega_d t + \phi + \pi/2] \tag{4.5}$$

On the other hand, if the targets are receding (negative Doppler) [14],

$$I(t)^{-} = k_2 E_0 \cos[\omega_d t - \phi] \quad Q(t)^{-} = k_2 E_0 \cos[\omega_d t - \phi - \pi/2] \tag{4.6}$$

The sign of the Doppler shift, and hence the direction of the target is determined by noting the phase relationship between I(t) and Q(t). [14]

Q(t) is $\pi/2$ slower with respect to I(t), therefore $\omega_d > 0$

Q(t) is $\pi/2$ leading with respect to I(t) , therefore $\omega_d < 0$

4.4 Feedback

To reduce the coupling (Tx leakage) signal in the system, a negative feedback loop was suggested. A signal is generated from the receiver output of equal amplitude but opposite phase and then fed back into the receiver path. This section details the approach taken to design the feedback loop as well as the simulation and implementation thereof.

4.4.1 Approach to Coupling Reduction

The approach taken to reduce the Tx leakage signal within the system was to implement a negative feedback loop within the receiver. A copy of the receiver output is fed back into the input of the receiver. This copy should be of equal or greater amplitude but opposite phase to that of the input signal. This feedback loop would adaptively reduce the Tx leakage signal added to the received signal due to the coupling between the Tx and Rx antennas. A block diagram of the proposed feedback loop is given in Figure 4.5.

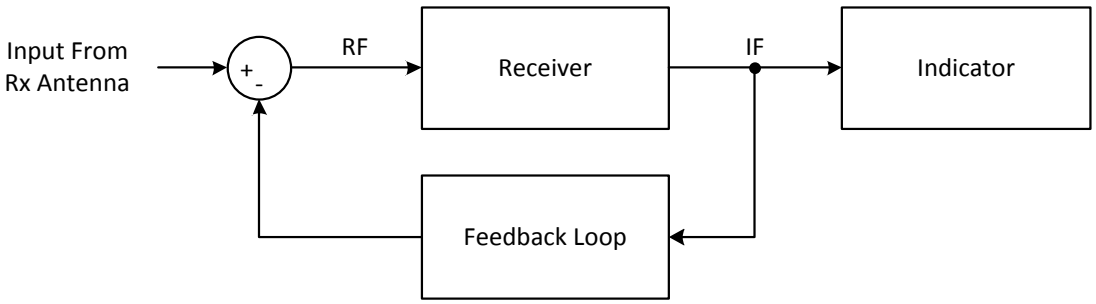

Figure 4.5 – Block diagram showing feedback loop

Placing a high-pass filter in the receiver chain with a cut-off frequency above that of the transmitter leakage signal would suppress it, but this is not a practical solution. The transmitter leakage signal is so large that it could possibly over-drive the receiver, meaning that the LNAs in the receiver would saturate. Placing a low-pass filter in a negative feedback loop would have the same effect of suppressing low frequencies as the high-pass filter. It would also adaptively reduce the size of the received signal so as not to over-drive the receiver.

The idea for the negative feedback loop was adapted from the application of the reflected power canceller (RPC) in the Bofors/Signaal "PILOT", FM-CW tactical navigation radar. [21] [22] Figure 4.6 shows a block diagram of the RPC implemented in the PILOT radar.

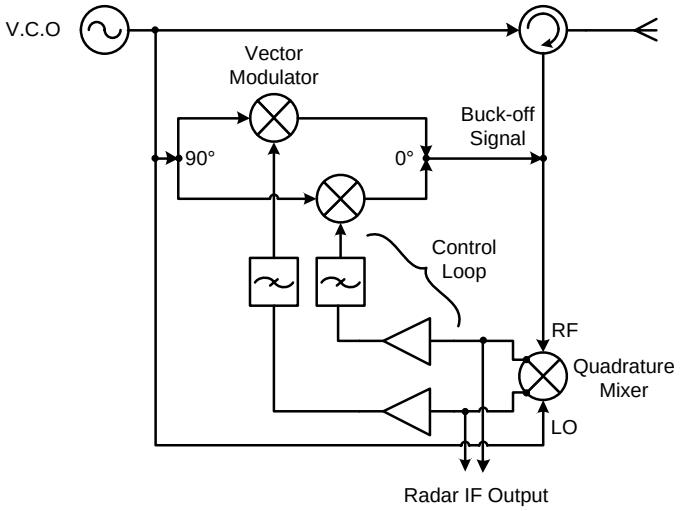

Figure 4.6 –Diagram of RPC in PILOT radar [21]

A similar approach to the RPC above was also considered for this project, but this approach employs digital cancellation [23] [24], as illustrated in Figure 4.7.

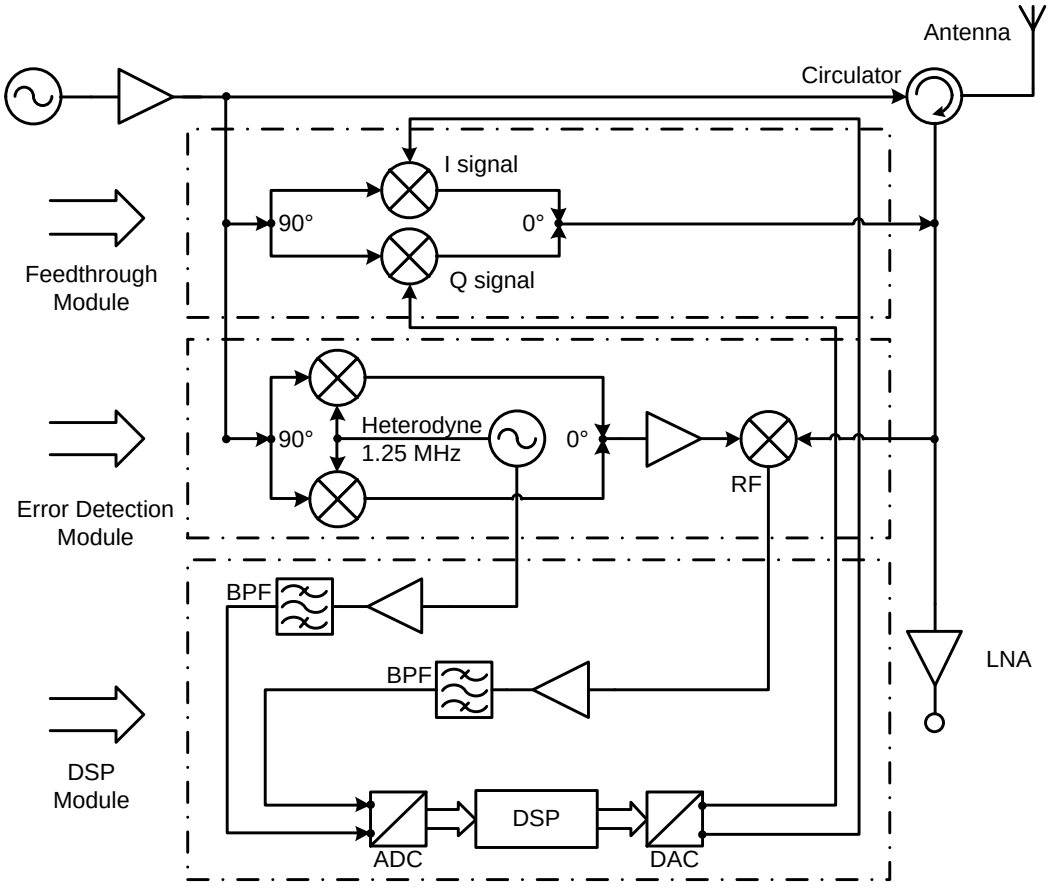

Figure 4.7 – Diagram of digital leakage cancellation scheme [23]

From the above two RPC schemes a design was created for this project to implement the concept of a negative feedback loop. A block diagram showing the design of the feedback loop to be used in this project is shown in Figure 4.8. For the purpose of explaining the feedback loop as part of the receiver, the block diagram shows a simplified circuit without the quadrature modulation.

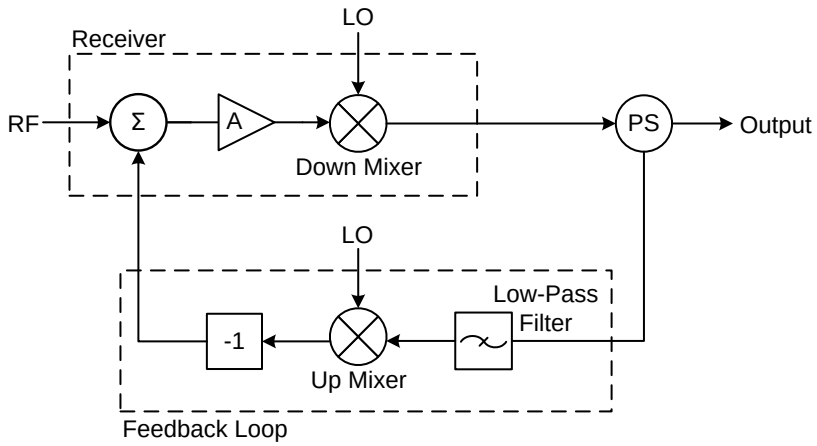

Figure 4.8 –Diagram of receiver with feedback loop showing components

The RF signal from the antenna is first amplified; this controls the gain of the feedback loop and consequently the amount of transmitter leakage suppression of the system. The signal is then mixed down to baseband with a copy (LO signal) of the transmitted signal.

The feedback loop takes a copy of the receiver output signal and filters out all frequency components above baseband. This feedback filter controls the frequency range of the suppression in the system. Any "target" signal found below the cut-off frequency of the feedback filter, will be suppressed. More importantly it will suppress the transmitter leakage signal. Therefore this filter controls the minimum range of the radar.

The feedback signal is then mixed back up to the original bandwidth of the system and is made negative with respect to the original signal.

The transmitter leakage signal appears as a close-in "target" in the frequency spectrum of the output of the radar system. For example, if the two antennas are place 0.6m apart, the coupling signal appears as a "target" at 30 kHz in the Fourier transformed space as can be seen in Figure 4.9 and Figure 4.10.

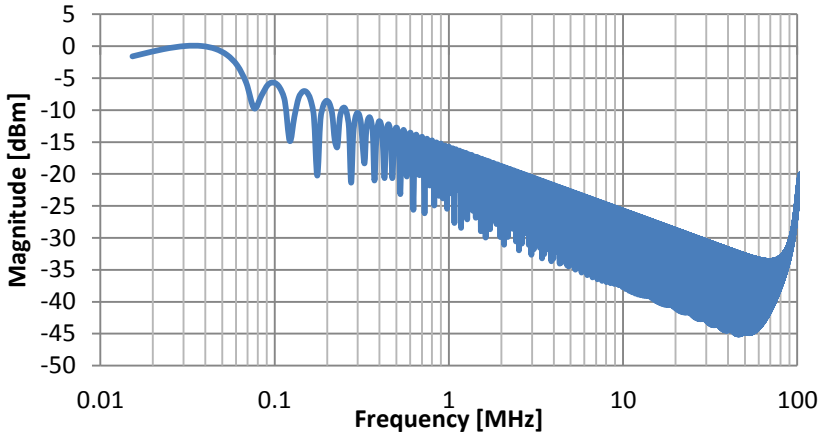

Figure 4.9 – Frequency spectrum of receiver without feedback showing coupling signal. See Figure 4.10 for low frequency detail

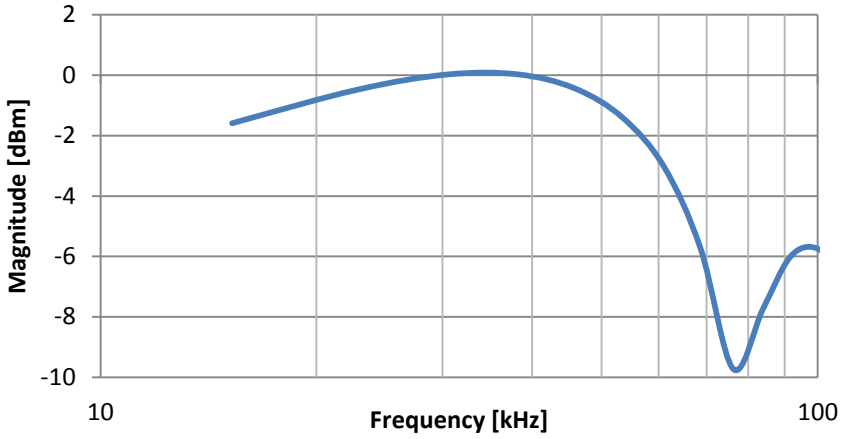

Figure 4.10 – Zoomed-in view of Figure 4.9

The placement of the two antennas at a distance d apart gives a signal time delay of τ. This time delay can be determined by Equation (4.7) [11].

$$\tau = \frac{d}{c} \tag{4.7}$$

Where, τ = time delay in seconds,

d = distance in meters,

c = speed of light.

The frequency at which such a signal with this time delay will appear can be determined by Equation (4.8) [11].

$$F_{\tau} = \frac{\tau \times F_{sweep}}{T_{sweep}} \tag{4.8}$$

Where, F_{τ} = frequency at which the signal appears due to time delay,

F_{sweep} = frequency sweep of FM-CW transmitter (in this case 300 MHz),

T_{sweep} = sweep length of FM-CW transmitter (in this case 20 us).

Figure 4.11 shows how the feedback loop is integrated into the radar system including both I and Q channels.

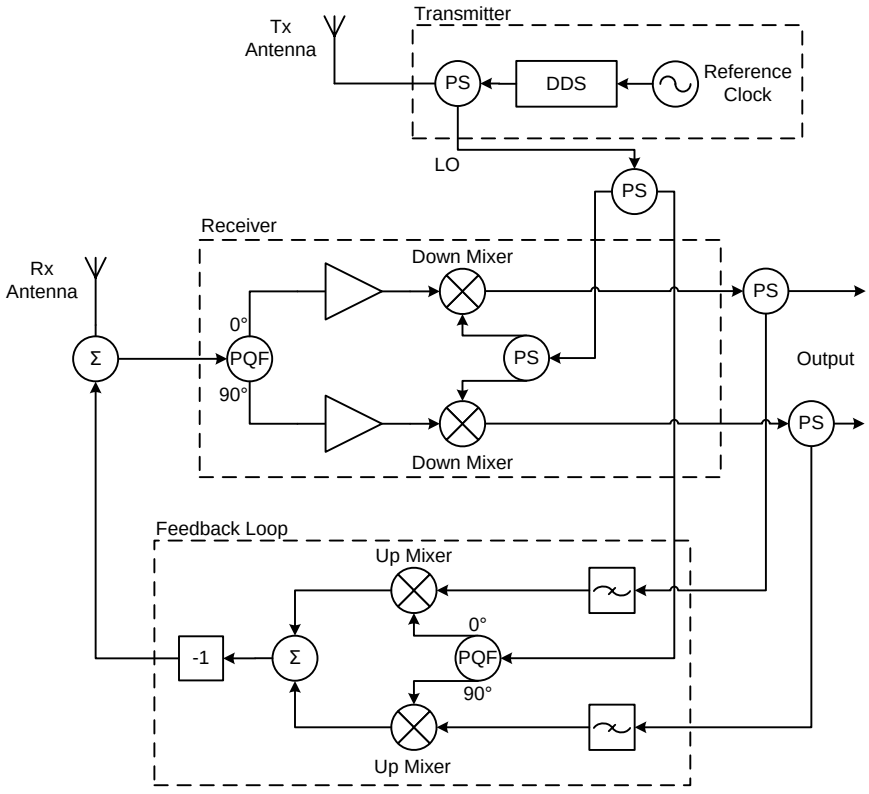

Figure 4.11 – Diagram of radar system that includes the quadrature modulation and feedback loop

The block diagram of Figure 4.12 is a simplified form of the diagram in Figure 4.8.

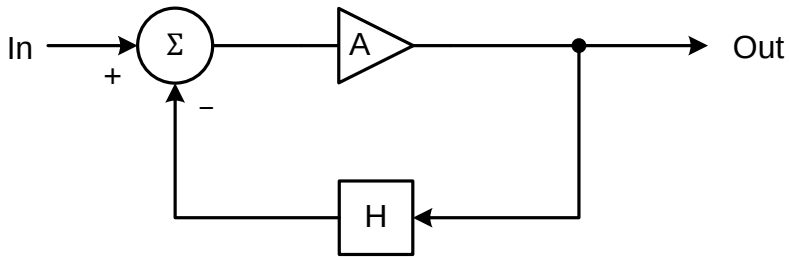

Figure 4.12 – Simplified block diagram of the feedback loop

The transfer function, *G*, of the feedback loop in Figure 4.12 is given by the following equation:

$$G = \frac{Out}{In} = \frac{A}{1 + AH} \tag{4.9}$$

Where, *In* = input signal,

Out = output signal,

A = amplification,

H = transfer function of the low-pass filter.

The frequency response of an n[th] order Butterworth filter, the low-pass filter *H*, is in the form of [25]:

$$H(\omega) = \frac{1}{1 + \left(\omega / \omega_{LPc}\right)^{n}} \tag{4.10}$$

Where, ω_{LPc} = 3dB low-pass cut-off frequency,

n = order of the filter.

Therefore, the transfer function of Equation (4.9) becomes:

$$G = \frac{A}{1 + A\left[\frac{1}{1 + \left(\omega / \omega_{LPc}\right)^{n}}\right]}$$
$$\approx \frac{A}{1 + A\left[\frac{1}{\left(\omega / \omega_{LPc}\right)^{n}}\right]} \qquad \because \omega \gg \omega_{LPc} \tag{4.11}$$
$$= \frac{A}{1 + \left(\frac{\omega}{(A)^{1/n}\,\omega_{LPc}}\right)^{-n}}$$

The new transfer function is now in the form of a high-pass filter [25]:

$$H_{HPF}(\omega) = \frac{1}{1 + \left(\omega / \omega_{HPc}\right)^{-n}} \tag{4.12}$$

Where, ω_{HPc} = 3dB high-pass cut-off frequency.

Therefore the new "cut-off frequency" for the feedback loop is:

$$\omega_{HPc} = (A)^{1/n}\,\omega_{LPc} \tag{4.13}$$

Equation (4.13) indicates that the amplifier A contributes to the high-pass cut-off frequency ω_{HPc}. To determine the value of the amplifier, in dB, the following equation can be used:

$$A_{dB} = 20\log_{10}\left(\left(\frac{\omega_{HPc}}{\omega_{LPc}}\right)^{n}\right) \qquad (4.14)$$

For example, using a 4th order Butterworth low-pass filter with $\omega_{LPc} = 30kHz$ and a 40dB amplifier will give the feedback loop a high-pass cut-off frequency of $\sim 100kHz$.

4.4.2 Simulation

A simulation of the simplified block diagram in Figure 4.12 has been written using MATLAB. A copy of the MATLAB code is attached in Appendix A.4.

The parameters of the components of the simulated feedback loop are as follows:

- A = 40 dB Amplifier
- H = 4th Order Butterworth low-pass filter with a cut-off frequency of 30 kHz

The frequency response of the low-pass filter H, Equation (4.10), which forms part of the feedback loop, is plotted in Figure 4.13.

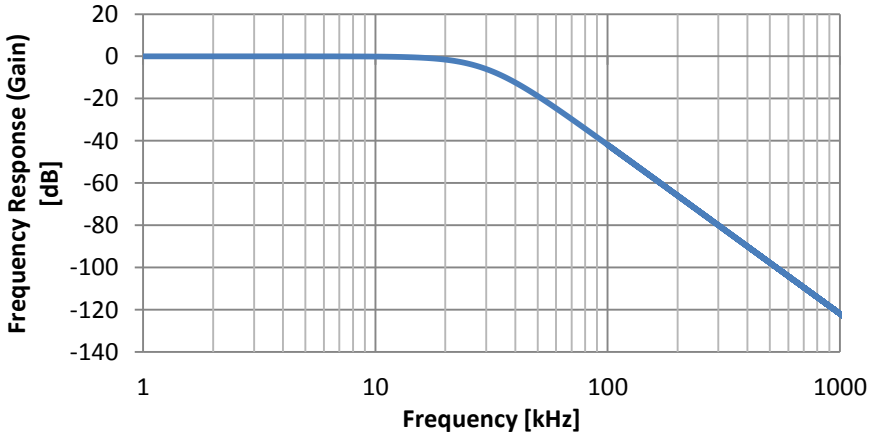

Figure 4.13 – Simulated frequency response of the low-pass filter

This shows that the filter has a 3 dB cut-off frequency at 30 kHz and a slope of 80 dB per decade which is expected of a 4th order Butterworth filter.

Next, the frequency response of the feedback loop is calculated and displayed in Figure 4.14.

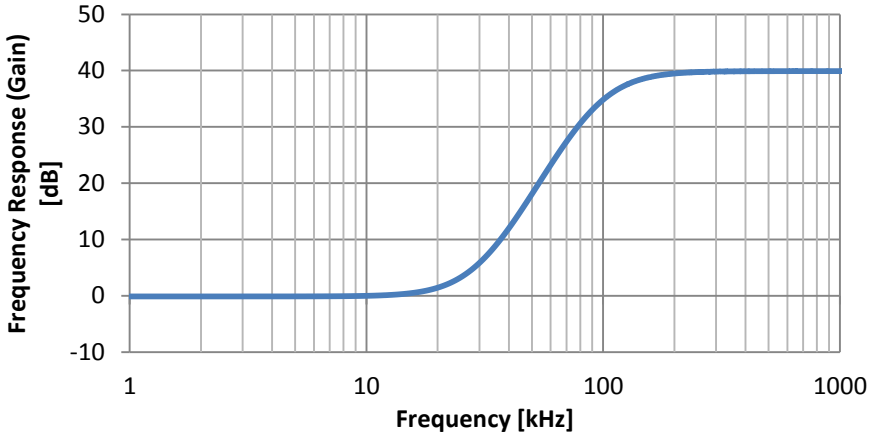

Figure 4.14 – Simulated frequency response of the feedback loop

From Figure 4.14 it can be seen that the feedback loop now responds more-or-less like a high-pass filter. The upper "cut-off" frequency is determined to be at ~100 kHz and the lower is that of the low-pass filter, namely 30 kHz. What this means is that any signal passing through the feedback loop with a frequency below 100 kHz will not be amplified by the 40 dB amplifier, in effect it would be suppressed.

Figure 4.15, Figure 4.16 and Figure 4.17 show the simulated output of the feedback loop with a test signal with varying frequencies applied to the loop. In each figure:

(a) Represents the output signal where the loop has been opened, therefore no feedback is present and the signal is only amplified.
(b) Represents the output signal where the loop is closed.
(c) Represents the frequency response of the closed-loop feedback circuit.

In each figure can be seen that the output signal, where the feedback loop is closed, (b), closely follows the closed loop response.

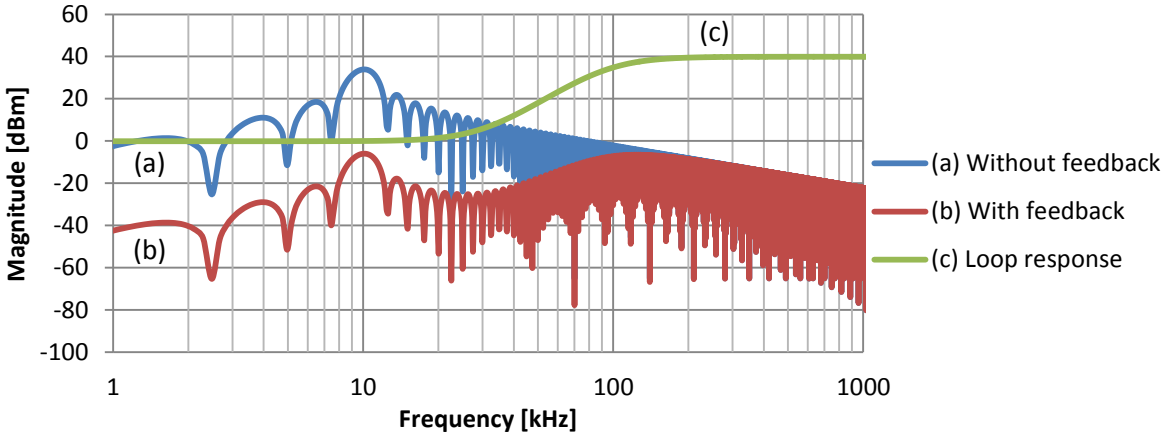

Figure 4.15 – Simulated output of feedback loop. Input test signal at 10 kHz

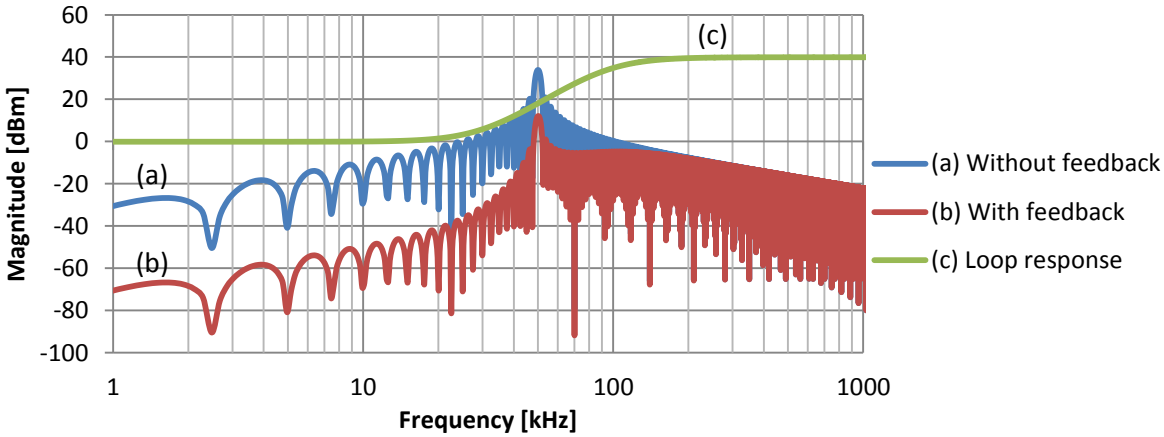

Figure 4.16 – Simulated output of feedback loop. Input test signal at 50 kHz

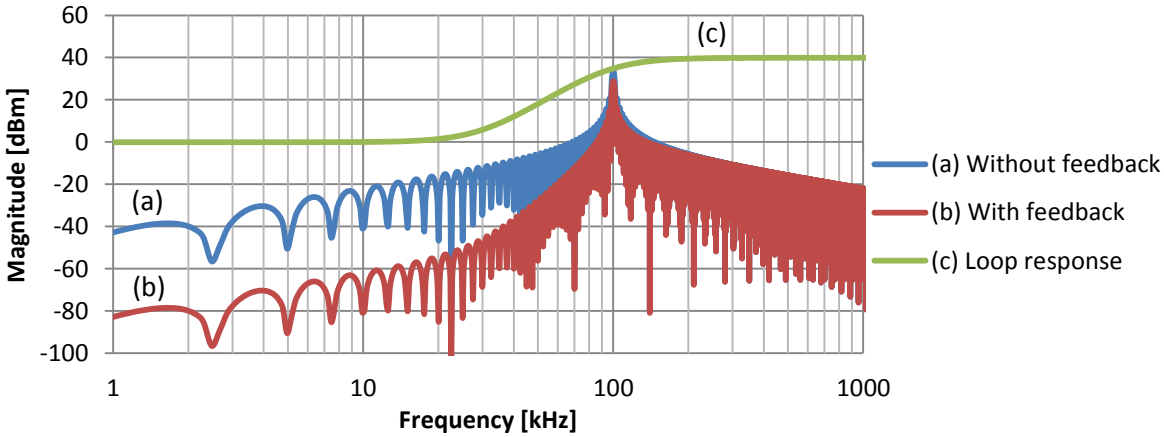

Figure 4.17 – Simulated output of feedback loop. Input test signal at 100 kHz

In conclusion, the simulation and the above results confirm that the feedback loop is an acceptable method to reduce the coupling within a radar system.

4.4.3 Hardware Implementation

Now that the design for the feedback loop was completed and it was determined from the simulation that it is effective at coupling cancellation, the hardware implementation can be started. Again, for explanation of the feedback loop, the quadrature modulation was left out.

Figure 4.18 shows a block diagram of the hardware setup including the feedback loop.

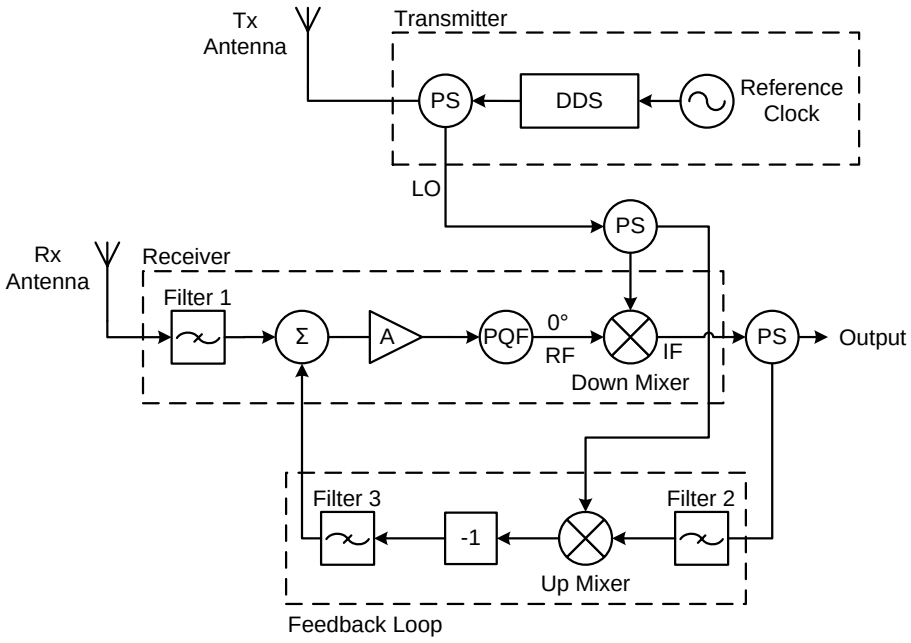

Figure 4.18 –Diagram of radar system with feedback (showing only one channel)

Filter 1 is a low-pass filter with a cut-off frequency of 355 MHz. It is used to remove any frequency components received by the Rx antenna not within the bandwidth of the system. The amplifier marked A is a 40 dB amplifier and forms the feedback gain of the loop. Filter 2 is the baseband low-pass filter with a cut-off frequency of 30 kHz. It removes the $f_{RF}+f_{LO}$ component created by the mixer in the receiver. Filter 3 is a low-pass filter with a cut-off frequency of 355 MHz and is used to remove frequency components not in the system

bandwidth and to improve the symmetry of the receiver input. The results of the feedback loop are given and discussed in Chapter 6.

Chapter 5

System Component Implementation

In this chapter the block diagram developed in Chapter 4 is broken down into its individual components. Each of these is discussed separately with suitable components being chosen to implement each. Each component is then tested and their results are presented.

5.1 Direct Digital Synthesizer

A direct digital synthesizer (DDS) is a type of frequency synthesizer that is digitally controlled, "programmed", to generate a frequency- and phase-tuneable analog waveform. A basic DDS consists of a reference clock, a register map, numerically controlled oscillator (NCO) and a digital-to-analog converter (DAC). [26]

Figure 5.1 provides a functional diagram of a basic Direct Digital Synthesizer.

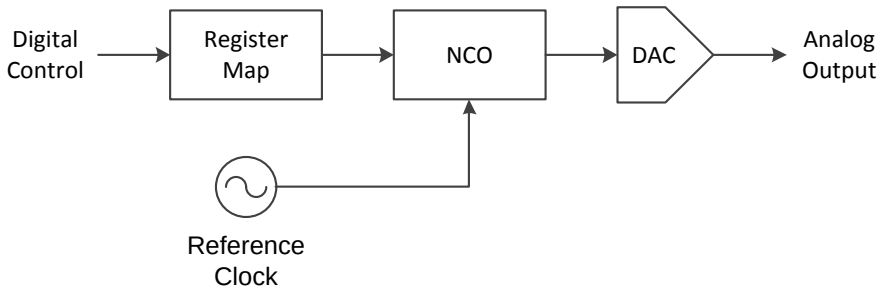

Figure 5.1 – Functional diagram of basic Direct Digital Synthesizer [26]

The NCO is controlled by programming a Frequency Tuning Word (FTW) and a Phase Offset Word (POW) into the register map. These two Words control the frequency and phase of the output waveform respectively.

The DDS chosen for this project is the AD9910 from Analog Devices. This device has the ability to linearly sweep the frequency of the output waveform in reference to time. This allows the device to create the FM-CW signal used in the radar system.

The linear frequency sweep is accomplished by programming a Delta- Frequency Tuning Word (DFTW) and Delta- Frequency Ramp Rate Word (DFRRW) into the register map. These two Words control the Δf and Δt in Figure 5.2.

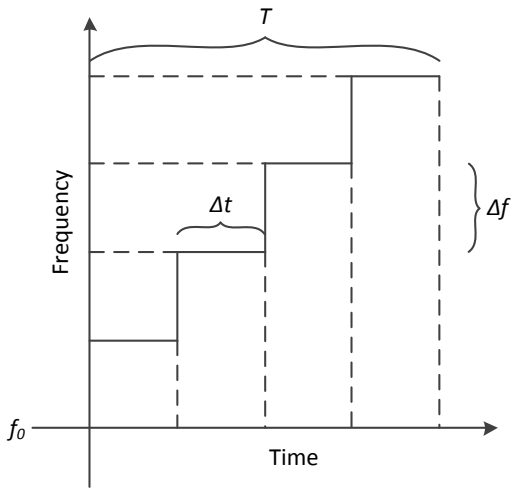

Figure 5.2 – Graph showing how a Linear Frequency Sweep is accomplished

After a period of time Δt the DDS increases the frequency of the output waveform by Δf. This is repeated until a time of T has passed and the frequency is restored to the value stored in the FTW register.

The equations for the FTW, DFTW and DFRRW are as follows [20]:

$$f_O = \frac{(FTW \times SYSCLK)}{2^N} \tag{5.1}$$

$$T = \frac{|f_F - f_S| \times 2^{34}}{SYSCLK^2} \times \frac{DFRRW}{DFTW} \tag{5.2}$$

$$\Delta f = \frac{DFTW \times SYSCLK}{2^{31}} \tag{5.3}$$

$$\Delta t = \frac{8 \times DFRRW}{SYSCLK} \tag{5.4}$$

Where, f_O = output frequency of the waveform,

FTW = Frequency Tuning Word,

$SYSCLK$ = system clock,

N = number of bits of the DDS (32 in the case of the AD9910),

T_{sweep} = period of the linear sweep,

f_F = frequency at which the linear sweep stops,

f_S = frequency at which the linear sweep starts,

$DFRRW$ = Delta- Frequency Ramp Rate Word,

$DFTW$ = Delta- Frequency Tuning Word,

Δf = frequency step of the linear sweep,

Δt = time step of the linear sweep.

The SYSCLK is the clock at which the DDS runs and is controlled by the reference clock. Once a decimal value for the FTW, DFTW and DFRRW has been calculated, it must be rounded to an integer and converted to a 32-bit binary value.

The FTW is a 32-bit integer and the POW a 16-bit integer. This allows for a frequency resolution of ~0.23Hz and phase resolution of 0.022°. The AD9910 is capable of generating frequencies of 400+ MHz when driven at a 1GHz internal clock speed (SYSCLK).

Figure 5.3 illustrates the measured output signal of linear sweep enabled DDS.

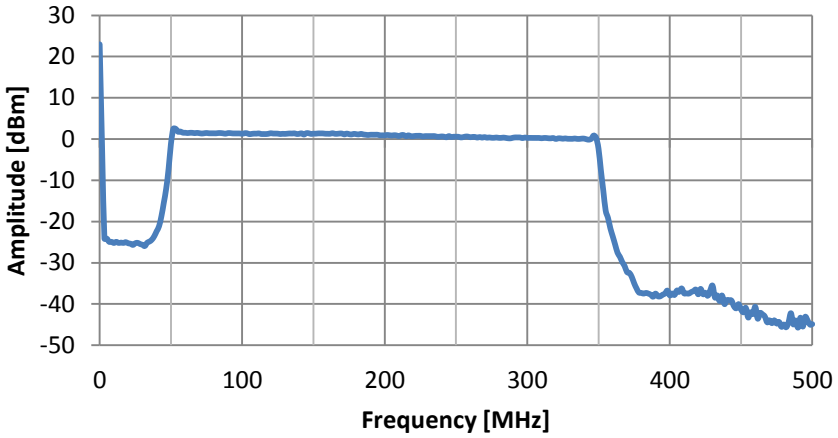

Figure 5.3 – Measured output signal of linear sweep enabled DDS

5.1.1 Reference Clock

The DDS needs a 1 GHz reference clock to run its internal clock. A 1 GHz low phase-noise ceramic oscillator is used for this purpose. Figure 5.4 shows the measured output of this oscillator.

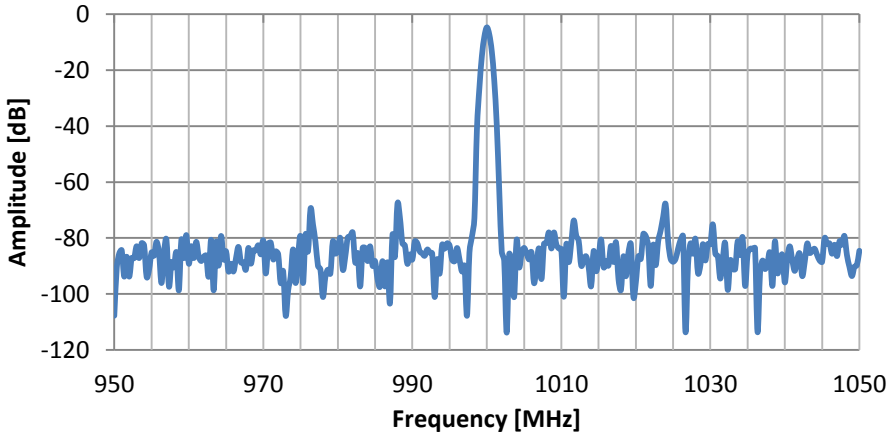

Figure 5.4 – Measured output signal of 1 GHz reference clock

5.2 Field-Programmable Gate Array (FPGA)

The device chosen for the acquisition and processing of the radar data as well as the digital control of the DDS, is the Cyclone III EP3C25 FPGA from Altera. The FPGA chip is mounted on a starter kit evaluation board which allows the user to directly configure and communicate with the Cyclone III device via the on-board USB interface.

Table 5.1 lists the main features of the Cyclone III started board.

Table 5.1 – The main features of the Cyclone III starter board [27]

Low-power consumption Altera Cyclone III EP3C25 chip in a 324-pin FineLine BGA (FBGA) package
Expandable through HSMC connector
32-Mbyte DDR SDRAM
16-Mbyte parallel flash device for configuration and storage
1 Mbyte high-speed SSRAM memory
Four user push-button switches
Four user LEDs

Table 5.2 lists the main advantages of the Cyclone III started board.

Table 5.2 – The main advantages of the Cyclone III starter board [27]

Facilitates a fast and successful FPGA design experience with helpful example designs and demonstrations.
Directly configure and communicate with the Cyclone III device via the on-board USB-Blaster™ circuitry and JTAG header
Active Parallel flash configuration
Low power consumption
Cost-effective modular design

The FPGA serves two purposes:

- Firstly it is used for controlling the DDS.
- Secondly to acquire the radar data.

These two topics are discussed in the following sections.

5.2.1 DDS Control

The FPGA is used for controlling, or "programming", the DDS. To do this, the FPGA sends the necessary data to the DDS to generate the FM-CW signal. The data that it sends to the DDS are the Frequency Tuning Word (FTW), the Phase Offset Word (POW), the Delta-Frequency Tuning Word (DFTW) and the Delta- Frequency Ramp Rate Word (DFRRW). These variables are described in more detail in Section 5.1.

The FPGA connects to the DDS evaluation board using the following pins:

- SDIO (serial data pin) – This pin is used to transfer the Tuning Words to the device.
- SCLK (serial data clock pin) – This pin is used to synchronize the data transfer with the device.
- CS (chip select pin) – This pin functions as a chip select control line and allows multiple devices to exist on a single serial bus.

- FUD (frequency update pin) – This pin is used to control the frequency update of the device. The signal sent to this pin corresponds to the resetting of the frequency sweep to the start frequency, Equation (5.2).
- IORESET (I/O reset pin) – The IORESET pin provides a means to re-establish synchronization with the device without affecting the contents of previously programmed registers.
- RESET (device reset pin) – An active high on this pin forces the AD9910 to return to its default operating conditions.

A copy of the VHDL code loaded on the FPGA is attached in Appendix A.4.

5.2.1.1 Program Description

The program that controls the DDS is split into two parts.

- The first part is used to obtain values for the different variables of the DDS (FTW, DFTW, etc.). These variables are stored in the program and then sent to the second part of the program.
- The second part of the program takes these variables and converts them to binary data before sending them to the DDS.

Figure 5.5 visually represents the program that controls the DDS as a flow chart.

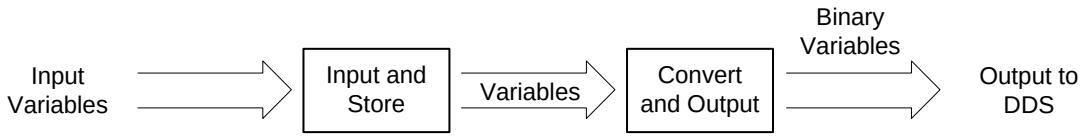

Figure 5.5 – Flowchart of DDS control program

5.2.2 Data Acquisition

Data acquisition was supposed to be accomplished using the FPGA evaluation kit and the THBD ADA daughter board that contains two 14-bit DAC and two 14-bit ADC channels. The FPGA software to permit the use of the THBD ADA for data acquisition could however not

be completed. All measurements were instead taken using a Rohdes & Schwarz FSH6 spectrum analyser and a Tektronix TDS3052B digital oscilloscope, as illustrated in Figure 5.6.

Figure 5.6 – Picture of Rohdes & Schwarz FSH6 spectrum analyser

5.3 Polyphase Quadrature Filter

Polyphase Quadrature Filters (PQF) are widely used in communications systems and are used in the modulation and demodulation of single sideband signals. [28]

For the purpose of quadrature modulation used in this radar system (Section 4.3), the PQF was chosen to split the LO signal from the transmitter into two signals in quadrature with each other. What this means is that the one signal, the signal in the Q channel, has a 90° phase difference compared to the other signal, the signal in the I channel.

The next section details the design, manufacturing and testing of the PQF component.

5.3.1 Design

The PQF is an RC (resistor-capacitor) polyphase network and the most commonly used have 4 segments per node. Each node has one resistor and capacitor, as shown in Figure 5.7. [29]

The general theory analysing n-phase systems [30] defines a polyphase signal as:

- A set of n vectors, each corresponding to a voltage
- The vectors are of equal magnitude
- The vectors are uniformly distributed over 360°.

Therefore a polyphase signal with n=4 vectors will have a 90° phase difference between each vector.

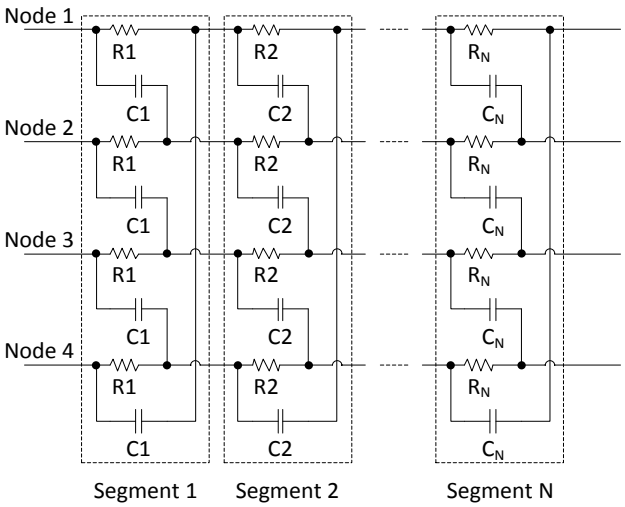

Figure 5.7 – General layout of Polyphase Quadrature Filter [29]

One segment is only capable of converting a signal into a polyphase signal for one frequency. To cover a range of frequencies, it is necessary to cascade these segments.

As a rule of thumb, the number of segments N can be determined by the following equation [29],

$$N = Log_2\left(\frac{f_{max}}{10 * f_{min}}\right) + \frac{M}{10} \tag{5.5}$$

Where, N = Number of segments of the Polyphase network,

f_{max} = Maximum frequency of the network,

f_{min} = Minimum frequency of the network,

M = Minimum suppression of the unwanted sideband.

The RC value of each segment is determined by [29],

$$R_x C_x = \frac{\left(\sqrt[N-1]{\frac{f_{max}}{f_{min}}}\right)^{(1-x)}}{2\pi \cdot f_{min}} \quad x = 1, 2 \ldots N \tag{5.6}$$

In practice, all the capacitors are chosen to be the same. This is done because low tolerance resistors are more readily available and affordable than capacitors.

With $f_{max} = 350MHz$, $f_{min} = 50MHz$ and the sideband suppression M chosen as 60dB, the number of segments N is calculated and rounded down to 5. With the number of segments known, the RC value for each segment is now calculated. The value for each capacitor is chosen to be 47pF. Figure 5.8 shows the final electrical diagram for the PQF showing all the segments as well as the input and outputs of the component.

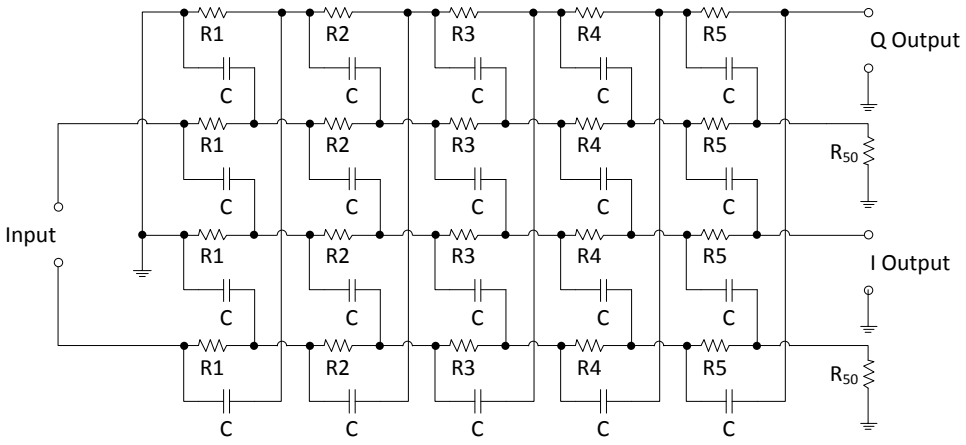

Figure 5.8 – Electrical diagram of final Polyphase Quadrature Filter design

Table 5.3 lists the component values for the PQF. The calculated values for the resistors, for example $R_1 = 9.675\Omega$, are not available as a real resistor, so a resistor with a value close to that of the calculated value is chosen.

Table 5.3 – Component Values for Polyphase Quadrature Filter

Component	Calculated Value	Real Component Value
C	47 pF	
R_1	67.73Ω	68Ω
R_2	41.64Ω	39Ω
R_3	25.60Ω	27Ω
R_4	15.74Ω	15Ω
R_5	9.675Ω	10Ω
R_{50}	50Ω	

With the design completed, the component was simulated using Spice to determine if it performed according to expectations. Figure 5.9 illustrates the simulated gain of the I and Q channels of the Polyphase Quadrature Filter.

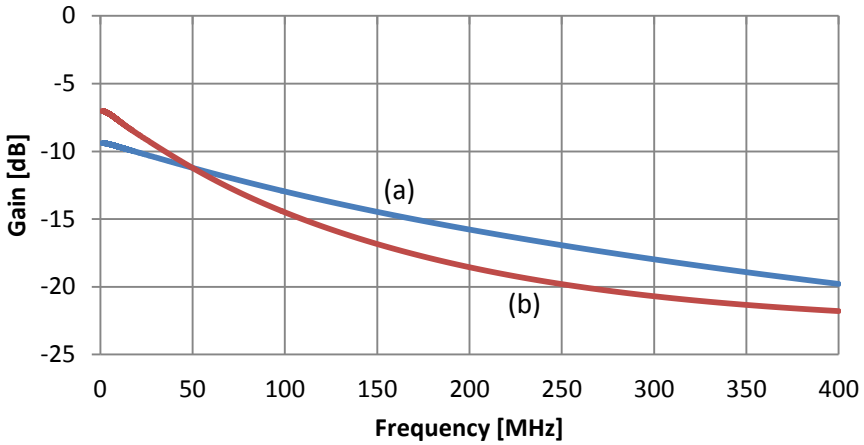

Figure 5.9 – Simulated gain of (a) I channel and (b) Q channel outputs of Polyphase Quadrature Filter

The gain of the I and Q channels shown in Figure 5.9, shows that there is a drop in signal power of between 11dB and 19dB for the I channel and between 11dB and 21dB for the Q channel over the 50 MHz to 350 MHz bandwidth. Although an I and Q channel gain that is similar and more flat would be preferred, this is acceptable.

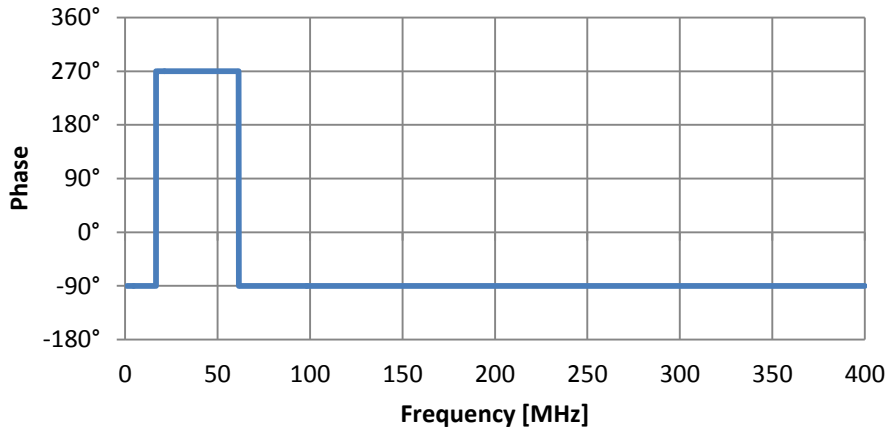

Figure 5.10 – Phase Difference between I and Q channel outputs of Polyphase Quadrature Filter

The phase difference between the I and Q channels shown in Figure 5.10 is exactly what was required. The jump in phase from -90° to +270° is due to the phase of the one signal becoming negative and the jump back to -90° is when the other signal also becomes negative.

5.3.2 Manufacturing and Testing

Figure 5.11 provides a picture of the manufactured PQF.

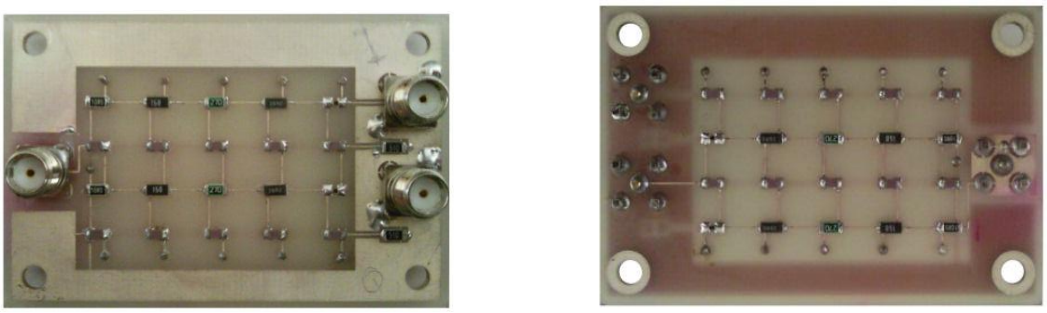

Figure 5.11 – Picture of manufactured PQF, top (left) and bottom (right)

The PQF was manufactured, and gain and phase measurements were taken of the component and the results are shown in Figure 5.12.

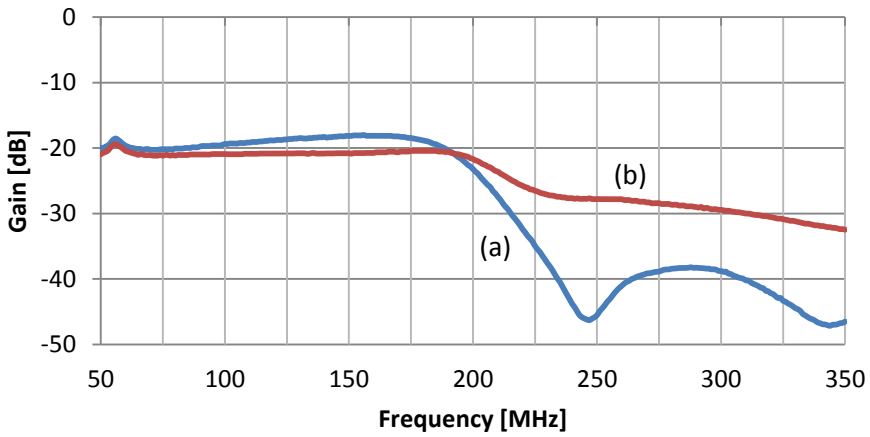

Figure 5.12 – Measured gain of (a) I channel and (b) Q channel of Polyphase Quadrature Filter

Measurements of the gain of the I and Q channels presented in Figure 5.12, shows that it differs from the Spice simulation but that it is acceptable. At about 200 MHz the gain of both channels of the PQF starts to drop. This can be a result of inferior built quality and RC components unable to manage such high frequencies. This limits the bandwidth of the system to a range of 50 to 200 MHz.

Figure 5.13 shows the measured phase response of the I and Q channels of the manufactured PQF. It shows that the phase varies depending on frequency, which is caused by a time delay between the input and output signal.

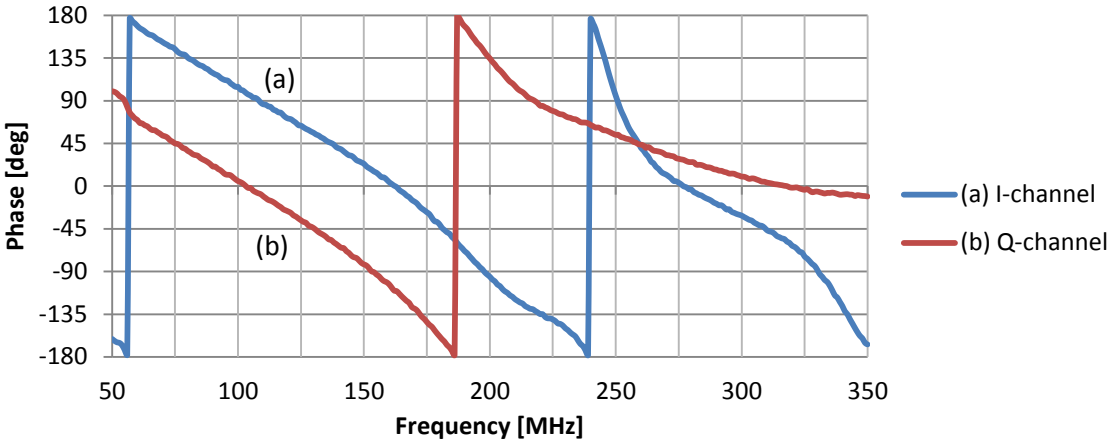

Figure 5.13 – Measured phase response of polyphase quadrature filter

Measurements of the phase difference between the I and Q channels, Figure 5.14, show that a 90° phase shift is acquired.

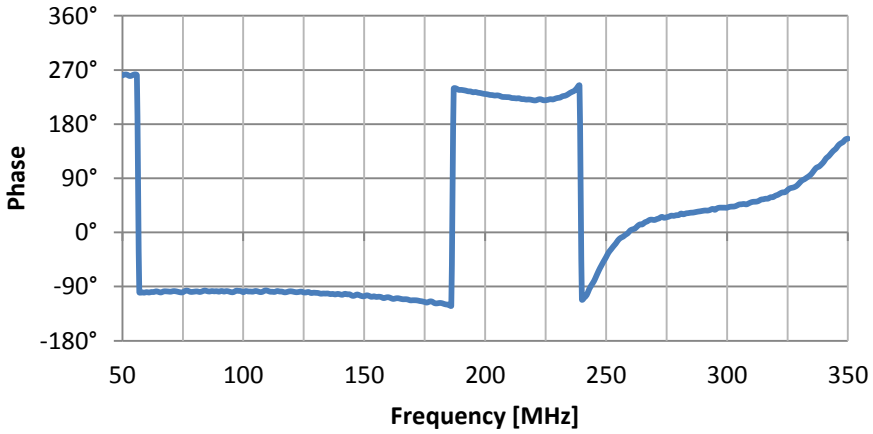

Figure 5.14 – Measurement of phase difference of Polyphase Quadrature Filter

Again the jump from -90° to +270° can be seen. Also after 200 MHz the phase difference also becomes erratic.

Although the manufactured PQF is not 100% accurate and that the signal becomes erratic after 200 MHz, the device is still usable in the radar system.

5.4 Quadrature Demodulator

In the segment of the system where the I and Q channels are fed back into the receiver (Section 4.4); a device was needed to combine these two channels and mix them back up to the correct frequency. This is done similarly to the quadrature modulation process, only in reverse. Figure 5.15 shows a block diagram of this process.

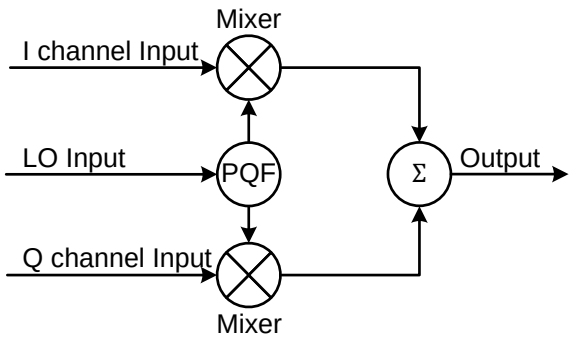

Figure 5.15 – Functional block diagram of quadrature demodulation

A polyphase quadrature filter is used to split the LO input into two LO signals at 90° phase difference to drive two mixers in quadrature. The I and Q channel signals are then mixed with the quadrature LO signals after which they have a 0° phase difference. These two signals are then combined to form the output signal.

5.5 Filters

5.5.1 400 MHz Low-pass Filter

A low-pass filter (LPF) was needed at the input of the receiver. This filter removes unwanted components in the Rx signal that are not within the bandwidth of the system. A

400 MHz LC Butterworth LPF with seven poles was designed and manufactured for this purpose.

Figure 5.16 shows the circuit diagram for this filter and Table 5.4 the component values.

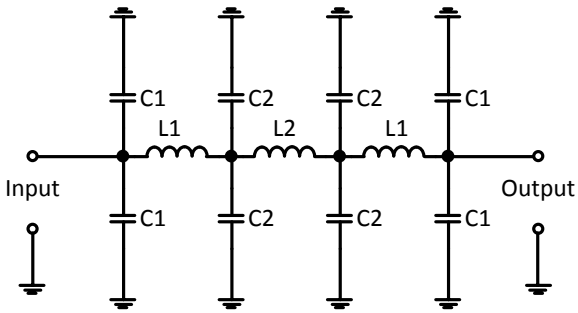

Figure 5.16 – Electrical diagram of 400 MHz low-pass filter

Table 5.4 – Component values for 400 MHz low-pass filter

Component	Physical Component Value
C_1	$3.3pF$
C_2	$6.4pF$
L_1	$24nH$
L_2	$30nH$

The circuit was simulated using Spice and the frequency response of Figure 5.17 was obtained. This showed a perfectly flat pass band and the -3dB cut-off frequency to be at about 470 MHz which was at an acceptable value.

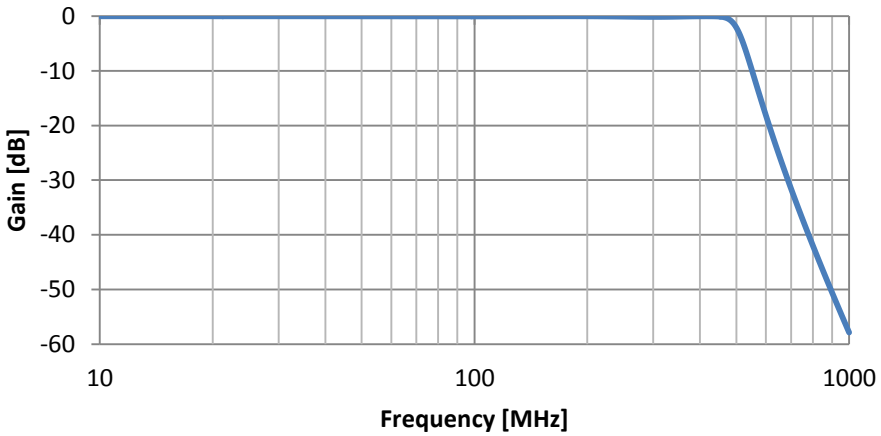

Figure 5.17 – Simulated frequency response of 400 MHz low-pass filter

The filter was manufactured, as shown in Figure 5.18, and the frequency response was measured. The frequency response results are shown in Figure 5.19.

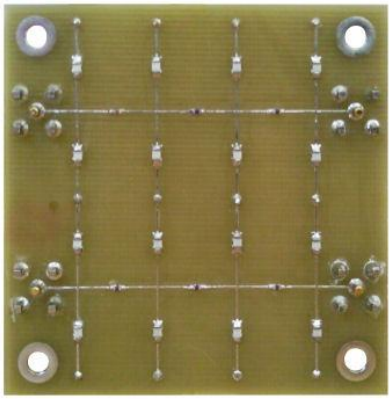

Figure 5.18 – Manufactured 400 MHz low-pass filter

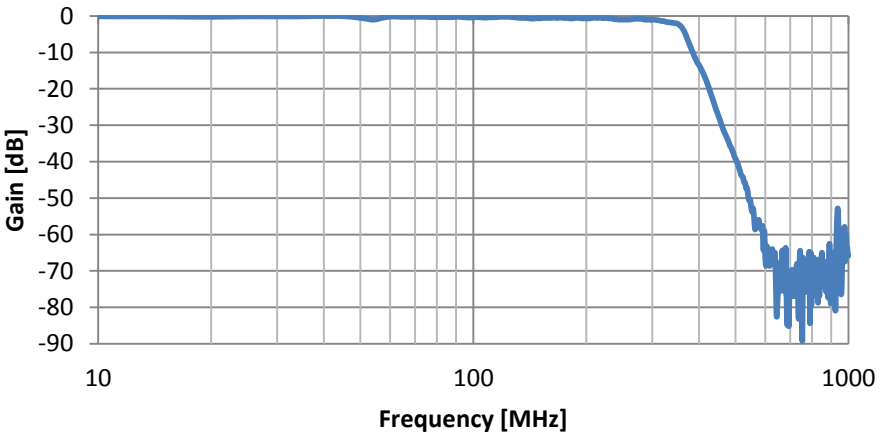

Figure 5.19 – Measured frequency response of 400 MHz low-pass filter

The results showed that the cut-off frequency has moved to 355 MHz and that it has a flat pass band with very little ripple. The movement of the cut-off frequency can be accounted to the inaccuracies of the LC components.

5.5.2 Baseband Filter

A baseband low-pass filter was needed for the feedback process discussed in Section 4.4. This LPF had to have a very low cut-off frequency of 30 kHz as well as a very steep slope. A 4th order Butterworth low-pass filter was chosen and designed [25]. Figure 5.20 shows the circuit diagram for this filter.

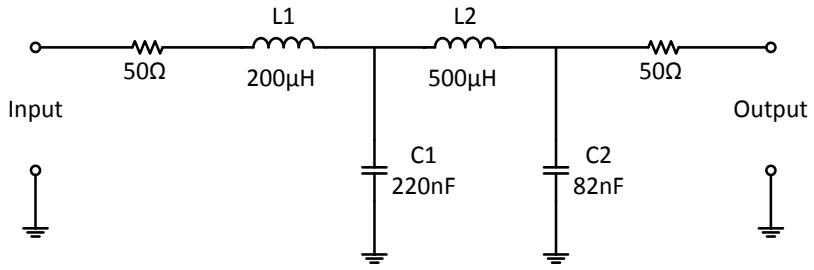

Figure 5.20 – Electrical diagram of baseband low-pass filter

The circuit was simulated using Spice and the frequency response of Figure 5.21 was obtained. This showed a perfectly flat pass band, the -3dB cut-off frequency to be at about 30 kHz and the slope to be 80 dB per decade.

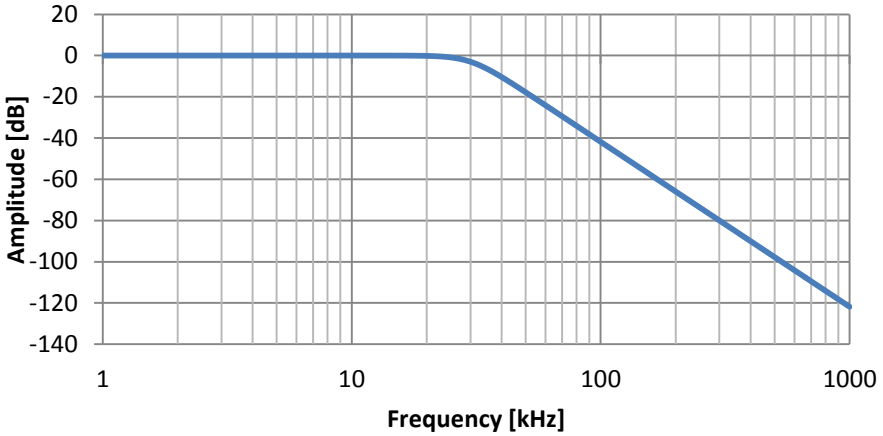

Figure 5.21 – Simulated frequency response of baseband low-pass filter

The filter was manufactured and the frequency response was measured. The frequency response results are shown in Figure 5.22

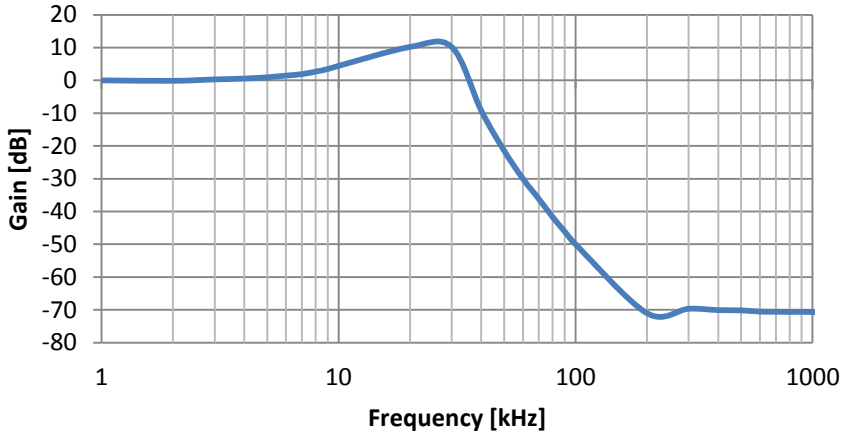

Figure 5.22 – Measured frequency response of baseband low-pass filter

The results showed the cut-off frequency is at 30 kHz, has a non-flat pass band (possibly from measurement inaccuracy) and a slope of 80 dB per decade.

5.6 Amplifiers

5.6.1 High Frequency Segment

Amplifiers were needed in the "high frequency" segment of the system. The high frequency segment refers to the part of the system where the frequency is in the range of 50 to 350 MHz. Amplifiers with a gain of 20dB were chosen for this project. These were the ZFL-500 amplifiers from Mini-Circuits. It features a frequency range of 0.05 to 500 MHz and has a low noise figure of typically 5.3dB. It is powered by a single +15V supply. Figure 5.23 shows a picture of this device.

Figure 5.23 – Picture of ZFL-500 amplifier

5.6.2 Inverting Amplifier

In the feedback loop the signal needed to be phase shifted by 180° so that the feedback signal could be subtracted from the receiver input signal. It was decided that the 180° phase shift should take place in the "low frequency" segment of the feedback loop, after the 30 kHz low-pass filter in this part of the loop. An easily designed and constructed inverting opamp circuit was chosen for this purpose. Figure 5.24 provides an electrical diagram of the Inverting Opamp circuit.

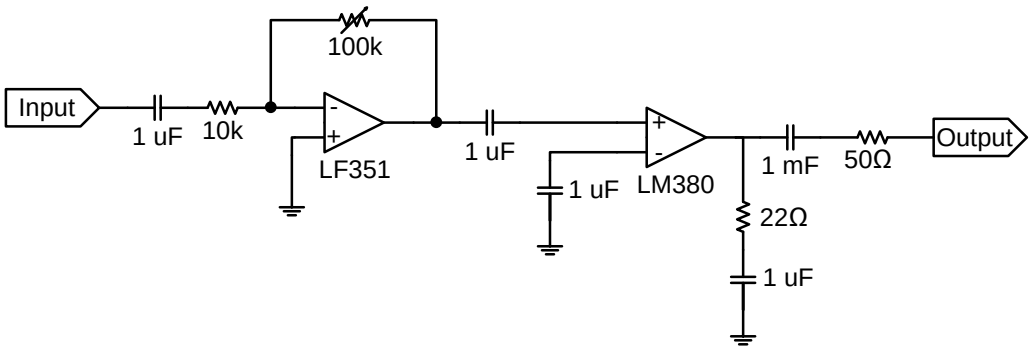

Figure 5.24 – Electrical diagram of Inverting Opamp circuit

For the inverting segment of this circuit, an LF351 inverting opamp was chosen with variable gain. Variable gain was needed due to the uneven output of the polyphase quadrature filter's I and Q channels seen in Figure 5.12. This would be used to match the amplitudes of the I and Q channels to each other in the low frequency segment. This opamp has a gain of 10 V/V (20 dB) and a bandwidth of 1 MHz. This opamp is however not able to supply enough current to drive the 50Ω impedance of the system.

To supply enough current, a second stage opamp was included in the inverting opamp circuit. The opamp chosen for this stage is the LM380, a 2W audio amplifier. This opamp was designed to be non-inverting, it has a fixed gain of 50 V/V (34 dB) and a bandwidth of 100 kHz.

The max gain for this amplifier is therefore 500 V/V (54 dB) and it has a bandwidth of 100 kHz.

5.7 Mixer

A mixer is a device that takes in two input signals, the LO and RF signals, and outputs an IF signal containing the sum and difference of the two input signals' frequencies.

Mathematically this can be written as [31]:

$$E_{out} = \left[A_{RF}\cos(\omega_{RF}t)\right]\times\left[A_{LO}\cos(\omega_{LO}t)\right] = \frac{A_{RF}A_{LO}}{2}\left(\cos[(\omega_{RF}-\omega_{LO})t]-\cos[(\omega_{RF}+\omega_{LO})t]\right) \quad (5.7)$$

Where, E_{out} = the mixer output signal,

A_{RF} , A_{LO} = the amplitudes of the RF and LO input signals,

ω_{RF} , ω_{LO} = the frequencies of the RF and LO input signals.

Visually this can be represented by the following graph in Figure 5.25.

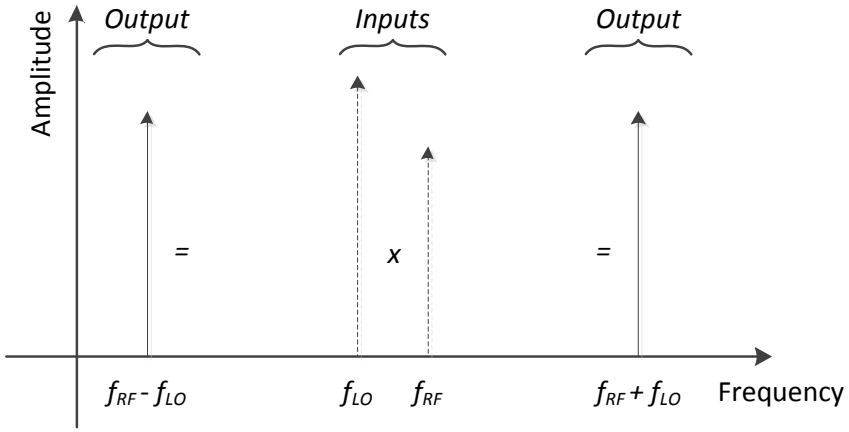

Figure 5.25 – Representation of mixing process

The mixing device chosen for this project is the ZX05-1L+ mixer from Mini-Circuits. It features LO and RF frequencies of 2 to 500 MHz and IF frequencies of DC to 500 MHz. It has an LO-RF isolation of typical 55dB and a conversion loss of max 7.2dB. Figure 5.26 shows a schematic and picture of this device.

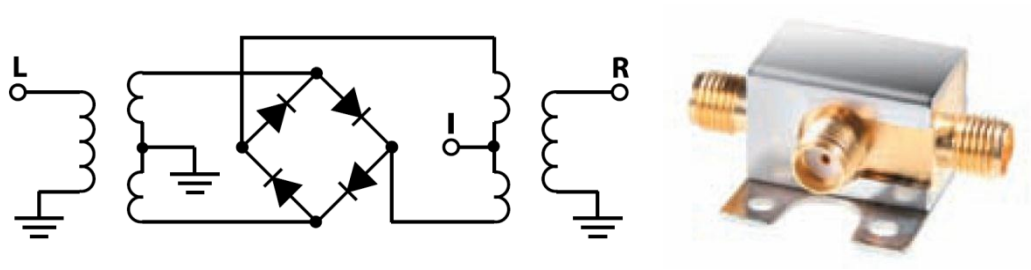

(a) (b)

Figure 5.26 – (a) Electrical diagram and (b) Picture of ZX05-1L+ Mixer

5.8 Power Splitter

A two way power splitter is a device that takes an input signal and divides it into two equal output signals. The two output signals have no altered frequency or phase compared to that of the input signal. The only difference is that the power of the output signal is half that of the input. The output signals can be written as

$$E_{out1}(\omega,\phi) = E_{out2}(\omega,\phi) = E_{in}(\omega,\phi) - 3dB \qquad (5.8)$$

The power splitter chosen is the ZFSC-2-1+ from Mini-Circuits. It has a frequency range of 5 to 500 MHz, a low insertion loss of typically 0.3dB and isolation between ports of typically 28dB. Figure 5.27 shows a diagram and picture of this device.

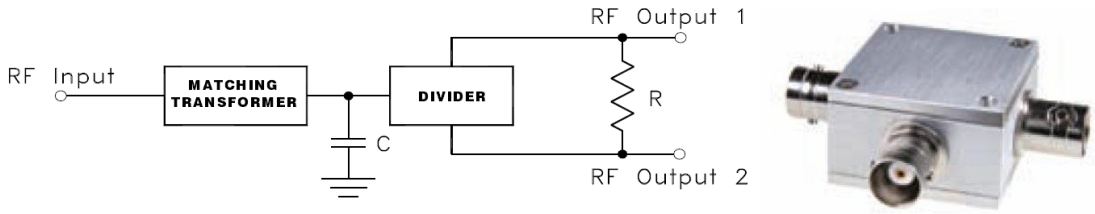

Figure 5.27 – (a) Electrical diagram and (b) Picture (BNC version shown) of ZFSC-2-1+ 2-way Power Splitter

The power splitter also functions as a power combiner when two signals are connected to the outputs of the device.

5.9 Delay Line

From the measurements taken in Section 6.1, it was decided not to use antennas for the measurements of the rest of the system, namely for the feedback. To replace the antennas, a delay line combined with a variable attenuator was chosen.

The delay line chosen was a 10m coaxial cable. This would introduce the necessary time delay in the Rx signal.

For the attenuator, the Agilent (HP) 8495B Manual Step Attenuator was chosen. It has a frequency range of DC to 18 GHz and a variable attenuation of 0 to 70 dB in 10 dB steps.

Figure 5.28 – Agilent (HP) 8495B Manual Step Attenuator

Chapter 6

Final Measurements and Conclusion

In this chapter the two possible solutions to the transmitter leakage problem are tested. In the case of the antennas, these are measured to determine the amount of isolation between them. For the feedback loop, the constructed radar system is tested and the amount of leakage cancellation measured. All measurements were taken using a Rohde & Schwarz FSH6 spectrum analyser and a Tektronix TDS3052B digital oscilloscope.

6.1 Antennas

The previous section on antenna simulations (Section 3.2) showed what could be expected from a number of antenna designs concerning the antenna criteria obtained. Now an antenna design had to be chosen to be used in the "practical" radar system. The important parameter to focus on when choosing an antenna for this project was the coupling of that antenna. The purpose of the project is to determine a method to reduce antenna coupling. Therefore the chosen antenna had to still exhibit a quantifiable amount of coupling.

Figure 6.1 – Monopole antenna

The antenna design decided upon was the dipole design. This design showed a fair amount of coupling in its simulation. It was important that the antennas had coupling so that when testing the feedback loop, transmitter leakage could be present. Two of the monopoles seen in Figure 6.1 were used to realize this design. Input impedance, reflection coefficient, coupling and gain measurements were taken of this antenna design to compare it to the simulation results.

6.1.1 Measurement Setup

The two monopole antennas were placed 0.6 m from each other in the orientation and position that can be seen in Figure 3.1. Measurements were then taken of the antennas using the spectrum analyser. The spectrum analyser was set up to sweep over a larger frequency range than the bandwidth of the system, namely 0 to 500 MHz. At this large bandwidth the spectrum analyser was only able to produce a sweep rate of 50 ms.

6.1.2 Results

Figure 6.2 illustrates the measured input impedance of the monopole antenna.

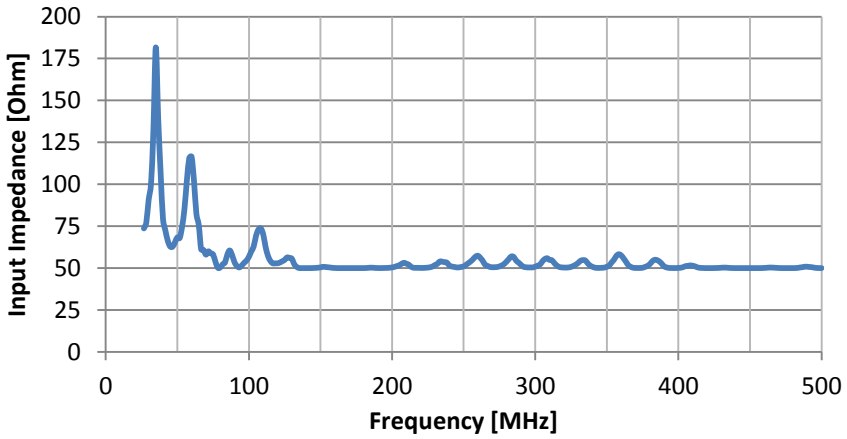

Figure 6.2 – Measured input impedance of monopole antenna

Figure 6.2 shows that the desired 50 Ohm impedance matches the antenna to the rest of the system.

Figure 6.3 illustrates the measurements of the antenna's reflection coefficient.

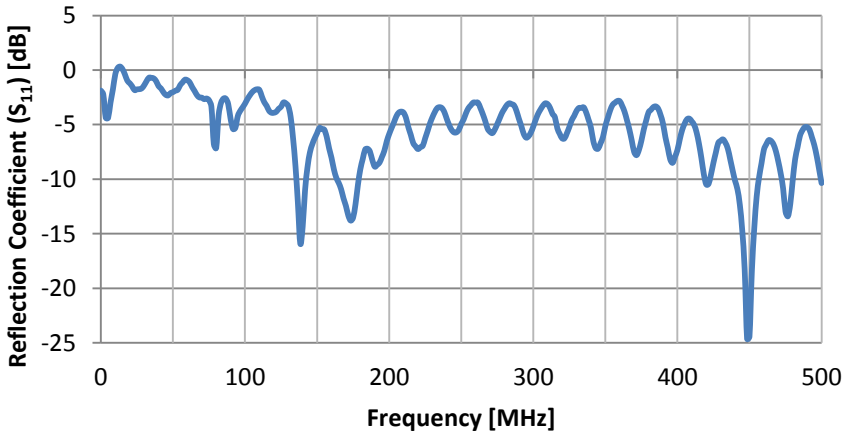

Figure 6.3 – Measured reflection coefficient of monopole antenna

Figure 6.3 shows that the antenna becomes resonant at 140 MHz and especially at 450 MHz. Although not the ideal resonant frequency, this is not a vital requirement for the project.

Figure 6.4 illustrates the coupling measured between two monopole antennas.

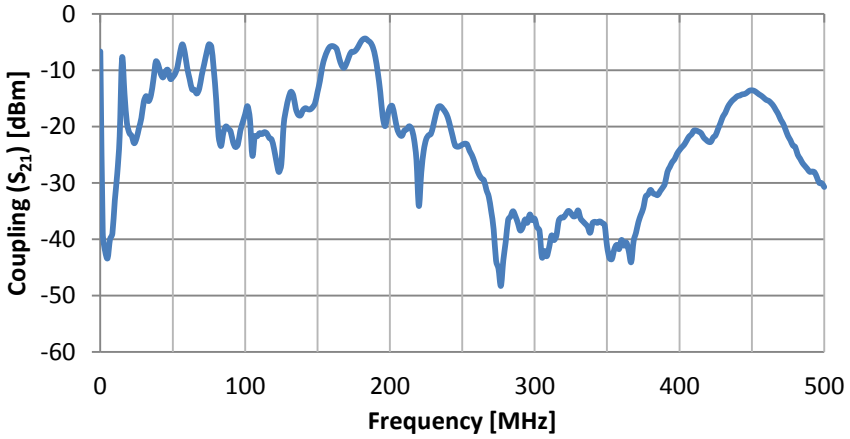

Figure 6.4 – Measured coupling between two monopole antennas

Figure 6.4 shows that the coupling between the two monopole antennas is indeed quite high, especially below 250 MHz. This is the important parameter required of the antennas chosen for this project. It allows for suitable measurements of the transmitter leakage signal in the radar system and the attempt to reduce this signal.

6.1.3 Conclusion

The measurements of the applied antenna design show that although the antennas have a different resonant frequency from that of the simulated antennas, it does have similar levels of coupling.

After a re-evaluation of the antennas characteristics it was decided not to use these for further measurements. The antennas had too small a bandwidth if compared to the radar system. Also, variation in the gain of the antennas would not allow for accurate measurements of the feedback loop. External factors such as objects placed close to the antennas and movement around them could possibly interfere with the signal transmitted between them. A delay line in combination with a variable attenuator would give much more accurate readings and was implemented into the system.

6.2 Feedback Loop

For this section, the radar system designed in Chapter 4 was combined with the negative feedback loop designed in Section 4.4. The final radar system design can be seen in the diagram of Figure 6.5.

During the course of taking measurements of the system, it was found that if the amplitude of the receive signal and that of the feedback signal (the two signals combined at the receiver input) are not matched (of equal or similar amplitude), little or no feedback would occur. What this means is that the total gain of the feedback loop is too low. This is a rather understandable observation. If the loop gain is too low, the feedback signal would be too small if compared to the receive signal, and it would be unable to suppress any transmitter leakage signal present in the receive signal.

To resolve the low loop gain, extra amplification was added to the output of the feedback loop as well as another variable attenuator similar to the one discussed in Section 5.9. This made it possible to match the two signal amplitudes. When taking measurements, it was always ensured that the amplitude of the feedback signal was matched to that of the receive signal.

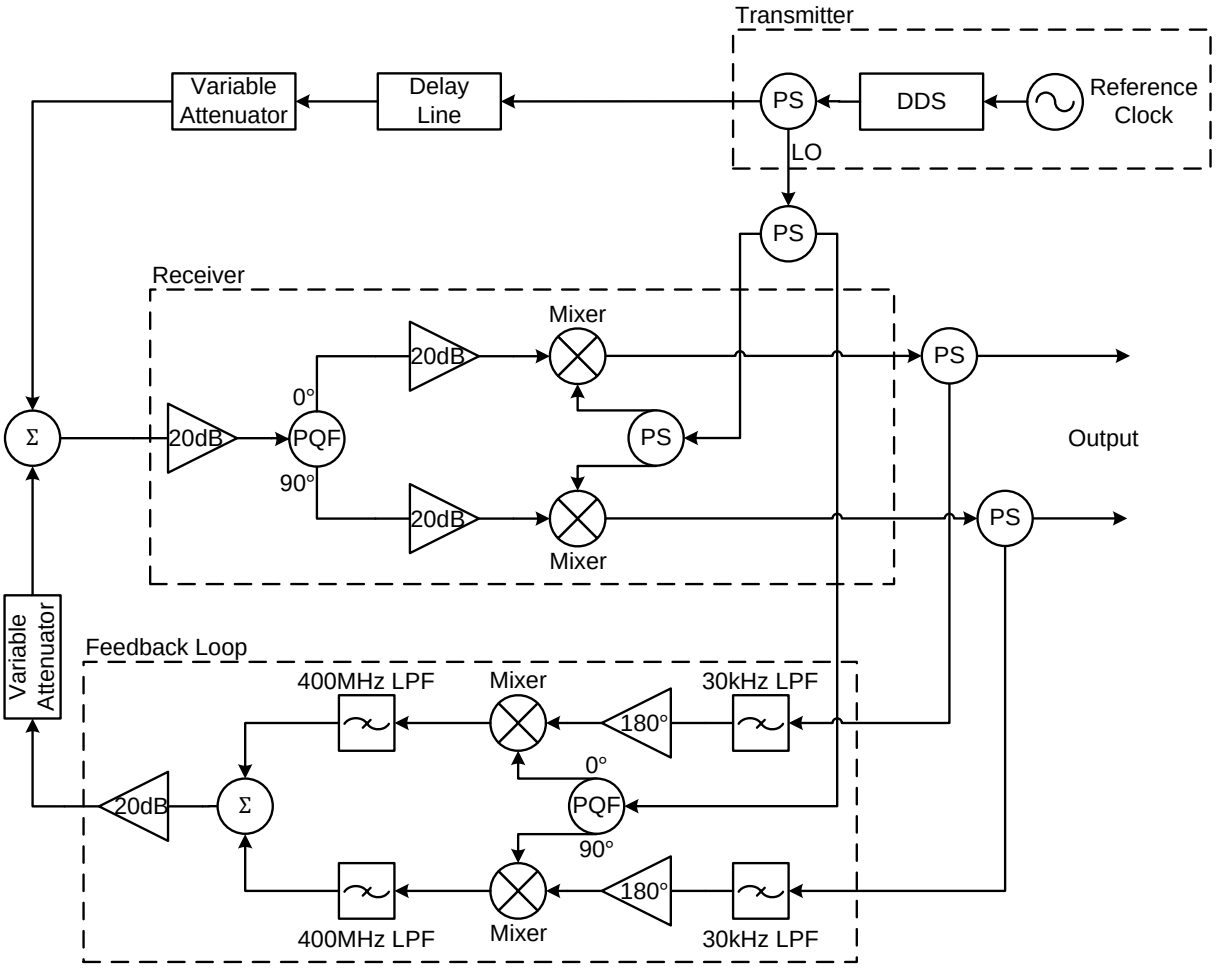

Figure 6.5 – Diagram showing the final system design

6.2.1 Measurement Setup

While taking measurements of the radar system, all components were placed on a common ground plane. This was done to reduce possible interference between system components and for easy access to the ground voltage level. Power supplied to the system was as follows; +15 V and -15 V for the amplifiers, 3.3 V and 1.8 V for the DDS and 5 V for the reference clock. These were checked with a digital multimeter.

Measurements to the system where the frequency is in the "higher" range, namely 50 to 350 MHz, were accomplished with the spectrum analyser. The spectrum analyser in combination with its VSWR Bridge, Rhode & Schwarz FSH-Z3, is able to measure frequency and phase responses. The spectrum analyser was set up to sweep from 10 to 400 MHz; the

analyser has a lower frequency limit of 10 MHz when taking frequency response measurements, at a sweep rate of 20 ms. The input signal was applied to the antenna/delay line input of the combiner at the entrance of the receiver; the output was then measured at the output of the feedback loop as it connects to the aforementioned combiner. The spectrum analyser would also be used to drive the LO signals in the system and therefore the DDS is entirely disconnected from the system.

The spectrum analyser was also used to check input and output power levels for each component. This was done to ensure that all components were supplied with the correct power levels. The oscilloscope was also employed to check input and output voltage levels for every component, especially the amplifiers, to ensure that saturation of the component did not occur.

6.2.2 Results

What one would expect from the results of the measurements of the feedback loop, if everything works perfectly, is that the phase response of the receiver measured from its input to its output would be 0° and from the receiver input to the feedback loop output would be 180°. However, the phase response is expected to vary somewhat due to the phase variance of the polyphase quadrature filter, as can be seen in Figure 6.6.

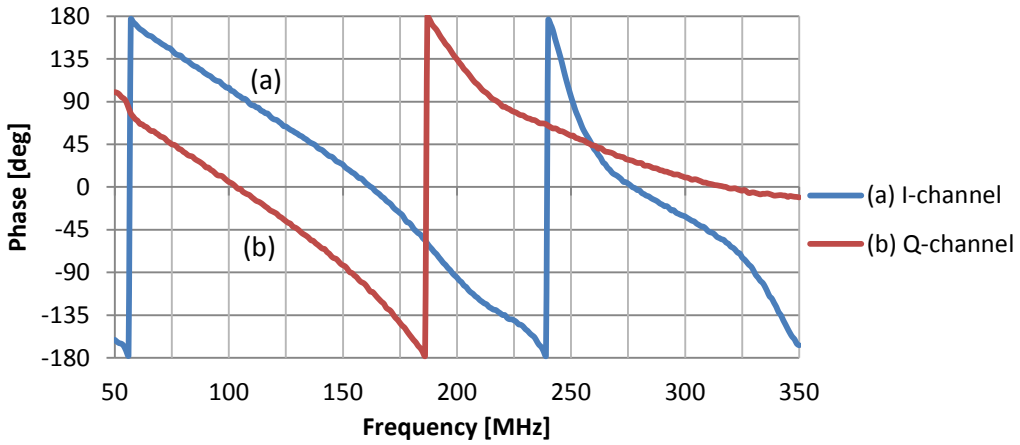

Figure 6.6 – Measured phase response of polyphase quadrature filter

This variance in the phase response is caused by a time delay in the PQF which it then introduces into the receiver and feedback loop. This time delay can be calculated using the following derivative equation:

$$delay \quad [s] = \frac{d(Phase) \quad [rad]}{d(frequency) \quad [rad/s]} \tag{6.1}$$

Figure 6.7 shows the calculated time delay of the PQF versus frequency.

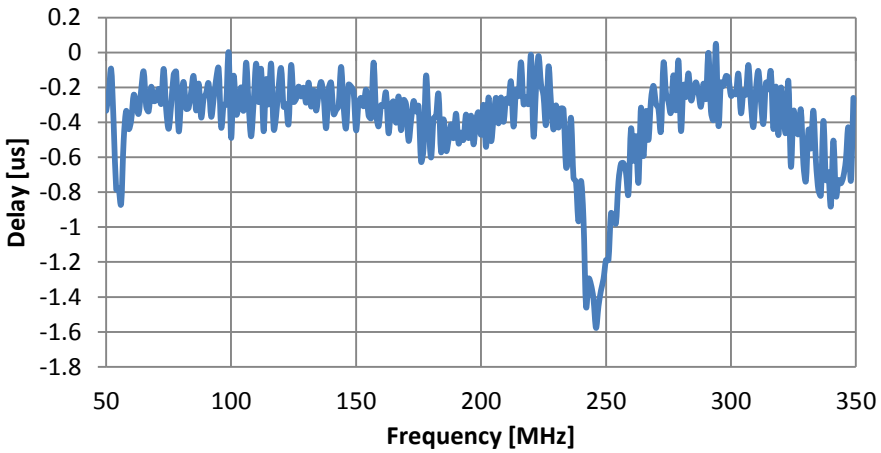

Figure 6.7 – Calculated time delay of the PQF

Frequency measurements were now conducted on the feedback loop. Open and closed loop measurements were taken and compared. What is meant by open loop, is that this is when the feedback signal is not fed back into the receive signal and closed loop is when it is indeed fed back in.

Figure 6.8 shows the measured frequency response of the open and closed feedback loop.

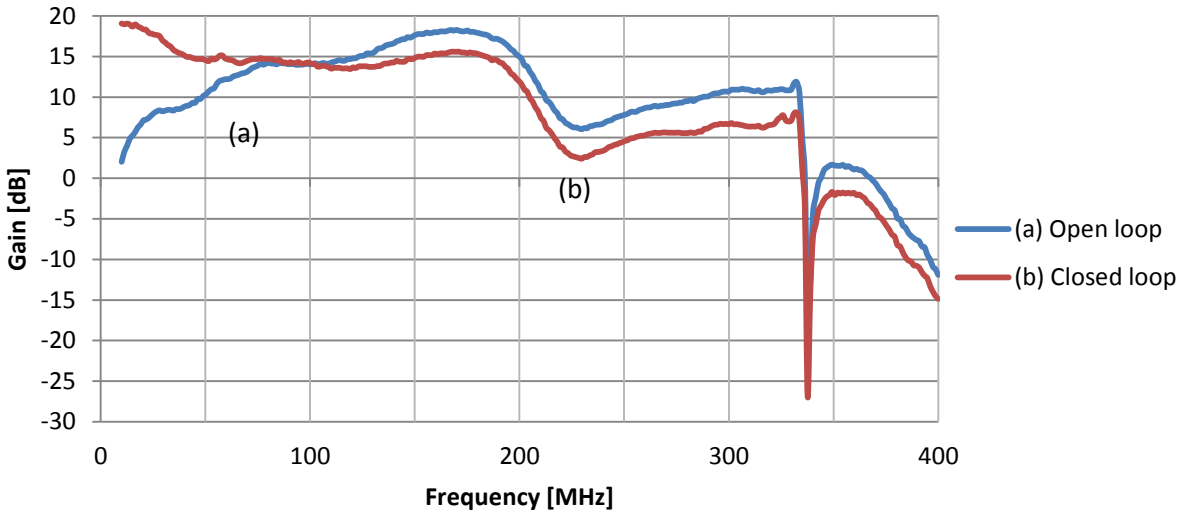

Figure 6.8 – Measured frequency response of open and closed feedback loop

The gain of both the open and the closed loop system is more or less 15 dB between 50 and 250 MHz. After this the gain starts to drop. This can be accounted to the frequency response of the PQF in the receiver chain, as illustrated in Figure 5.12, which shows a similar drop in gain after 200 MHz. The extreme dip in the gain at ~340 MHz cannot be accounted for.

The gain of the system is at 15 dB and not 40 dB as it was designed to be. This is due to the insertion and conversion losses of the components in the chain, mainly the PQF and mixers in the receiver chain.

Figure 6.9 shows the measured phase response of the open and closed feedback loop.

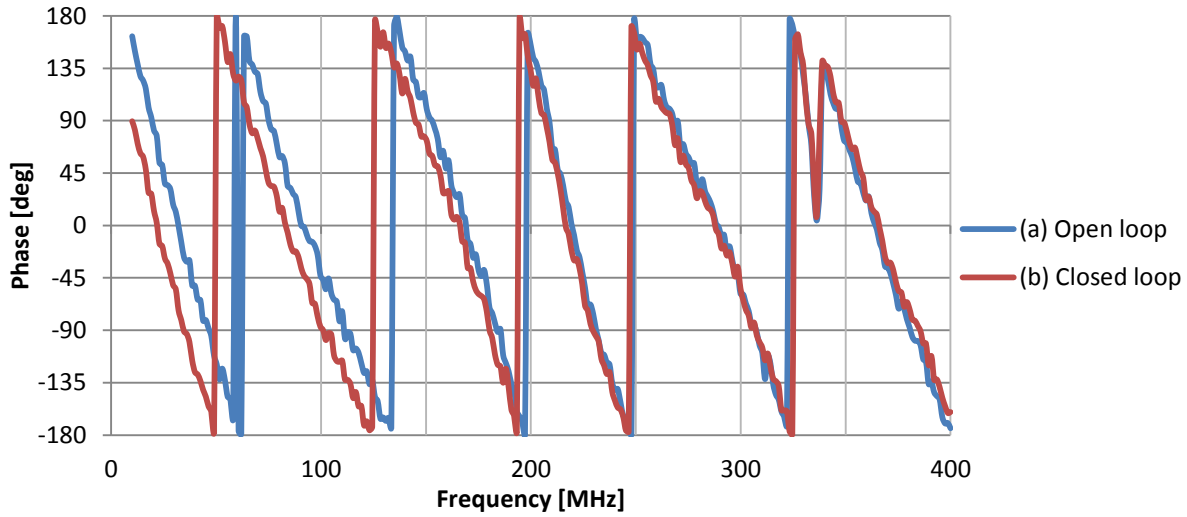

Figure 6.9 – Measured phase response of open and closed feedback loop

As can be seen in the phase response of the feedback loop in Figure 6.9, the phase varies as was anticipated. The amount of phase variance is however more than expected and is most likely caused by the addition of time delays introduced in the system by other components such as the power splitters and filters and by the cables used to connect the components to each other.

What can be anticipated from this variance in the feedback loop phase, is that suppression of any transmitter leakage signal in the receive signal will only occur at certain segments of the system bandwidth. Applying a CW signal to the system and measuring the receive and feedback signals' voltage with the oscilloscope, showed that the feedback is 180° out of phase with respect to the receive signal at ~100MHz. The system is also 180° out of phase at other frequencies, but for further testing 100 MHz would be used.

6.3 Coupling Suppression

6.3.1 Measurement Setup

For this section of measurements where the output of the system is in the "lower" frequency range, at close to baseband level between the down mixer in the receiver

channel and the 30 kHz low-pass filter in the feedback loop, measurements were accomplished using the oscilloscope. For frequency measurements in this frequency range, the oscilloscope utilizes an FFT function with a rectangular sampling window.

The DDS was now connected back into the system and the configuration looks like that of Figure 6.5. Because the system is 180° out of phase at 100 MHz and not across the entire bandwidth, the DDS was set to sweep from 95 to 105 MHz. Because of this smaller frequency sweep, the sweep rate had to be adjusted. Varying the sweep rate of the DDS would create a "transmitter leakage signal" at different frequencies due to the inclusion of the delay line at the receiver input.

Measurements were taken from the output of the system, namely the output of the down mixers in the receive chain. Again taking measurements where the feedback loop is opened and closed, these were compared to determine the gain of the receiver and therefore if transmitter leakage suppression is successful. Measurements were also taken at different sweep frequencies, namely 195 to 205 MHz and 295 to 305 MHz. This would show if suppression is successful where the feedback loop is not 180° out of phase with respect to the receiver.

6.3.2 Results

What would be expected of the results would be that at a sweep of 95 to 105 MHz the frequency response of the receiver would closely follow that of the simulation presented in Figure 4.14.

Figure 6.10 shows the measured frequency response of the output of the system and from it can be seen that suppression does in fact occur and that it follows the response of the simulation, although limitedly.

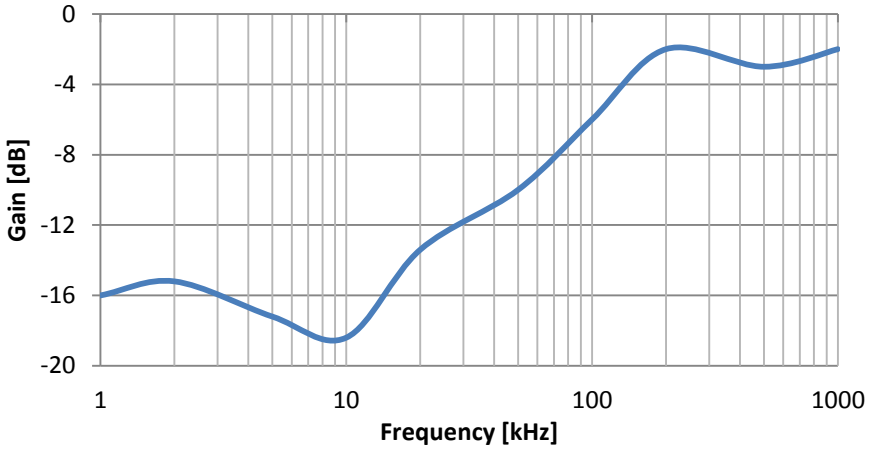

Figure 6.10 – Measured output frequency response at a sweep of 95 to 105 MHz

The lower gain of the measured output when compared to that of the simulation can again be accounted to insertion and conversion losses in the system components that are not taken into account in the simulation. Suppression of signals below 30 kHz can be seen to be between 12 and 16 dB. The reason for this lower amount of suppression is due to the overall lower amount of loop gain within the feedback loop.

Figure 6.11 and Figure 6.12 show measurements of the output frequency response but at different sweep frequencies, namely 195 to 205 MHz for the former and 295 to 305 MHz for the latter. At these frequencies the feedback loop was measured to not be 180° out of phase with respect to the receive signal. As was expected, although suppression does occur, it does not follow the frequency response of the simulation. Therefore the correct suppression of the transmitter leakage signal would not occur. Target information that could appear at these frequencies would instead be suppressed.

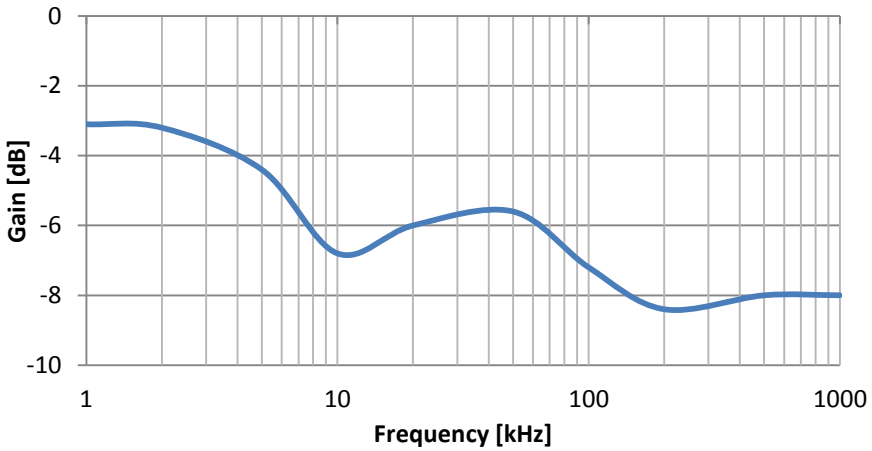

Figure 6.11 – Measured system output at a sweep of 195 to 205 MHz

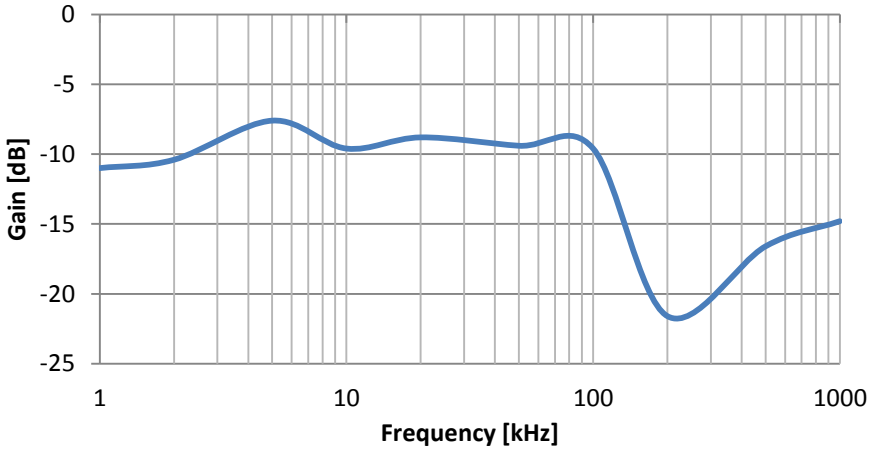

Figure 6.12 – Measured system output at a sweep of 295 to 305 MHz

6.4 Conclusion

In summary, two different methods to reduce or suppress the transmitter leakage signal that occurs in a bistatic FM-CW radar system were investigated. The first focussed on the antennas of the radar system. In an effort to reduce the amount of coupling between the antennas, different antenna designs were looked at to see if an antenna could be designed that would have a lesser quantity of coupling.

From the simulation of a number of antenna designs, it was determined that it is indeed possible to design an antenna with reduced coupling. The coupling would however never

be zero when using FM-CW. When placing a transmit and receive antenna so close without isolating them from each other, coupling would always occur. Therefore another method to reduce the transmitter leakage signal was investigated.

This other method was the implementation of a negative feedback loop within the receiver of the radar system. The feedback loop would suppress any signal received up to a certain frequency and after that frequency it would let it pass without disruption. In effect the feedback loop would respond similar to a high-pass filter, as can be seen from its simulation, but with the added advantage of not allowing the leakage signal to over-drive the receiver.

The mathematical theory behind the working of the feedback loop and the simulation thereof proved that it can indeed suppress the leakage signal. But, a simulation is the ideal case by nature and does not take into account imperfections in components and external factors.

If the polyphase quadrature filter and other components did not introduce a time delay within the system, then the feedback loop would be able to operate over the entire bandwidth it was designed for. This is however not the case as can be seen from the measurements taken of the system.

What the results do show is that it is indeed possible to construct a radar system with a negative feedback loop to suppress the transmitter leakage signal incurred in the system by the antennas. More ideal components would however be needed.

This radar system was constructed by using components bought from well established companies as well as components designed and manufactured personally. As expected it was these components that were personally manufactured that gave the most problems.

6.5 Further Development

To improve on the time delay issue befalling this project, a PCB layout of the system can be investigated. Instead of having components connected by SMA and other cables to each other, as it is in this project and can be seen in Figure 6.13, laying the entire system out on a PCB would improve on the time delay within the feedback loop.

The polyphase filter is also a large contributor to the time delay issue. A redesign of the component is needed. A smaller more compact layout using resistors and capacitors more suited for the frequency range would greatly reduce the time delay of the PQF. Other devices that split the signal into quadrature channels could also be considered to replace the PQF.

The simulation of the feedback loop used a very simplified model of the loop. By adding more detail to the model, such as component losses and frequency and phase responses, a more realistic simulation could be achieved. Each component in the receiver and feedback loop should be fully modelled and then added to the simulation model. The simulation could then be used to determine what other factors besides the time delay caused the system to only work within a restricted bandwidth.

For further development of the system, the implementation of the FPGA as an indicator to process data, Section 4.1, could be completed. This aspect of the project could however not be completed due to time limitations.

Another aspect that can be explored is the digitisation of the feedback loop. This would allow for easy modifications of the feedback gain and frequency that suppression takes place. This would also make it possible to easily add the feedback loop to any number of radar systems where signal leakage is an issue.

To improve on the amount of leakage suppression further, a combination of low coupling antennas and a negative feedback loop should be used. If the antennas permit less

transmitter leakage signal into the receiver, the feedback loop would be more adept at suppressing such signals.

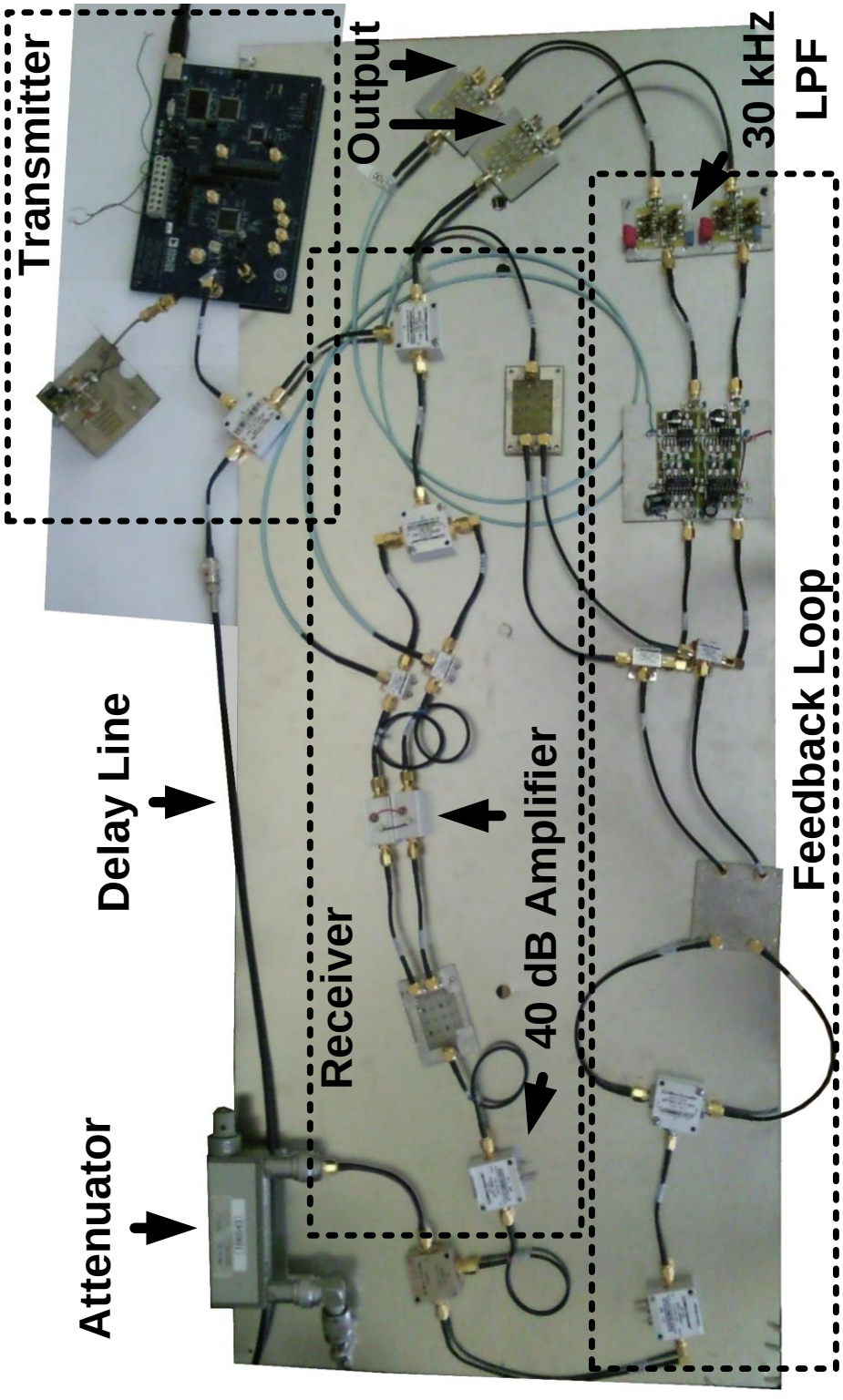

Figure 6.13 – FM-CW radar system with negative feedback loop

Bibliography

[1] **Buchwald, J. Z.** *The Creation of Scientific Effects: Heinrich Hertz and Electric Waves.* University of Chicago Press, 1994.

[2] **Knott, E. F., Shaeffer, J. F. and Tuley, M. T.** *Radar Cross Section.* SciTech Publishing, Inc., 2004.

[3] **Watson Jr, R. C.** *Radar Origins Worldwide: History of Its Evolution in 13 Nations Through World War II.* Trafford Publishing, 2009.

[4] *Radar Speed Signs.* [Online] RadarSign Website. http://www.radarsign.com/Pages/Products/DriverFeedbackSigns.aspx.

[5] **Daniels, D. J.** *Ground Penetrating Radar.* The Institution of Engineering and Technology, London, United Kingdom, 2007. Vol. 1.

[6] **Woods, B.K.** *Development of an Active Pulsed Radar Receiver for a Mono-Static Borehole-Radar Tool.* Department of Electrical and Electronic Engineering, University of Stellenbosch. Stellenbosch, March 2003. MSc Thesis.

[7] **Boshoff, J.** [Personal communication]. 2008. Maritime Archaeologist. Iziko Museums, Cape Town..

[8] **Van der Merwe, P. J.** *The Design of a Monostatic, Ultra Wide Band, VHF, Pulse Radar for Detection of Close-in Targets.* Department of Electrical and Electronic Engineering, University of Stellenbosch. Stellenbosch, March 2003. MSc Thesis.

[9] **Palma, C.** *Astronomy 801 - Stellar Velocities.* [Online] Penn State University Website, 2010. https://www.e-education.psu.edu/astro801/content/l4_p7.html.

[10] **Russell, D. A.** *The Doppler Effect and Sonic Booms.* [Online] Kettering University Website, 2010. http://paws.kettering.edu/~drussell/Demos/doppler/doppler.html.

[11] **Skolnik, M. I.** *Introduction to Radar Systems.* 3rd Edition. McGraw-Hill, 2001.

[12] **McGraw-Hill Companies, Inc.** *Continuous-wave radar.* [Online] McGraw-Hill Science & Technology Encyclopedia, 2010. http://www.answers.com/topic/continuous-wave-radar.

[13] *Doppler radar.* [Online] Argonne National Laboratory, NEWTON Website, 2010. http://www.newton.dep.anl.gov/askasci/gen99/gen99055.htm.

[14] **Van Genderen, P.** *Radar System Design.* Stellenbosch. Radar System Design Short Course, 2008.

[15] **Carroll, J. M.** *Continuous-Wave Radar.* [Online] McGraw-Hill Companies Inc, AccessScience.com, 2010. http://www.accessscience.com/content.aspx?searchStr=Continuous-wave+radar&id=159400.

[16] *Continuous wave radar.* [Online] Statemaster.com Encyclopedia, 2010. http://www.statemaster.com/encyclopedia/Continuous_wave-radar.

[17] *Trackman.* [Online] St Andrews Links Website, 2010. http://www.standrews.org.uk/Playing-golf-in-St-Andrews/Academy/Instruction/The-Academy/Technology/Trackman.aspx.

[18] **Mahafza, B. R.** *Introduction to Radar Analysis.* CRC Press, 1998.

[19] **Atkins, G.** *T2FD - The Forgotten Antenna.* [Online] Hard-Core-DX.com, 2010. http://www.hard-core-dx.com/nordicdx/antenna/wire/t2fd.html.

[20] **Analog Devices.** *AD9858 - 1 GSPS Direct Digital Synthesizer.* Datasheet.

[21] **Stove, A. G.** *Linear FM-CW Radar Techniques.* 1992. Radar and Signal Processing, IEEE Proceedings.

[22] **Beasley, P. D. L., Stove, A. G. and Reits, B. J.** *Solving the Problems of a Single Antenna Frequency Modulated CW Radar.* Radar Conference, 1990. Record of the IEEE 1990 International Conference.

[23] **K. Lin and Y. E. Wang.** *Real-time DSP for Reflected Power Cancellation in FMCW Radars.* Proc. 60th IEEE Veh. Technol. Conf., Sep. 26–29, 2004, vol. 6.

[24] **K. Lin, Y. E. Wang, C. Pao, Y. Shih.** *A Ka-Band FMCW Radar Front-End With Adaptive Leakage Cancellation.* IEEE Transactions on Microwave Theory and Techniques, Vol. 54, No. 12. 2006.

[25] **Fourie, C J.** *Basic Filter Theory.* University of Stellenbosch, Electronics 315 Class Notes, 2006.

[26] **Analog Devices.** *A Technical Tutorial on Digital Signal Synthesis.* [Online] Website of the IEEE Long Island Section, 2010. http://www.ieee.li/pdf/essay/dds.pdf.

[27] **Altera Corporation.** *Cyclone III FPGA Starter Board Reference Manual.* June 2008.

[28] **Crols, J. and Steyaert, M.** *CMOS Wireless Transceiver Design.* Kluwer Academic Publishers, 1997.

[29] **Niessen, W. J.** *Understanding and Designing Sequency Asymmetric Polyphase Networks.* 2006.

[30] **Fortesque, C. L.** *Methods of Symmetrical Co-Ordinates Applied to the Solution of Polyphase Networks.* [Online] 1918. 34th Annual Convention of the American Institute of Electrical Engineers, Atlantic City, N.J.. http://thunderbox.uwaterloo.ca/~ccanizar/papers/classical/Fortescue.pdf.

[31] **Machado, G. A. S.** *Low-power HF Microelectronics: A Unified Approach.* IET Publishers, 1996.

Appendix

A.1 Wu-King Antenna Model

The Wu-King antenna is a resistively-loaded monopole antenna. This means that instead of a solid wire forming the monopole, the wire is interspersed with resistive elements. The values for these resistive elements increase exponentially the further from the feed they are placed. These values are an important variable in the design of the Wu-King Antenna. The purpose of modelling the antenna is to determine for what values of the resistive elements the best results can be obtained. Figure A.1 shows the model for the Wu-King Dipole Antenna.

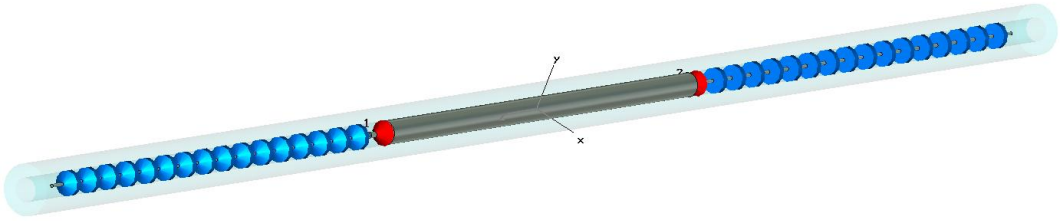

Figure A.1 – Model of Wu-King Antenna showing the interspersed resistive elements

In the antenna model used, the resistive elements are given starting values that range from 58 Ohm to 1680 Ohm. These values are then scaled by a factor. With CST's ability to perform a parametric sweep on this factor different results are obtained for different factor values. From the results the factor is then obtained and in-turn the values of the resistive elements.

The gain of the Wu-King drops thus worsens, as the factor value is increased.

The input impedance and reflection coefficient stay more or less the same for different factor values leaving only coupling and gain as defining criteria. As the factor is increased, so the coupling improves but the gain decreases and vice versa. Therefore a balance between coupling and gain must be found.

A.2 Folded Dipole Antenna Derivations

This section documents two derivations of the Folded Dipole antenna. They are very similar to the Folded Dipole in Section 3.1.3, but with minor differences:

a) This folded dipole's end points are not terminated at the feed; an air gap is left between the feed and end points.
b) This folded dipole's end points are terminated ate the feed, however at the mid-point between the feed and the end an air gap is left open.

Figure A.2 illustrates the input impedance results of the Folded Dipole Antenna Derivations.

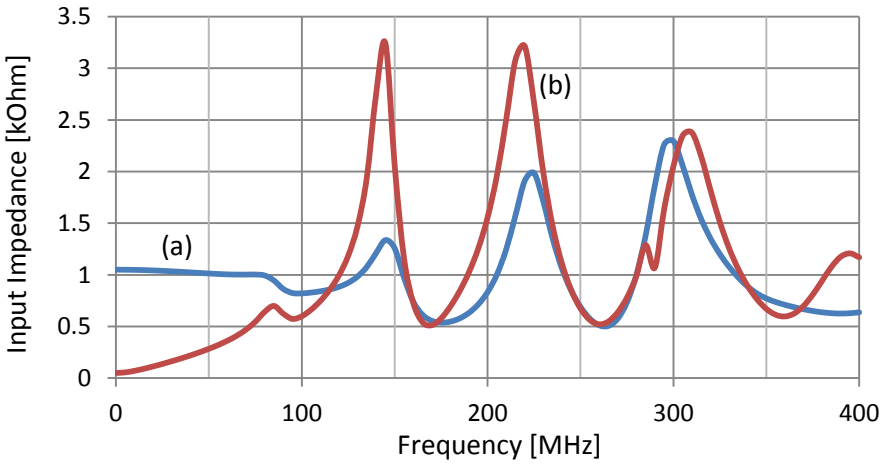

Figure A.2 – Simulated input impedance of Folded Dipole Antenna Derivations

Figure A.3 illustrates the reflection coefficient results for the Folded Dipole Antenna Derivations.

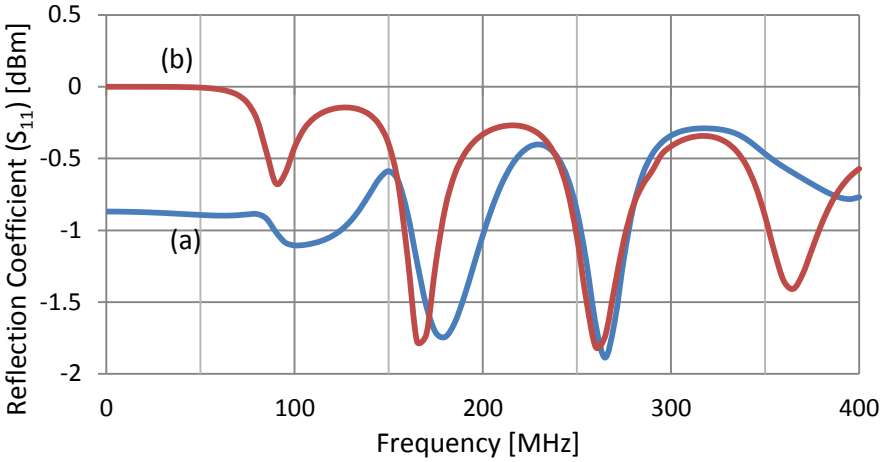

Figure A.3 – Simulated reflection coefficient of Folded Dipole Antenna Derivations

Figure A.4 illustrates the coupling results of the Folded Dipole Antenna Derivations.

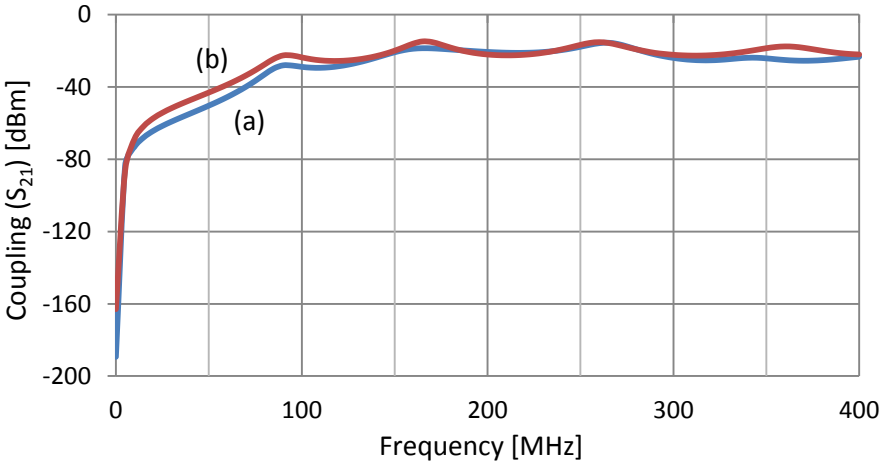

Figure A.4 – Simulated coupling of Folded Dipole Antenna Derivations

A.3 Quadrature Demodulator

The ADL5386 Quadrature Modulator from Analog Devices was first used as the quadrature demodulator. The device however failed at the very last minute and with limited time

could not be replaced by another. Because a lot of time was spent using this device, for the sake of completeness its use is documented in this section.

In the segment of the system where the I and Q channels are fed back into the receiver (Section 4.4); a device was needed to combine these two channels and mix them back up to the correct frequency. This is done by the ADL5386 Quadrature Modulator from Analog Devices which features a frequency range of 50 to 2200 MHz. Figure A.5 shows a functional block diagram of this device.

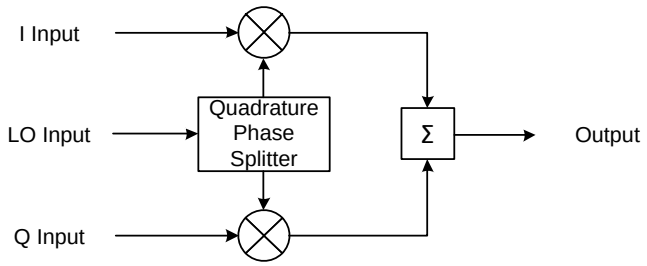

Figure A.5 – Functional block diagram of ADL5386 Quadrature Modulator

The device takes the LO input and splits it into two LO signals at 90° of phase difference to drive two mixers in quadrature. The I and Q channel signals are then mixed with the quadrature LO signals after which they have a 0° phase difference. These two signals are then combined to form the output signal.

Both the I and Q channel inputs are differential. Therefore connecting the I and Q channel signals only to the negative ports and grounding the positive ports creates an output signal that is negative. This means that the output signal has a 180° phase difference to the in-phase signal. This is done so that the output signal when combined with the received signal at the receiver is subtracted from that signal.

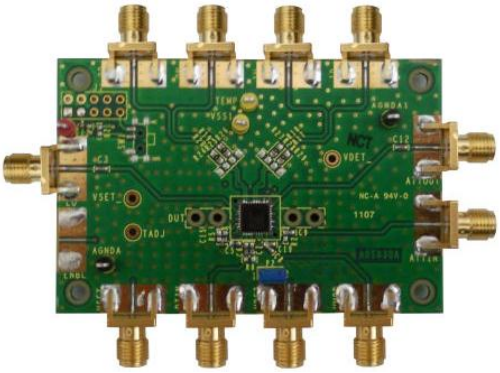

Figure A.6 – Picture of quadrature modulator evaluation board

A.3.1 Bias Circuit for the Quadrature Modulator

The I and Q inputs of the Quadrature Modulator requires a DC bias level of +0.5V. A DC bias Circuit was designed and built.

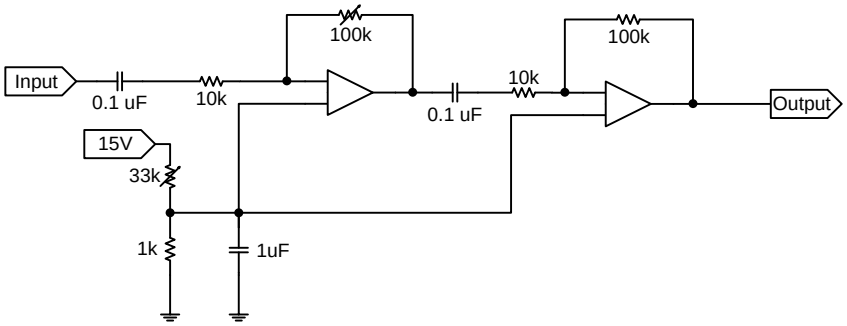

Figure A.7 – DC bias for Quadrature Modulator

A.4 MATLAB Simulation Code

This section documents the MATLAB code for the simulation of the simplified feedback model in Section 4.4.2.

```
clear;

openloop = 1;                           % Variable to open the feedback loop

Fs = 1e9;                               % Sampling freq.
Ts = 1/Fs;                              % Sampling period

n = 4;                                  % Filter order
```

```
Flpc = 30e3;                            % Low-pass filter cut-off freq.
Adb = 40;                               % Loop gain in dB
A = 10^(Adb/20);
Fhpc = (A^(1/n))*Flpc;                  % Resultant feedback loop cut-off freq.

L = 40e4;                               % Length of signal

time = (0:L+n-1)/Fs;                    % Time vector
x = cos(2*pi*100e3*time);               % Test signal

NFFT = 10*2^nextpow2(L);
f = Fs/2 * linspace(0,1,NFFT/2);

h=1./(1+((f)./Flpc).^(n));              % Transfer function of low-pass filter

if openloop
    g=(A.*h);                           % Open loop transfer function
else
    g=A./(1+A.*h);                      % Closed loop transfer function
end

xFFT = fft(x,NFFT)/(L);

TP1 = A.*xFFT;                          % Output of circuit WITHOUT feedback
TP2 = g.*xFFT(1:NFFT/2);                % Output of circuit WITH feedback
TP3 = g;

%-------------------------------------------------------------------------

figure(20)
    clf,
    semilogx(f,20*log10(abs(TP1(1:NFFT/2))),'r-'),
    hold on
    semilogx(f,20*log10(abs(TP2(1:NFFT/2))),'b-'),
    semilogx(f,20*log10(abs(g)),'k');
    hold off,
    xlabel('Frequency [Hz]'),
    ylabel('Magnitude [dBm]'),
    grid on,
    xlim([1e3,1e6]);
```

A.5 FPGA Code

This section documents the VHDL code for the programming the AD9858 FPGA. The AD9858.vhd is the program object used to obtain values for the different variables of the DDS; FPGA_top.vhd then takes these variables and converts them to binary data before sending them to the DDS.

A.1.1 AD9858.vhd

```
library ieee;
use ieee.std_logic_1164.all;
use ieee.std_logic_unsigned.all;

entity AD9858 is
```

A.5 FPGA Code

```
 port(
  nReset  : in  std_logic;
  Clk     : in  std_logic; -- 10 MHz

  CFR         : in std_logic_vector(31 downto 0);
  DFTW        : in std_logic_vector(31 downto 0);
  DFRRW       : in std_logic_vector(15 downto 0);
  FTW0        : in std_logic_vector(31 downto 0);
  POW0        : in std_logic_vector(13 downto 0);
  FTW1        : in std_logic_vector(31 downto 0);
  POW1        : in std_logic_vector(13 downto 0);
  FTW2        : in std_logic_vector(31 downto 0);
  POW2        : in std_logic_vector(13 downto 0);
  FTW3        : in std_logic_vector(31 downto 0);
  POW3        : in std_logic_vector(13 downto 0);
  Profile     : in std_logic_vector( 1 downto 0);
  FUD_Period  : in std_logic_vector(31 downto 0); -- T = x * 200 ns; off when 0

  DDS_IOReset : out   std_logic;
  DDS_SDIO    : inout std_logic;
  DDS_SClk    : out   std_logic;
  DDS_nCS     : out   std_logic;
  DDS_Reset   : out   std_logic;
  DDS_PS      : out   std_logic_vector(1 downto 0);
  DDS_FUD     : out   std_logic
 );
end entity AD9858;
--------------------------------------------------------------------------------

architecture a1 of AD9858 is
 signal state     : std_logic_vector( 3 downto 0);
 signal retstate  : std_logic_vector( 3 downto 0);
 signal count     : std_logic_vector( 5 downto 0);

 signal Data      : std_logic_vector(39 downto 0);

 signal tCFR      : std_logic_vector(31 downto 0);
 signal tDFTW     : std_logic_vector(31 downto 0);
 signal tDFRRW    : std_logic_vector(15 downto 0);
 signal tFTW0     : std_logic_vector(31 downto 0);
 signal tPOW0     : std_logic_vector(13 downto 0);
 signal tFTW1     : std_logic_vector(31 downto 0);
 signal tPOW1     : std_logic_vector(13 downto 0);
 signal tFTW2     : std_logic_vector(31 downto 0);
 signal tPOW2     : std_logic_vector(13 downto 0);
 signal tFTW3     : std_logic_vector(31 downto 0);
 signal tPOW3     : std_logic_vector(13 downto 0);

 signal tFUD1     : std_logic;
```

A.5 FPGA Code

```
 signal tFUD2     : std_logic;
 signal FUD_Count : std_logic_vector(31 downto 0);
--------------------------------------------------------------------------------

begin
 process(Clk, nReset) is
 begin
  if nReset = '0' then
   state       <= (others => '0');
   count       <= (others => '0');
   Data        <= (others => '0');

   tCFR        <= (others => '0');
   tDFTW       <= (others => '0');
   tDFRRW      <= (others => '0');
   tFTW0       <= (others => '0');
   tPOW0       <= (others => '0');
   tFTW1       <= (others => '0');
   tPOW1       <= (others => '0');
   tFTW2       <= (others => '0');
   tPOW2       <= (others => '0');
   tFTW3       <= (others => '0');
   tPOW3       <= (others => '0');

   tFUD1       <= '0';
   tFUD2       <= '0';
   FUD_Count   <= (others => '0');

   DDS_IOReset <= '1';
   DDS_SClk    <= '0';
   DDS_nCS     <= '1';
   DDS_Reset   <= '1';
--------------------------------------------------------------------------------

  elsif rising_edge(Clk) then
   case state is
    when "0000" =>
     DDS_Reset   <= '0';
     DDS_IOReset <= '0';
     DDS_nCS     <= '0';
     state       <= "0001";
--------------------------------------------------------------------------------

    when "0001" =>
     if CFR /= tCFR then
      tCFR     <= CFR;
      Data     <= X"00" & CFR;
      count    <= "100111"; -- 39
      retstate <= "0010";
```

```
      state    <= "1110";
     else
      state    <= "0010";
     end if;
-------------------------------------------------------------------------------

    when "0010" =>
     if DFTW /= tDFTW then
      tDFTW    <= DFTW;
      Data     <= X"01" & DFTW;
      count    <= "100111"; -- 39
      retstate <= "0011";
      state    <= "1110";
     else
      state    <= "0011";
     end if;
-------------------------------------------------------------------------------

    when "0011" =>
     if DFRRW /= tDFRRW then
      tDFRRW   <= DFRRW;
      Data     <= X"02" & DFRRW & X"0000";
      count    <= "010111"; -- 23
      retstate <= "0100";
      state    <= "1110";
     else
      state    <= "0100";
     end if;
-------------------------------------------------------------------------------

    when "0100" =>
     if FTW0 /= tFTW0 then
      tFTW0    <= FTW0;
      Data     <= X"03" & FTW0;
      count    <= "100111"; -- 39
      retstate <= "0101";
      state    <= "1110";
     else
      state    <= "0101";
     end if;
-------------------------------------------------------------------------------

    when "0101" =>
     if POW0 /= tPOW0 then
      tPOW0    <= POW0;
      Data     <= X"04" & "00" & POW0 & X"0000";
      count    <= "010111"; -- 23
      retstate <= "0110";
      state    <= "1110";
```

```
     else
      state    <= "0110";
     end if;
-------------------------------------------------------------------------------

    when "0110" =>
     if FTW1 /= tFTW1 then
      tFTW1    <= FTW1;
      Data     <= X"05" & FTW1;
      count    <= "100111"; -- 39
      retstate <= "0111";
      state    <= "1110";
     else
      state    <= "0111";
     end if;
-------------------------------------------------------------------------------

    when "0111" =>
     if POW1 /= tPOW1 then
      tPOW1    <= POW1;
      Data     <= X"06" & "00" & POW1 & X"0000";
      count    <= "010111"; -- 23
      retstate <= "1000";
      state    <= "1110";
     else
      state    <= "1000";
     end if;
-------------------------------------------------------------------------------

    when "1000" =>
     if FTW2 /= tFTW2 then
      tFTW2    <= FTW2;
      Data     <= X"07" & FTW2;
      count    <= "100111"; -- 39
      retstate <= "1001";
      state    <= "1110";
     else
      state    <= "1001";
     end if;
-------------------------------------------------------------------------------

    when "1001" =>
     if POW2 /= tPOW2 then
      tPOW2    <= POW2;
      Data     <= X"08" & "00" & POW2 & X"0000";
      count    <= "010111"; -- 23
      retstate <= "1010";
      state    <= "1110";
     else
```

```
      state    <= "1010";
     end if;
-------------------------------------------------------------------------------

    when "1010" =>
     if FTW3 /= tFTW3 then
      tFTW3    <= FTW3;
      Data     <= X"09" & FTW3;
      count    <= "100111"; -- 39
      retstate <= "1011";
      state    <= "1110";
     else
      state    <= "1011";
     end if;
-------------------------------------------------------------------------------

    when "1011" =>
     if POW3 /= tPOW3 then
      tPOW3    <= POW3;
      Data     <= X"0A" & "00" & POW3 & X"0000";
      count    <= "010111"; -- 23
      retstate <= "1100";
      state    <= "1110";
     else
      state    <= "1100";
     end if;
-------------------------------------------------------------------------------

    when "1100" =>
     tFUD1 <= '1';
     state <= "1101";
-------------------------------------------------------------------------------

    when "1101" =>
     tFUD1 <= '0';
     state <= "0001";
-------------------------------------------------------------------------------

    when "1110" =>
     DDS_SClk <= '1';
     state    <= "1111";
-------------------------------------------------------------------------------

    when "1111" =>
     DDS_SClk <= '0';
     Data     <= Data(38 downto 0) & '0';

     if count = "000000" then
      state <= retstate;
```

```
     else
      state <= "1110";
     end if;

     count <= count - '1';
-------------------------------------------------------------------------------

    when others =>
   end case;
-------------------------------------------------------------------------------

   if    FUD_Period = X"00000000" then
    tFUD2     <= '0';
   elsif FUD_Count  = X"00000000" then
    tFUD2     <= not tFUD2;
    FUD_Count <= FUD_Period - '1';
   else
    tFUD2     <= '0';
    FUD_Count <= FUD_Count  - '1';
   end if;
  end if;
 end process;
-------------------------------------------------------------------------------

 DDS_SDIO <= Data(39);
 DDS_PS   <= Profile;
 DDS_FUD  <= tFUD1 or tFUD2;
end architecture a1;
-------------------------------------------------------------------------------
```

A.1.2 FPGA_top.vhd

```
library ieee;
use ieee.std_logic_1164.all;
use ieee.std_logic_unsigned.all;

PACKAGE THDB_ADA_package IS
   COMPONENT AD9858
      PORT(    nReset          : in  std_logic;
                       Clk                    : in  std_logic; -- 10 MHz

                       CFR          : in std_logic_vector(31 downto 0);
                       DFTW         : in std_logic_vector(31 downto 0);
                       DFRRW        : in std_logic_vector(15 downto 0);
                       FTW0         : in std_logic_vector(31 downto 0);
                       POW0         : in std_logic_vector(13 downto 0);
                       FTW1         : in std_logic_vector(31 downto 0);
```

```
                        POW1        : in std_logic_vector(13 downto 0);
                        FTW2        : in std_logic_vector(31 downto 0);
                        POW2        : in std_logic_vector(13 downto 0);
                        FTW3        : in std_logic_vector(31 downto 0);
                        POW3        : in std_logic_vector(13 downto 0);
                        Profile     : in std_logic_vector( 1 downto 0);
                        FUD_Period   : in std_logic_vector(31 downto 0); -- T = x * 200 ns; off
when 0

                        DDS_IOReset : out   std_logic;
                        DDS_SDIO    : out std_logic;
                        DDS_SClk    : out   std_logic;
                        DDS_nCS     : out   std_logic;
                        DDS_Reset   : out   std_logic;
                        DDS_PS      : out   std_logic_vector(1 downto 0);
                        DDS_FUD     : out   std_logic
                        );
   END COMPONENT;
END THDB_ADA_package;

LIBRARY work;
USE work.THDB_ADA_package.ALL;

library ieee;
use ieee.std_logic_1164.all;
use ieee.std_logic_unsigned.all;

entity FPGA_top is
       port(   nReset         : in  std_logic;                                          --
Button to reset device
                        Clk_10M     : in  std_logic;
                        Profile     : in std_logic_vector( 1 downto 0);

                        DDS_IOReset : out   std_logic;
       -- I/O Reset pin
                        DDS_SDIO    : out     std_logic;
       -- Serial Data pin
                        DDS_SClk    : out   std_logic;
       -- System Clock (10Mhz)
                        DDS_nCS     : out   std_logic;
       -- not Chip Select pin
                        DDS_Reset   : out   std_logic
                        );
end entity FPGA_top;

architecture DDS of FPGA_top is

begin
       AD98581 :AD9858 port map(
```

```
                nReset,
                Clk_10M,
                X"00000078", -- CFR, (32)
                X"00000000", -- DFTW, (32)
                X"0000", -- DFRRW, (16)
                X"00418937", -- FTW0, (32) 00418937(0.5MHz) 00800000
                "00" & X"000", -- POW0, (14)
                X"00000000", -- FTW1, (32)
                "00" & X"000", -- POW1, (14)
                X"00000000", -- FTW2, (32)
                "00" & X"000", -- POW2, (14)
                X"00000000", -- FTW3, (32)
                "00" & X"000", -- POW3, (14)
                Profile, -- Profile, (2)
                X"00000000", -- FUD_Period, (32) -- T = x * 200 ns; off when 0
                DDS_IOReset, -- : out std_logic;
                DDS_SDIO, -- : inout std_logic;
                DDS_SClk, -- : out std_logic;
                DDS_nCS, -- : out std_logic;
                DDS_Reset -- : out std_logic;
                );
end architecture DDS;
```